AD-A163 696 LUBRICANT FOAMING AND AERATION STUDY PART 2(U) 1/2
RENSSELAER POLYTECHNIC INST TROY NY S ROSS DEC 85
AFWAL-TR-84-2001-PT-2 F33615-80-C-2017

UNCLASSIFIED F/G 11/8 NL

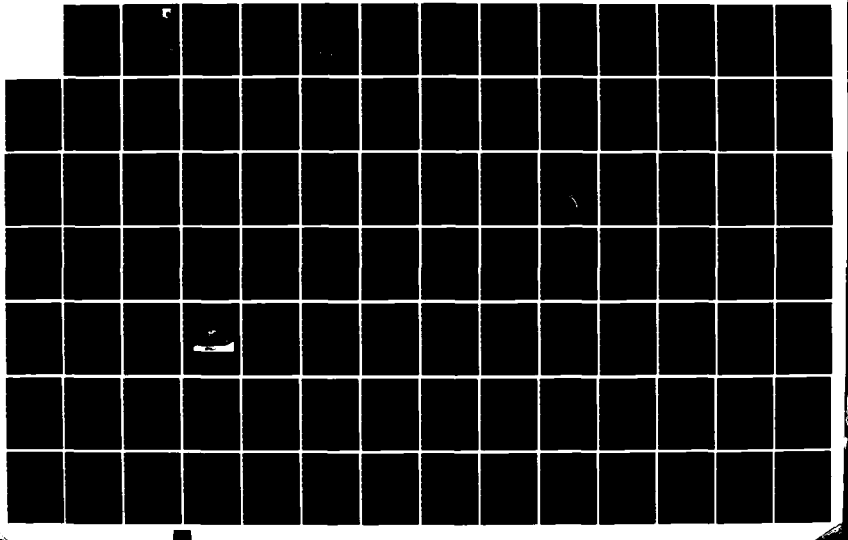

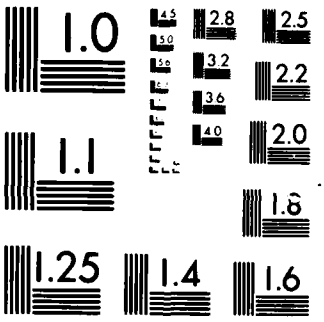

AFWAL-TR-84-2001, Part II

LUBRICANT FOAMING AND AERATION STUDY, PART II

Sydney Ross

Rensselaer Polytechnic Institute
Troy, NY 12180-3590

December 1985

Final Report for Period March 1984-July 1985

AERO PROPULSION LABORATORY
AIR FORCE WRIGHT AERONAUTICAL LABORATORIES
AIR FORCE SYSTEMS COMMAND
WRIGHT-PATTERSON AIR FORCE BASE OH 45433

NOTICE

When Government drawings, specifications, or other data are used for any purpose other than in connection with a definitely related Government procurement operation, the United States Government thereby incurs no responsibility nor any obligation whatsoever; and the fact that the Government may have formulated, furnished, or in any way supplied the said drawings, specifications, or other data, is not to be regarded by implication or otherwise as in any manner licensing the holder or any other person or corporation, or conveying any rights or permission to manufacture, use, or sell any patented invention that may in any way be related thereto.

This report has been reviewed by the Office of Public Affairs (ASD/PA) and is releasable to the National Technical Information Service (NTIS). At NTIS, it will be available to the general public, including foreign nations.

This technical report has been reviewed and is approved for publication.

Phillip W. Centers
PHILLIP W. CENTERS
Project Engineer

Howard F. Jones
HOWARD F. JONES
Chief, Lubrication Branch

FOR THE COMMANDER

Robert D. Sherrill
ROBERT D. SHERRILL
Chief, Fuels and Lubrication Division

"If your address has changed, if you wish to be removed from our mailing list, or if the addressee is no longer employed by your organization please notify AFWAL/POSL, WPAFB, OHIO 45433 to help us maintain a current mailing list."

Copies of this report should not be returned unless return is required by security considerations, contractual obligations, or notice on a specific document.

SECURITY CLASSIFICATION OF THIS PAGE

REPORT DOCUMENTATION PAGE

1a. REPORT SECURITY CLASSIFICATION: UNCLASSIFIED	1b. RESTRICTIVE MARKINGS:
2a. SECURITY CLASSIFICATION AUTHORITY:	3. DISTRIBUTION/AVAILABILITY OF REPORT: Approved for public release; distribution unlimited.
2b. DECLASSIFICATION/DOWNGRADING SCHEDULE:	
4. PERFORMING ORGANIZATION REPORT NUMBER(S):	5. MONITORING ORGANIZATION REPORT NUMBER(S): AFWAL-TR-84-2001, Part II
6a. NAME OF PERFORMING ORGANIZATION: Rensselaer Polytechnic Inst. / 6b. OFFICE SYMBOL (If applicable):	7a. NAME OF MONITORING ORGANIZATION: Aero Propulsion Laboratory (AFWAL/POSL) Air Force Wright Aeronautical Lab (AFSC)
6c. ADDRESS (City, State and ZIP Code): Troy, N.Y. 12180-3590	7b. ADDRESS (City, State and ZIP Code): Wright-Patterson Air Force Base, OH 45433
8a. NAME OF FUNDING/SPONSORING ORGANIZATION / 8b. OFFICE SYMBOL (If applicable):	9. PROCUREMENT INSTRUMENT IDENTIFICATION NUMBER: F33615-80-C-2017
8c. ADDRESS (City, State and ZIP Code):	10. SOURCE OF FUNDING NOS.

PROGRAM ELEMENT NO.	PROJECT NO.	TASK NO.	WORK UNIT NO.
62203F	3048	06	14

11. TITLE (Include Security Classification): Lubricant Foaming and Aeration Study, Part II

12. PERSONAL AUTHOR(S): Sydney Ross

13a. TYPE OF REPORT	13b. TIME COVERED	14. DATE OF REPORT (Yr., Mo., Day)	15. PAGE COUNT
Final	FROM 3/1/84 TO 7/1/85	December 1985	128

16. SUPPLEMENTARY NOTATION:

17. COSATI CODES		
FIELD	GROUP	SUB. GR.
11	08	
14	02	

18. SUBJECT TERMS (Continue on reverse if necessary and identify by block number): Foam Bubble Rise; Lubricant, Foam Testing, Monolayer Lubrication, Surface Elasticity, Surface Tension, Dynamic Surface Tension; Capillary-wave Damping.

19. ABSTRACT (Continue on reverse if necessary and identify by block number)

This investigation is directed toward obtaining a fundamental understanding of lubricant foaming and aeration. On the practical side, foam tests showed that the surface activity of additives varies from one production batch to another, requiring continuing testing before acceptance. On the fundamental side, three independent techniques were developed to measure dynamic (nonequilibrium) surface tensions of oils containing additives, to obtain simpler correlative physical properties of oil surfaces than the complex multivariant effects that underlie the phenomena of foaming and aeration. These techniques to detect and measure dynamic surface tensions are: measuring changes of surface tension on cycling area contractions and expansions; measuring the damping of capillary ripples; and measuring the rate of ascent of a single bubble in an oil solution. These techniques are able to disclose the presence of surface activity in oil solutions, even before it develops to the state of an overt foam problem.

20. DISTRIBUTION/AVAILABILITY OF ABSTRACT: UNCLASSIFIED/UNLIMITED ☒ SAME AS RPT. ☐ DTIC USERS ☐	21. ABSTRACT SECURITY CLASSIFICATION: UNCLASSIFIED
22a. NAME OF RESPONSIBLE INDIVIDUAL: PHILLIP W. CENTERS	22b. TELEPHONE NUMBER (Include Area Code): (513)255-6608 / 22c. OFFICE SYMBOL: AFWAL/POSL

DD FORM 1473, 83 APR — EDITION OF 1 JAN 73 IS OBSOLETE.

UNCLASSIFIED

SECURITY CLASSIFICATION OF THIS PAGE

PREFACE

Lubricant Foaming and Aeration Study, Part II, is a continuation of AFWAL-TR-84-2001. The objective of the effort is to obtain a fundamental understanding of the causes of foaminess and gas retention in turbine-engine lubricants. The work was done in the Colloid and Surface Chemistry Laboratories, Department of Chemistry, Rensselaer Polytechnic Institute, Troy, N.Y. 12181, by Professor Sydney Ross, Dr Gaudenz Furler, Mr D.F. Townsend, and Mr Erik J. Bock, during the period March 1984 to July 1985. The effort was sponsored by the Aero Propulsion Laboratory, Air Force Wright Aeronautical Laboratories, Air Force Systems Command, Wright-Patterson AFB, Ohio, under Contract F33615-80-C-2017. The work was accomplished under Project 3048, Task 304806, Work Unit 30480614, Foaming and Aeration Characteristics of Turbine Lubricants, with Mr Phillip W. Centers as Project Engineer .

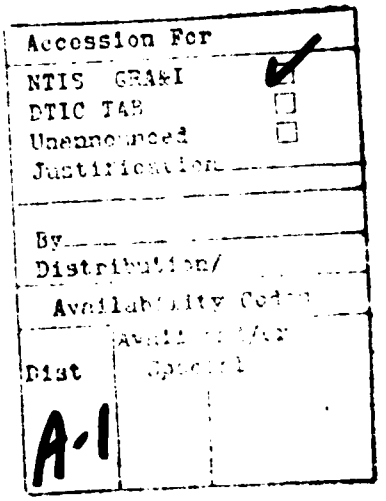

TABLE OF CONTENTS

LIST OF ILLUSTRATIONS

FIGURE PAGE

FIGURE PAGE

FIGURE PAGE

LIST OF TABLES

SECTION I

INTRODUCTION

The relation of the foaminess of a solution to dynamic, or nonequilibrium, surface tension is now a feature of a well established theory to explain the stability of liquid lamellae. The shift of emphasis in the present Report from a direct study of foams to their underlying cause is advantageous, as dynamic surface tensions are closer to reflecting fundamental physical properties of a solution such as surface viscosity and elasticity.

The results included in this Report relate chiefly to different techniques to create and to measure dynamic surface tensions. Of these techniques, only one, the cyclic variation of area of a solution, is followed by means of actual measurements of changing surface tension: the other techniques use secondary effects of local gradients of surface tension, such as the retardation of the rate of ascent of a bubble or the increased damping of capillary ripples.

Methods to measure dynamic surface tension and the hydrodynamic theories of the various methods are still active areas of research activity. In the work reported here we have introduced or modified techniques, and made use of recent theories, in each of three methods to study dynamic surface tension.

The dynamic surface tension consequent on the cyclic variation of surface area of a solution is an attempt to simulate the gradients of surface tension that are required for the stabilizing of liquid lamellae in a foam. The results of this technique come the closest to correlating with the actual production of foam in the standard test.

The retardation of the ascent of a bubble in an oil solution is valuable to discover the relative surface activities of various additives in oil solutions. Current theories of this effect received experimental verification in the course of this work.

The damping of capillary ripples is a method requiring sophisticated computer hardware and software, which has been successfully attained in this study. As with the theory of bubble rise, the results obtained provide experimental verification of current theory of damping of capillary ripples in solvents. Time was lacking, however, to follow this with the study of dynamic surface tension of additives in solution.

Section II

MATERIALS

1. Synthetic Lubricants as Solvents

Table 1 shows the synthetic ester lubricants and the various solutes that were tested for surface activity. We tested two model solutes that are not included in normal lubricant formulations. These showed the effect of structure on surface activity. All materials were used as is.

2. Model Aqueous Systems.

Table 2 shows the solutes used in water to act as models of surface-active behavior for the dynamic-surface-tension apparatus and the foam stability apparatus. Distilled water obtained from a general supply was redistilled from alkaline permanganate into phosphoric acid and distilled once again into a quartz container. 1-Butanol was obtained from Fisher Scientific Co. and was purified using C_{18} Sep-Pak cartridges. Polydimethylsiloxane, GE SF96-100 (the number average molecular weight is about 6600 g/mole,) was used as is. Sodium dodecyl sulfate was obtained from J.T. Baker Co. as 99% electrophoretic grade. It was dissolved in water, chilled below its Krafft point and filtered. It was then dissolved in nearly boiling absolute ethanol and recrystallized three times, each time allowing the crystals to ripen overnight at room temperature; the crystals were finally dried with acetone.

Table 1. Synthetic Lubricants and Solutes Tested for Surface Activity.

Designation	Name	Function	Source
Base Stock 704 or Mobil Ester P-41 or Tmp-heptanoate	Trimethylolpropane heptanoate (2,2-Diheptanoyloxymethyl-n-butyl heptanoate)	Synthetic Lubricant	Stauffer Chemical Mobil Oil Corp.
Emolein 2917	Dipropylene glycol bis-nonanoate	Synthetic Lubricant	Emery Industries Inc.
O-77-10 Blend	Tmp-heptanoate + Neopentyl glycol esters	Synthetic Lubricant	U.S. Air Force
Hercolube C	A pentaerythritol ester	Synthetic Lubricant	Hercules Chemical Co.
TEL-4041		Typical Formulated Lubricant	U.S. Air Force
N-Phenyl-1-naphthylamine		Antioxidant	Eastman Kodak Co.
Tricresyl phosphate		Dispersant Viscosity Index Improver	Fisher Scientific Co.
Polydimethylsiloxane		Antifoam	General Electric Co.
Polypropylene glycol		Potential Surface-Active Solute	Aldrich Chemical Co.
2,6,8-Trimethyl-4-nonanol		Potential Surface-Active Solute	Wiley Organics
Sebacic acid	Decanedioic acid	Load Carrying Addititve	U.S. Air Force
3,7-Dioctyl phenothiazine		Antioxidant	U.S. Air Force
Acryloid HF866	Conc. solution of alkyl methacrylate polymer in a sebacate-ester carrier oil	Dispersant Viscosity Index Improver	Rohm and Haas Co.
Triphenyl phosphite		Load-carrying Additive	U.S. Air Force

Table 2. Model Aqueous Systems of Surface Active Solutes.

Name	Purity	Source
Distilled Water	Triply Distilled	A central supply and then distilled from alkaline permaganate followed by a third distillation from phosphoric acid
1-Butanol	Reagent Grade	Fisher Scientific
Sodium Dodecyl Sulfate	Recrystallized 99% Electrophoretic Grade	J.T. Baker Co.
Polydimethylsiloxane		General Electric Co.
Polypropylene Glycol		Aldrich Chemical Co.

SECTION III

FOAM STABILITY MEASUREMENTS

1. Instrumentation

The type of foam that is met in the foaming of lubricating oils is a relatively unstable, or transient, foam. The instrumentation best adapted to measure the stability of such foams makes use of dynamically regenerated foam rather than a static foam, as the latter subsides too rapidly to be convenient to measure. A cylindrical container, a fixed rate of gas efflux, and a temperature of 80° C is specified for the method 3213 of Test Method standard 791.[1] Method 3213 is favored by the Aero Propulsion Laboratory of the Air Force Systems Command as it has been found to correlate well with the behavior of lubricants in practice, inasmuch as an oil that floods the test cylinder at 80° C is unacceptable under operating conditions in an aircraft engine. As a laboratory test, however, Method 3213 has too much the nature of an On-Off or Go-No Go test, that is, the separation in response between zero foam and foam flooding is too sudden. When a gradation in surface activities with temperature or with concentration of solute exists, a foam test more capable of finer degrees of response is required; and for this purpose we have introduced and used the variation of the foam volume with the rate of gas efflux, retaining the apparatus used in Method 3213, including the cylindrical foam container. For even finer degrees of measurement, a conical container is substituted for the cylinder. We have also found it expedient for comparisons of dynamic surface tensions measured at room temperature to conduct certain foam tests at temperatures below 80°C. The ratio of the volume of foam to the rate of gas efflux, measured in a regime where their relationship is directly proportional, gives the unit of foaminess advocated by Bikerman,[2] designated Σ, and equal to the lifetime in seconds of a bubble in the foam. When Method 3213 is used, the result is reported as a volume of foam at steady-state conditions: when the Bikerman test is used the result is reported as Σ in seconds. The temperature of the test is always specified.

2. Foam Synergism with Two Solutes in Tmp-Heptanoate

Surface activity is the result of a lack of enough interaction between solute and solvent to ensure that the solute is at its lowest potential energy when in the bulk phase. If sufficient interaction is lacking, the solute may find a lower potential in the surface or even as an insoluble phase. Apart from the van-der-Waals (otherwise known as the London-dispersion) forces of attraction, which always function between any two molecules, the commonest type of specific solvent-solute interaction is a Lewis acid-Lewis base

---

[1] See Appendix A

[2] J.J. Bikerman, Trans. Faraday Soc., 36, 634 (1938); Idem, "Foams," Springer-Verlag, New York, 1973, pp 78-80.

combination. If the solute and the solvent are both Lewis bases, this interaction is lacking; their mutual interaction is therefore small; and the solute may well become segregated at the surface, where the heteromolecular interaction with the solvent is replaced by a homomolecular interaction with like molecules. Any degree of segregation at the surface, no matter how slight, results in surface activity; and conduces to foaminess of the solution.

We began a search to discover more solutes that would evince surface activity in tmp-heptanoate; and to ascertain if such solutes are Lewis bases, since tmp-heptanoate as an ester is itself a Lewis base. Although many chemical types were tested, only Lewis-base compounds such as amines and esters, if present in high enough concentrations, caused foaming in tmp-heptanoate.

Two esters, tricresyl phosphate and ethyl salicylate, were found to cause foaming in tmp-heptanoate; these, when present together, give us another example of foam synergism. Quantitative measurements of foam stability, expressed as Σ in seconds, obtained by the Watkins' conical foam-test device, at room temperature, for various compositions of the two solutes in tmp-heptanoate, are reported as isaphroic (equal foaminess) contours in Figure 1. The values of Σ are the slopes of the linear region of a plot of $A^{3/2}$ vs flowrate, where A is the cross-sectional area of the cone at the equilibrium height of the foam.

3. Foaminess of Solutions of Tmp-Heptanoate containing Polydimethylsiloxane alone and in Mixtures with other Solutes

The solution of polydimethylsiloxane (100cSt) in tmp-heptanoate at a concentration of 6.34 ppm does not foam at room temperature or at 80°C on bubbling nitrogen gas through the solution. The bubbles emanating from the porous ball are unusually large, however, quite unlike those that originate at the ball in the absence of the polydimethylsiloxane. The more concentrated solution, 14.1 ppm, does not foam at room temperature, but foams progressively more as the temperature is raised up to 80°C. The bubbles that form are again unusually large, suggestive of coalescing action within the body of the solution. The unusual character of the foam is further illustrated when its stability is measured: a value of Σ = 21.0 seconds is obtained at low rates of gas flow up to 7 ml/second; but the stability drops at a higher rate of gas flow (16.7 ml/second.) This effect again points to a coalescence of bubbles under the condition of higher agitation associated with the higher gas-flow rate. Also notable in this respect is the observation that single bubbles on the surface of these solutions are stable, unlike the unstable bubbles on the surface of the solvent in the absence of polydimethylsiloxane. These facts indicate that the polydimethylsiloxane, as the source of a destabilizing action on the foam bubbles, is present as a partially insoluble constituent. At temperatures above room temperature, the polydimethylsiloxane is partly soluble and is a profoamer, while the insoluble fraction continues to cause coalescence.

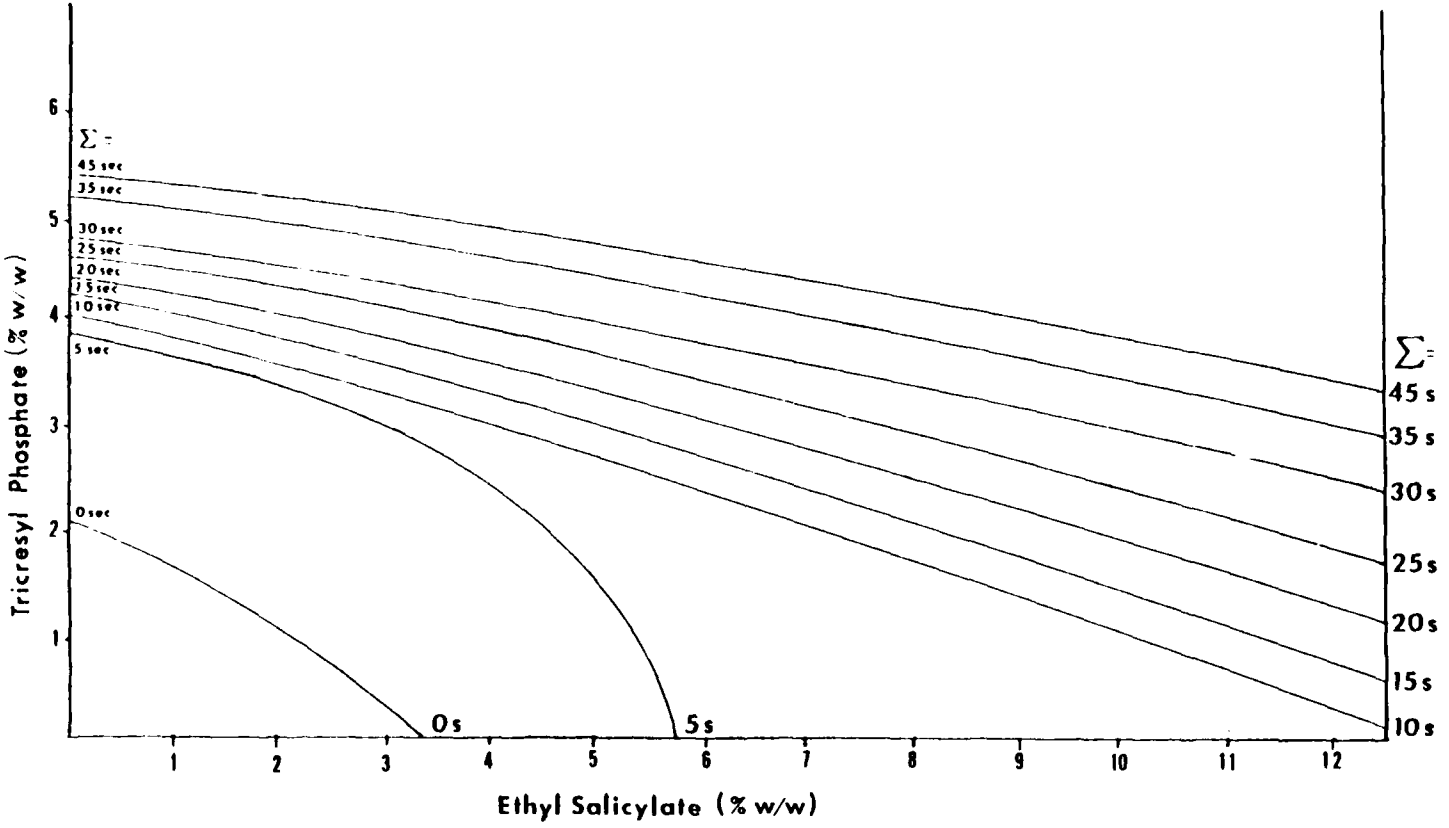

Figure 1. Isaphroic Contours of Binary Solutions of Tricresyl Phosphate and Ethyl Salicylate in Tmp-heptanoate at 22°C.

Our next series of experiments was to see if the bubble-coalescing activity of polydimethylsiloxane would be exercised in the presence of other profoaming solutes, such as N-phenyl-1-naphthylamine at a concentration of 4.0% w/w. A solution of this composition and concentration was prepared, with 6.34 ppm polydimethylsiloxane in addition. This solution, when freshly prepared, is defoamed at high flowrates of nitrogen gas (> 7 ml/second;) but not at low flowrates. After continued bubbling for about thirty minutes, the defoaming action "fatigues" and the foam is now remarkably stable, at room temperature and all the way up in temperature to 80°C. It is composed of small bubbles and climbs out of the column. The result of a measurement by Test Method 3213 at 80°C is > 500 ml. The presence of the 6.34 ppm polydimethylsiloxane, therefore, confers a short-lived defoaming action, but ultimately makes the solution much more foamy than it is in the absence of the silicone. The solution of N-phenyl-1-naphthylamine (Lot A12A) alone at 4% w/w concentration in tmp-heptanoate has a foam stability value of Σ = 19.2 seconds at 69.4°C (the highest temperature measured) and a maximum foam stability of 67.3 seconds at 40.2°C. Thus, even traces of a low-molecular weight silicone polymer acts as a synergist to enhance foam when combined with a profoaming additive in the oil.

Another solution of N-phenyl-1-naphthylamine (Lot A12A), 4% w/w, with 13.7 ppm polydimethylsiloxane, was also tested. This solution gave no evidence of any defoaming action at any time, even when freshly mixed; and enhanced the foaminess of the solution in the same way, and possibly to a greater degree, than its predecessor with less silicone.

We intend to follow up this newly disclosed example of foaming synergism, using concentrations of N-phenyl-1-naphthylamine (Lot A12A) or phenothiazine below the levels at which foaminess is observed, to discover whether the presence of a few parts per million of a silicone polymer in the oil induces foam in an admixture that otherwise does not foam at all. So closely connected in their causes are the two phenomena of profoaming and defoaming, that we might well discover defoaming action also provided by silicone polymers under different conditions of molecular weight, concentration, or temperature.

Reported above is an example of foaming synergism in solutions of tmp-heptanoate, caused by trace concentrations of polydimethylsiloxane (100 cSt) in the presence of some common oil anti-oxidants, such as N-phenyl-1-naphthylamine (Lot A12A) or phenothiazine. We now report further studies, using much lower concentrations of the oil additive and also of the silicone synergist. The results are included in Table 3, for mixtures in tmp-heptanoate of trace amounts of polydimethylsiloxane (100 cSt) along with (and without) N-phenyl-1-naphthylamine (Lot A12A), 2% (w/w)

Table 3 The Stability of Foam for various Concentrations and Temperatures with 100 cSt PDMS* and N-Phenyl-1-Naphthylamine (Lot A12A) in Tmp-Heptanoate.

Concentration of 100 cSt PDMS (ppm)	Concentration of N-Phenyl-1-Naphthylamine (% w/w)	Temp. (?C)	(sec)
6.34	0	22-80	0
0	2	22-80	0
6.34	2	22-80	>100
1.96	0	22-80	0
1.96	2	22.0	0
1.96	2	44.7	17.5
1.96	2	55.6	68.9
1.96	2	66.0	41.5
1.96	2	79.2	52.3
0.49	0	22-80	0
0.49	2	22.0	0
0.49	2	70.1	26.7
0.49	2	79.0	27.6

The Table shows the effect of higher temperatures, at which the foam becomes more stable. *PDMS = polydimethylsiloxane

4. Foaminess Tests on Various Lubricants and Solutes

Three different lubricants were tested by Foam Method 3213, with the results reported in Table 4.

Table 4. Results of Standard Foam Volume Test 3213 for 0-77-10, Emolein 2917, and TEL-4041.

System	Foam Volume (ml)
0-77-10 + 2% w/w N-phenyl-1-naphthylamine	0
0-77-10 + 2% w/w N-phenyl-1-naphthylamine + 2% w/w Tricresyl phosphate	240
Emolein 2917 + 2% w/w N-phenyl-1-naphthylamine	0
Emolein 2917 + 2% w/w N-phenyl-1-naphthylamine + 2% w/w Tricresyl phosphate	0
Emolein 2917 + 2% w/w N-phenyl-1-naphthylamine + 4% w/w Tricresyl phosphate	5
TEL-4041	5

Emolein 2917 had little foam stability when tested at 80°C with the same synergistic combination of solutes that produced foam when dissolved in tmp-heptanoate: namely, 2% (w/w) N-phenyl-1-naphthylamine + 2% (w/w) tricresyl phosphate. The blend 0-77-10, composed of tmp-heptanoate plus neopentyl glycol esters, tested in the same way and with the same combination of solutes at the same concentrations, showed about half the foaminess of the unblended tmp-heptanoate. The neopentyl glycol esters are, therefore, less susceptible than tmp-heptanoate to the effect of these solutes as surface-active agents, presumably because the neopentyl esters are better solvents than tmp-heptanoate for these additives.

The test lubricant, TEL-4041, showed little foam stability by Foam Method 3213 at 80° C and was not tested further.

All the solutions tested were tested again for the possible effect of water, by adding two or three drops of water, which were then allowed to remain in contact for two hours, before re-measuring the foaminess. No measurable effects were observed.

As already noted, solutes that exhibit surface activity in these synthetic-ester lubricants are rarely met. We have discovered a class of compound that causes Emolein 2917 to foam at room temperature. Small-chain alcohols (butanol, hexanol, octanol) were observed to produce foam when dissolved in Emolein 2917, but only at very high concentrations (ca. 20%.) Branched-chain secondary alcohols were then tried: diisobutyl carbinol [2,6-dimethyl-4-heptanol] and 2,6,8-trimethyl-4-nonanol produce foam in Emolein 2917 at 5% w/w. These solutes become less surface active at higher temperatures; and do not produce foam at temperatures above about 35° C.

Figure 2 shows the variation of the foam height with flow rate of nitrogen at 21° C for a solution of 2,6,8-trimethyl-4-nonanol (5% w/w) in Emolein 2917. The gas is introduced through a tube fitted with a fritted disc ("coarse" grade) concentric with its stem (Fisher Scientific Catalog No. 11-137-5B); the foam is produced in a cylinder of inside diameter 46.2 mm. The foaminess is measured as a retention time, which for the data reported in Figure 2 is 9.5 seconds. The retention time (rt) is a foamability parameter defined[3,4] as the slope of the linear part of the curve of dependence of total gas volume on gas-flow rate. In Figure 2, the data are described by two straight-line portions of the graph; in keeping with other published data, however, the upper line is more often the only linear portion obtained, and so it is used here to facilitate future comparisons. The rt value is equal to the average time necessary for a unit gas volume to pass through the whole system, i.e., solution plus foam.

---

[3] K. Malysa, R. Cohen, D. Exerowa and P. Krugljakov, J. Colloid Interface Sci., 80, 1 (1981)

[4] K. Malysa, K. Lunkenheimer, R. Miller and C. Hartenstein, Colloids and Surfaces, 3, 329 (1981).

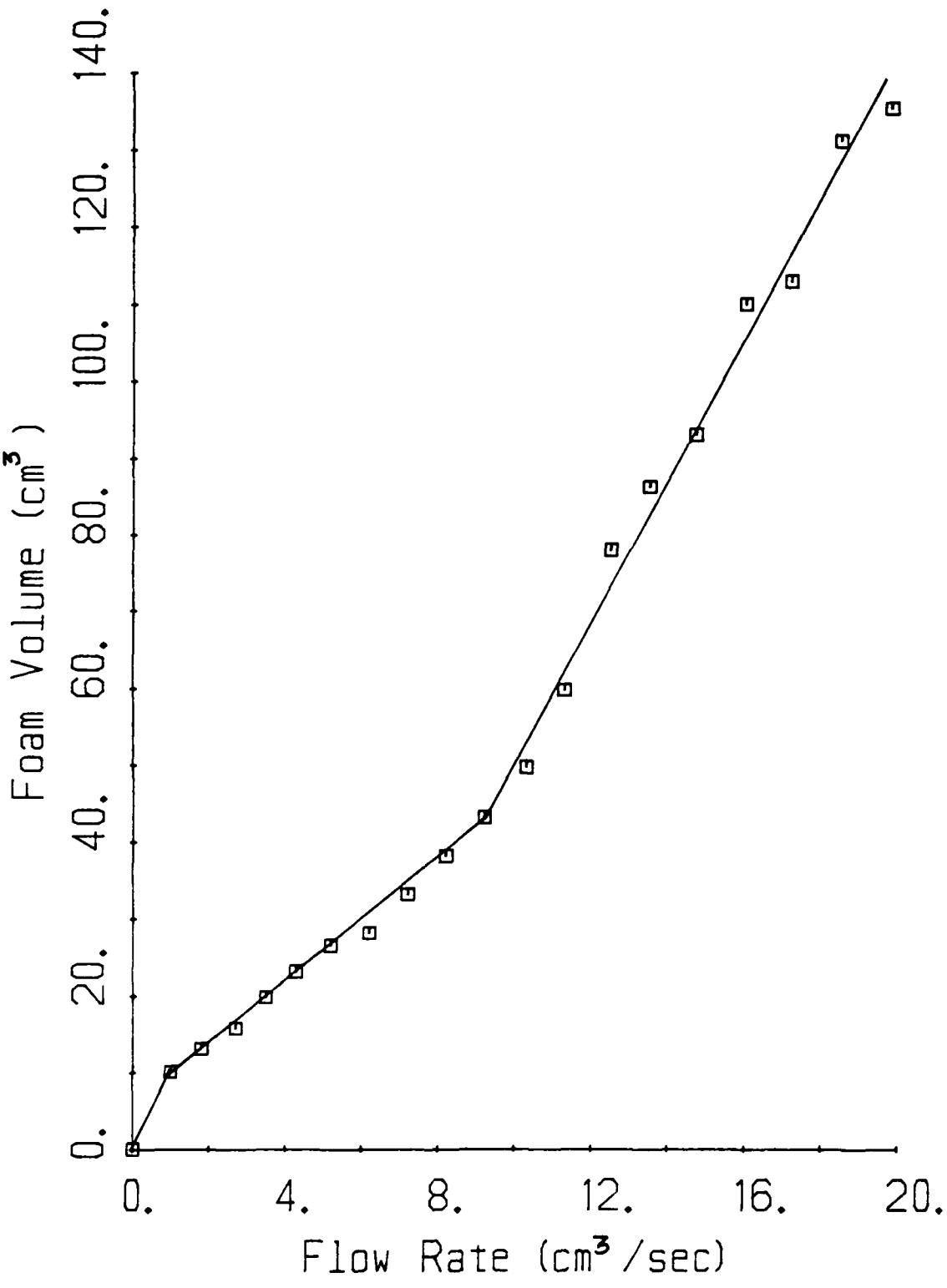

Figure 2. Variation of Volume of Gas in the Foam with Flow Rate for a Solution of 5% w/w 2,6,8 Trimethyl-4-nonanol in Emolein 2917 at 21°C.

Continuing the pursuit of solutes that cause foam production in Emolein 2917, we find that a solution of 2,6,8-trimethyl-4-nonanol at 5.0% w/w in Emolein 2917 does not show a hysteresis loop on the surface contraction/extension device, although the static surface tension drops from 30.0 mN/m to 29.0 mN/m, and the solution also produces stable foam.

Another solute that causes Emolein 2917 to produce foam is polypropylene glycol. It seems reasonable to try this material as a profoaming solute because the profoaming action of branched-chain secondary alcohols, already discovered, leads us to conclude that substituent methyl groups in a solute confer profoaming activity in these neopentyl glycol esters as solvents. Also, not forgotten, is that the polydimethylsiloxanes, known long since as profoaming solutes in solutions of synthetic ester lubricants, contain a large number of substituent methyl groups. Polypropylene glycol likewise has a number of substituent methyl groups. As expected, it too proved to be a profoaming solute in solution of Emolein 2917. The foam results for 5% w/w polypropylene glycol (weight-average molecular weight = 4000) dissolved in Emolein 2917 are reported in Table 5 and Figure 3. The solution does not foam until the temperature reaches about 35° C. Future work will observe the effects of molecular weight of this polymer from 750 to 4000 weight average.

Table 5. Foaminess of Polypropylene Glycol, Av.Mol.Wt. 4000, 5% w/w, in Emolein 2917.

Temperature (°C)	$\sum$ (sec)	Test Method 3213
21.7	0	-
46.5	16.2	-
55.1	16.3	-
65.2	25.7	-
79.5	14.5	150 ml

The foaminess of a solution of polypropylene glycol (average molecular weight of 4000 g/mole) at a concentration of 5.0% in Emolein 2917 at various temperatures were reported in Table 5. Further foaminess data were obtained and are reported for polypropylene glycols of various average molecular weights: viz. 725, 1000, 2000, and 3000 g/mole; at 5.0% concentration in Emolein 2917, and at various temperatures. Only one of these solutes showed foaminess, namely, the polypropylene glycol of average molecular weight = 3000 g/mole, which had a volume of 25 ml of foam at the test conditions of Method 3213 (80°C) but showed no foam at lower temperatures. None of the lower molecular weight polypropylene glycols showed foam at any temperature at this 5.00% concentration.

Foaminess of a solution of 4% w/w N-phenyl-1-naphthylamine (Lot A12A) in Mobil Ester P-41 was measured by Test Method 3213. This solute, at this concentration, in Base Stock 704, produced more than 500 ml of foam (see This Report, Part I, Section IV) but when

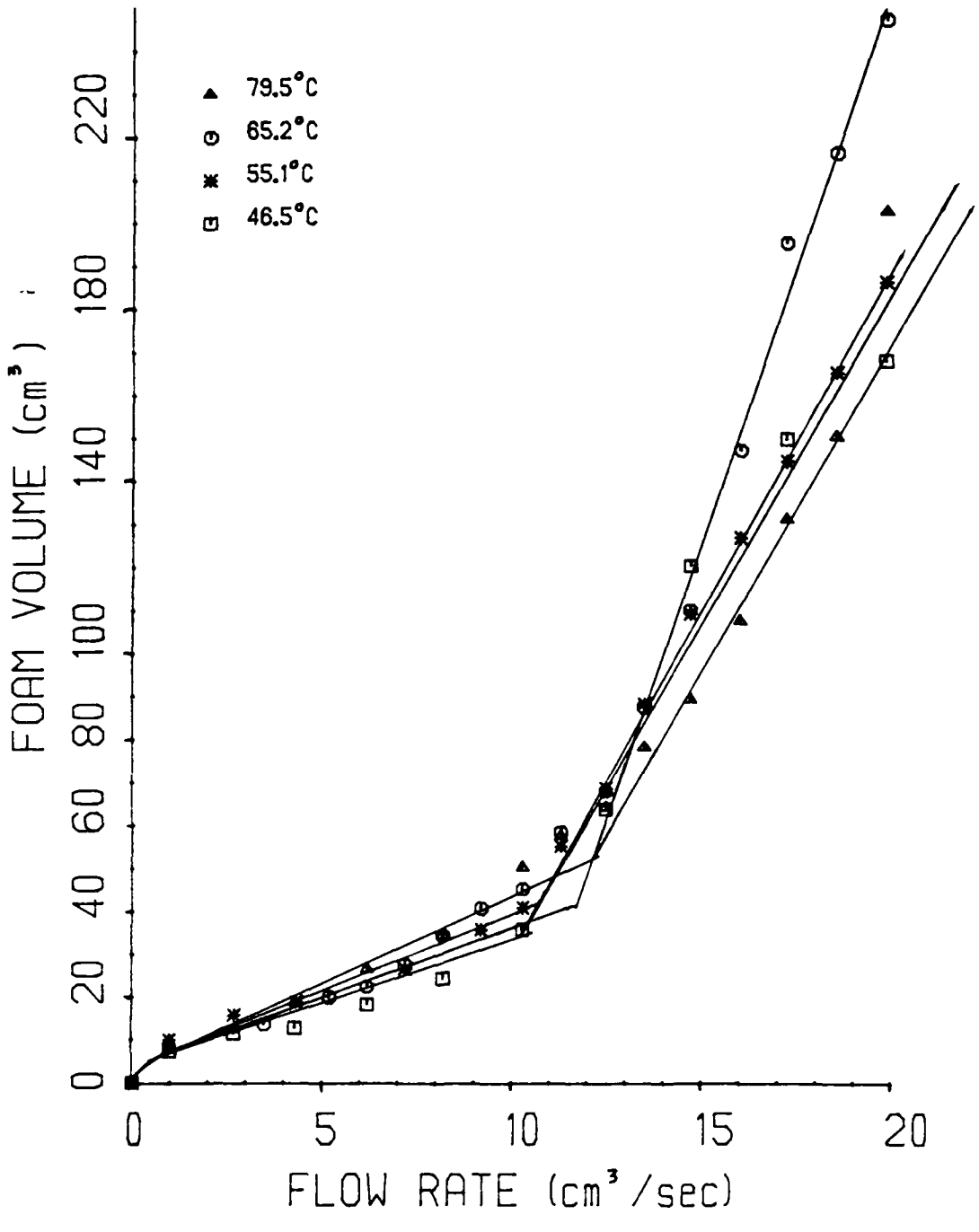

Figure 3. Variation of Volume of Gas in the Foam with Flow Rate for a Solution of 5% w/w Polyproylene Glycol, Av. Mol. Wt. 4000, in Emolein 2917 at Various Temperatures.

dissolved in another supply of oil of the same chemical composition, namely, Mobil Ester P-41, the same additive (but a different batch, Lot A13B) produced no foam at all. Similarly, the combination of 2% w/w N-phenyl-1-naphthylamine (Lot A13B) and 2% w/w tricresyl phosphate in Mobil Ester P-41 produced no foam, although the same combination (but from a different batch, Lot A12A) dissolved in Base Stock 704 produced more than 500 ml of foam. Even raising the concentrations of the amine to 5% and boosting the tricresyl phosphate to 10% in the Mobil Ester P-41 did not make the oil foam in the Test Method. The same result occurred again with 4% w/w phenothiazine dissolved in Mobil Ester P-41, that is, no foaminess; although the same solute at the same concentration dissolved in Base Stock 704 gave more than 500 ml of foam in the Test Method.

As well as unknown changes in the oil with the source of supply, we find that the additive N-phenyl-1-naphthylamine also varies from batch to batch: this solute from a different batch (Lot A13B), at 4% w/w in Base Stock 704 as solvent, showed no foaminess, although previously a solution of the same chemical from the same manufacturer, at the same concentration in the same solvent, had shown foaminess. Added tricresyl phosphate at 2% w/w did, however, cause more than 500 ml of foam to be produced, in accord with the previous finding of synergism between the two solutes.

Our supplies of the additive N-phenyl-1-naphthylamine were obtained from Eastman Kodak Co. from lots manufactured in 1981, 1982, and 1983. The results of our foam tests reveal that samples from the 1982 lots produced copious foam when dissolved in tmp-heptanoate; but that samples from the 1983 lots neither foamed as sole solutes nor in combination with tricresyl phosphate. It seems, therefore, that the manufacturer has gradually improved the purification of this additive.

SECTION IV

COMPRESSIONS AND DILATATIONS OF SOLUBLE ADSORBED FILMS

1. Introduction

The significance of the dynamic surface tension, as evinced by contraction-extension cycles of area of a solution, for the mechanism of the stability of foam lamellae, was descibed in Section VIII of This Report, Part I. A description of the apparatus and results obtained from it were also reported. These results are:

a. A pure solvent or a solution without surface activity shows no change of surface tension on contraction or extension of its surface;
b. a surface-active solute or an adsorbed monolayer causes the surface tension to decrease on contraction of the surface, and the surface tension to increase on extension of the surface. On cycling these changes of area, the dynamic surface tension displays hysteresis. Repeated cycling at a fixed frequency causes the system to reach a steady nonequilibrium state at which successive cycles repeat themselves.

Understanding how the hysteresis of surface tension arrives at its steady-state loop is important, because it reveals, at least qualitatively, the dynamics of adsorption and desorption.

The rates of adsorption and desorption are given by Langmuir[5] as follows:

$$u = k_1 \quad c \ (1 - \theta \ ) \qquad [1]$$

$$v = k_2 \quad \theta \quad \exp(-U/RT) \qquad [2]$$

where u is the rate of adsorption;
v is the rate of desorption;
θ is the fraction of the surface covered by an adsorbed monomolecular film;
U is the energy of adsorption; and
k_1 , k_2 are proportionality factors.

For a concentrated surface θ is large; therefore, the rate of adsorption is slow and the rate of desorption is rapid. The opposite is true for a dilute surface.

As well as the influence of the dynamics of adsorption, the behavior of soluble surface films on area cycling is determined by the relative surface concentration, which for a two-component system, is conveniently measured as the Gibbs excess concentration, Γ_2 molecules/cm^2, where

$$\Gamma_2 = -(1/kT) \ d\sigma / d \ \ln \ a_2 \qquad [3]$$

where a_2 is the activity of the bulk solution. The slope of the

---

[5] I. Langmuir, J. Amer. Chem. Soc., 39, 1848 (1917).

surface-tension isotherm is used to evaluate Γ_2 , and from Γ_2 in turn can be evaluated A, the area within which one molecule is found:

$$A = 10^{16}/\Gamma_2 \text{ sq. A.U./molecule} \quad [4]$$

These data are summarized as a spreading pressure-vs-area or Π vs A curve, where Π, the spreading pressure, is given by

$$\Pi = \sigma_o - \sigma \quad [5]$$

where σ_o is the surface tension of the solvent.

Spreading pressure-vs-area curves are two-dimensional analogs of pressure-vs-volume isotherms of gases, or, more exactly, of osmotic pressure-vs-dilution isotherms of solutions. Their general behavior can be described as consisting of two well marked portions: a dilute range of surface concentrations in which Π is low and large dilatations or compressions of the surface film can be made with hardly any change in the value of Π; and a concentrated range of surface concentrations in which large changes of Π result from small compressions or dilatations of the surface film. The dynamical behavior is further influenced by the rate of mechanical extensions and contractions of the surface compared to the rates of adsorption and desorption of the solute.

The points stressed above present aspects of the behavior of soluble adsorbed films that are pertinent to the interpretation of the dynamic surface tensions elicited by the area-cycling apparatus. To summarize:

a. In dilute surface films, the surface tension is not greatly reduced; compressions and dilatations of the surface film have only small effects on the surface tension, and the rate of adsorption is more rapid than the rate of desorption.
b. In concentrated surface films, the surface tension is close to its maximum amount of lowering; compressions and dilatations of the surface film have large effects on the surface tension, and the rate of desorption is more rapid than the rate of adsorption.

We shall show that the generalized description of behavior given above, based on the behavior of solutes of relatively low molecular weight, is followed fairly well by a weakly adsorbed solute such as is provided by the system 1-butanol+water; but is rather more complex for systems such as polymers in aqueous or nonaqueous solution.

Observing the surface-tension responses to the cyclical variation of the surface area for a system with a known equilibrium spreading pressure-vs-area curve and simple diffusion-controlled adsorption kinetics, makes interpreting the changes in the hysteresis curves easier. The system 1-butanol+water was chosen for this purpose. Results found with this system are applicable to nonaqueous systems for which the surface-concentration data are not known.

2. Experimental

The dynamic surface tensions were measured following the procedure decribed in This Report, Part 1, Section VIII. A water bath was added to obtain better thermal control of the solution during the measurement. Among the solutions measured, were aqueous solutions of 1-butanol, which were made by pipetting enough filtrate to make up two liters of a 0.819 M stock solution. Dilutions of the stock solution were made volumetrically. Dynamic surface tensions of aqueous solutions of sodium dodecyl sulfate were measured as well Solutions were made by weighing the solute into a two-liter volumetric flask; more dilute solutions were made from these as needed. The solutions of N-phenyl-1-naphthylamine and polydimethylsiloxane in tmp-heptanoate, were made by weighing both solute and solvent in a two-liter beaker.

3. Results

Figure 4 is the equilibrium spreading pressure-vs-area curve at 25.0°C for the system 1-butanol+water. Points P, Q and R correspond to the same letters in Figure 5, the adsorption isotherm, that is, surface concentration vs equilibrium bulk concentration. Figure 5 shows, for comparison, surface-concentration data for the system 1-butanol+water reported by Harkins and Wampler.[6] The dynamic surface tensions of solutions at the concentrations these points refer to are shown in Figure 6. Figure 6c shows the variation of surface tension with cycles of extensions and contractions of surface area of a 0.819 M solution of 1-butanol in water at 22.0°C and 1.02 cpm. The variation of surface tension with area forms a hysteresis loop, which moves away from equilibrium on successive iterations until it reaches a steady state; that is, no further change for five successive cycles. No effect on the surface tension was observed at slower cycling rates down to 0.02 cpm. Presumably the slow rates allow sufficient time for adsorption-desorption equilibria to be established.

Figure 6a shows the variation of surface tension with surface area of a 0.055 M aqueous solution of 1-butanol cycled at a frequency of 0.10 cpm. The surface tension decreases from its equilibrium value on successive contractions, until it reaches a steady state. The surface tension has a minimum value below its equilibrium at this frequency.

Figure 6b reports a 0.20 M aqueous solution of 1-butanol cycled at 1.02 cpm. The hysteresis starts out with an increase of surface tension and then slowly relaxes to a steady-state hysteresis loop that is above equilibrium at large surface areas and below equilibrium at small surface areas.

---

[6] W. D. Harkins and R. W. Wampler, J. Amer. Chem. Soc., 53, 850 (1931).

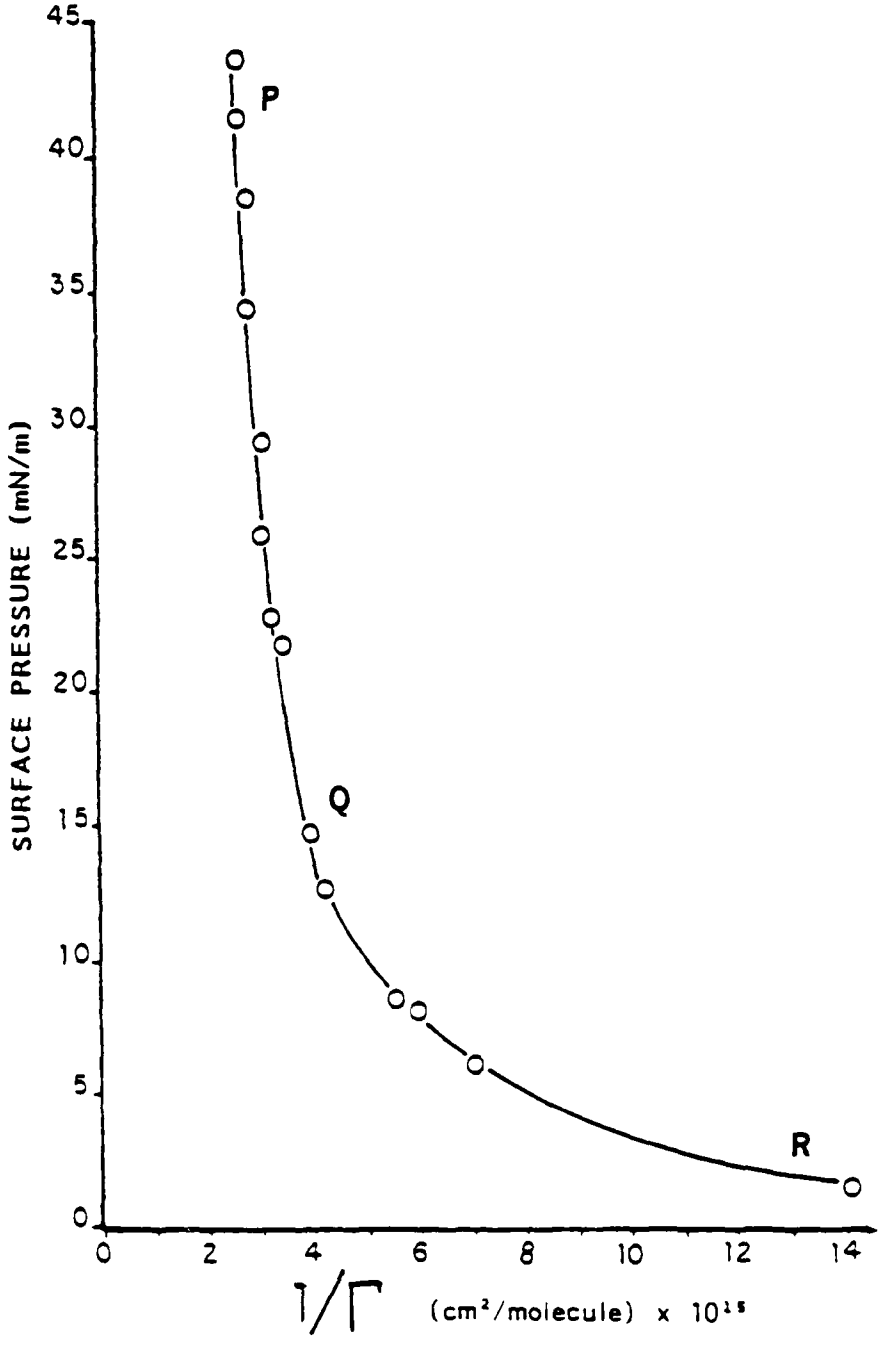

Figure 4. The Variation of the Equilibrium Surface Pressure with the Reciprocal of Surface Concentration for 1-Butanol in Water at 25.0°C.

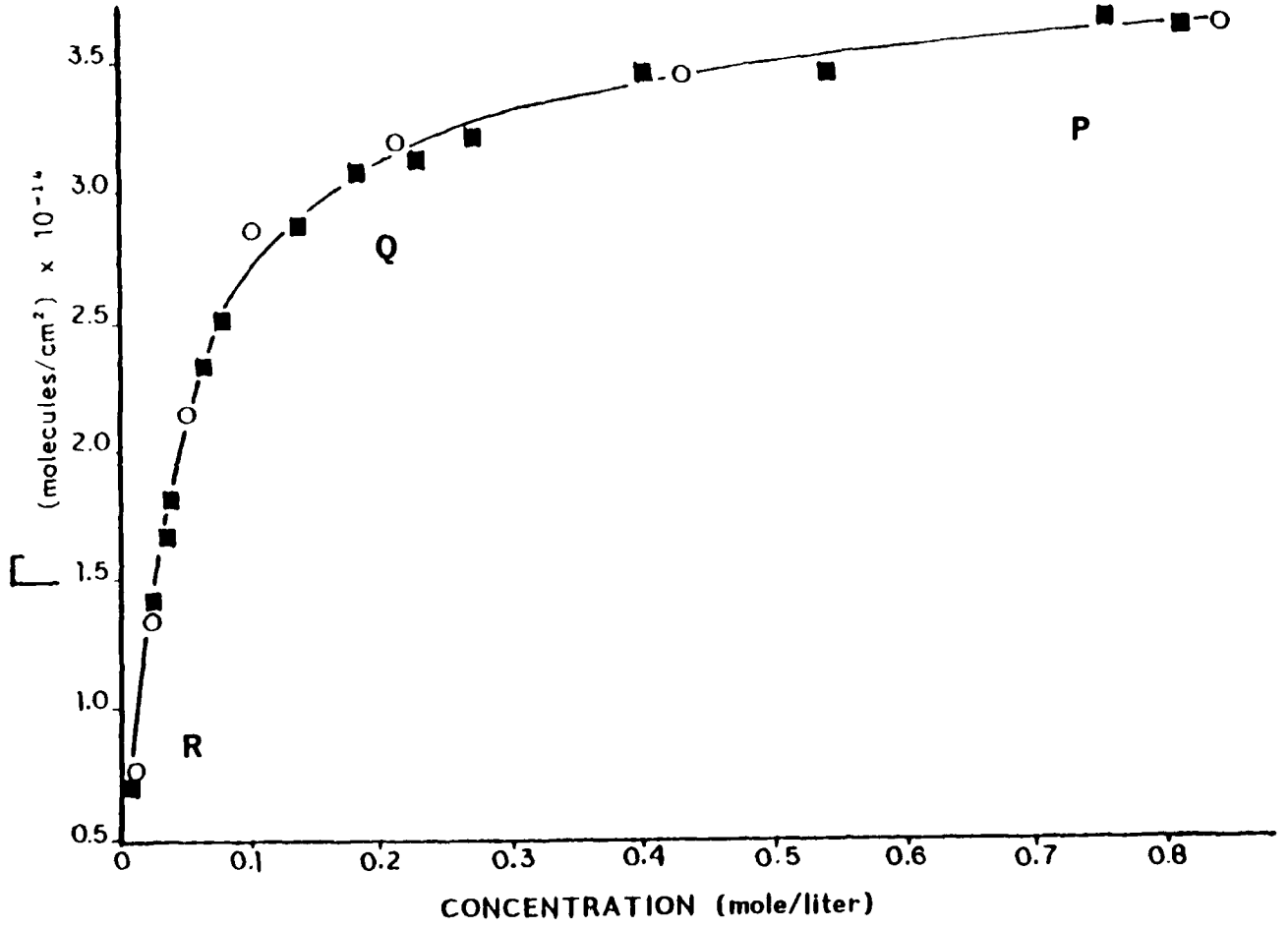

Figure 5. The Variation of Surface Concentration with the Bulk Concentration for 1-Butanol in Water at 25.0°C; (O) Harkins and Wampler ; (■) this Study.

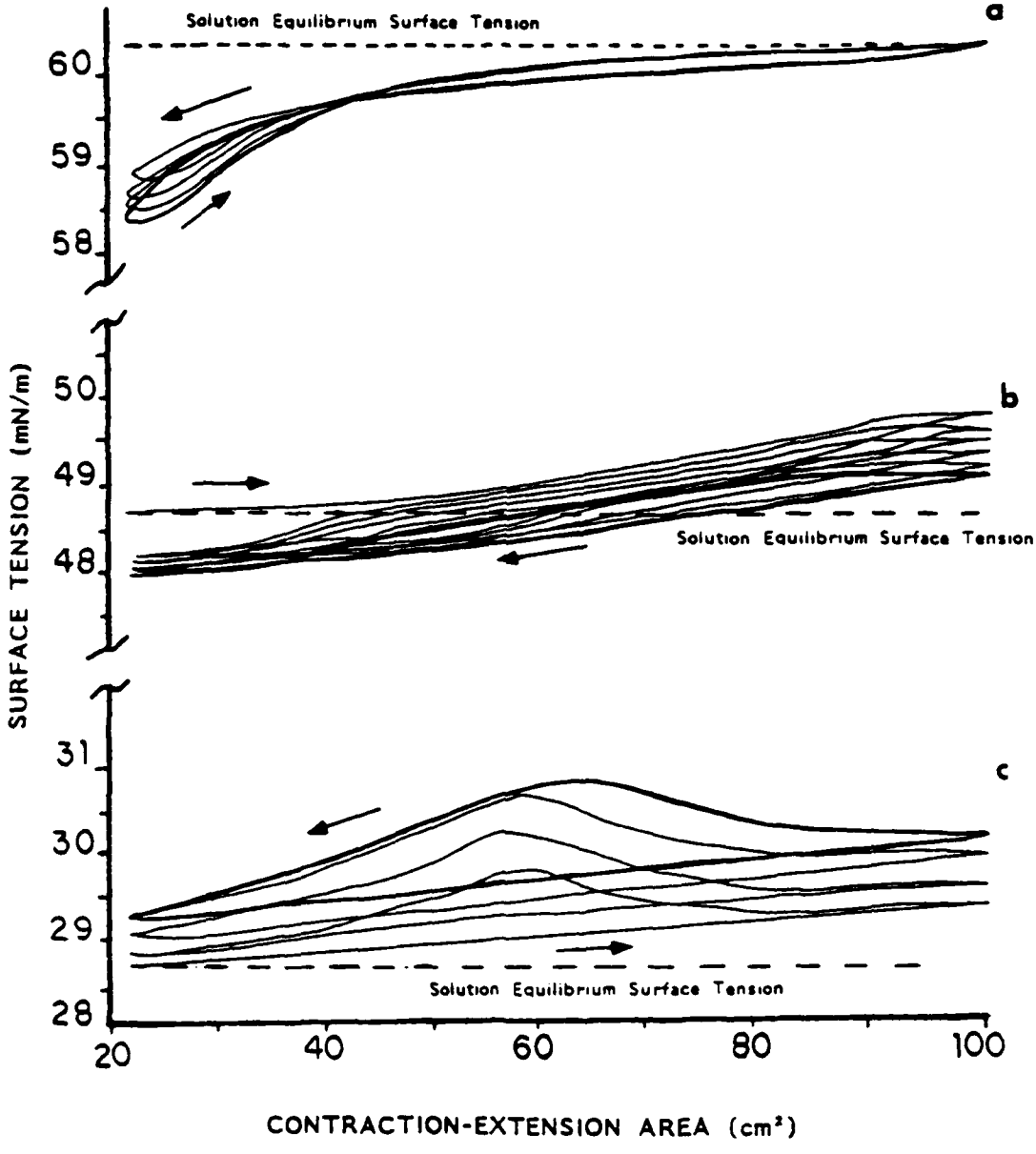

Figure 6. The Variation of Dynamic Surface Tension with Area of Solutions of 1-Butanol in Water, as the Hysteresis loops approach to Steady-State, at 25°C at the Following Conditions; (a) 0.055 M, and 0.10 cyc/min; (b) 0.20 M, and 1.02 cyc/min; (c) 0.819 M, and 1.02 cyc/min.

The variation of surface tension on changing the area of the surface was found for several other systems as well. Figures 7 and 8 show hysteresis loops progressing to a steady state for 1.6×10^{-5} M sodium dodecyl sulfate in water at 20°C and 3.5% (w/w) N-phenyl-1-naphthylamine (Lot A12A) in tmp-heptanoate at 60°C. Their similarity is obvious. Figures 7 and 8 refer to solutions that have an equilibrium surface tension near that of the solvent. The equilibrium surface tensions of mixtures of polydimethylsiloxane in tmp-heptanoate (Figures 9,10,11 and 12) are much lower than the surface tension of the solvent. The solutions tested were of polydimethylsiloxane (100 cSt) in tmp-heptanoate, at concentrations of 14.1, 6.34, 1.96 and 0.49 ppm in Figures 9,10,11 and 12 respectively. Figure 13 shows the hysteresis cycle of the solution of polydimethylsiloxane (100 cSt) of 0.49 ppm at 72.9°C. Only a slight change of the hysteresis loop from that of room temperature was observed.

4. Discussion

4.1 Dynamic Surface Tensions of Aqueous Solutions of 1-Butanol

The dynamic surface tensions of solutions have the surface tension of the solvent as their upper limit and the surface tension of a saturated surface as their lower limit. The variation of surface tension with the degree of surface coverage between these two limits is not linear: Its relationship is described by the equilibrium spreading pressure-vs-area isotherm, an example of which is shown in Figure 4. To find the point on this isotherm corresponding to a given bulk concentration, the surface concentration is matched with the bulk concentration, using Figure 5. The reciprocal of the surface concentration, that is, the area occupied by a molecule (see equation [4]) is plotted as the abscissa of Figure 4, so that the change of surface tension with area may be seen. Dilute solutions show little variation in surface tension over a wide range of changes of area changes (point R.) Concentrated solutions show large variations in surface tension with relatively small changes of area (point P.)

1-Butanol was selected as a model for this study because it is a small, nonionic molecule with relatively simple solution kinetics. The phenomena observed are broken up into three categories of solution type: dilute (Point R,) concentrated (Point P,) and intermediate (Point Q.)

A solution with a relatively low surface tension is probably near its lower limit; therefore, any dynamic change in the surface tension is more likely to be an increase, i.e., a dilatation of the adsorbed film. A solution with a relatively high surface tension is probably near its upper limit; therefore, any dynamic change in the surface tension is more likely to be a decrease, i.e., a compression of the adsorbed film. The dilute adsorbed film of a 0.055 M solution of 1-butanol in water, for example, has a relatively high equilibrium surface tension; and, sure enough, it can be compressed but not dilatated. Therefore the rate of desorption is much faster than the rate of adsorption, as predicted by the Langmuir adsorption

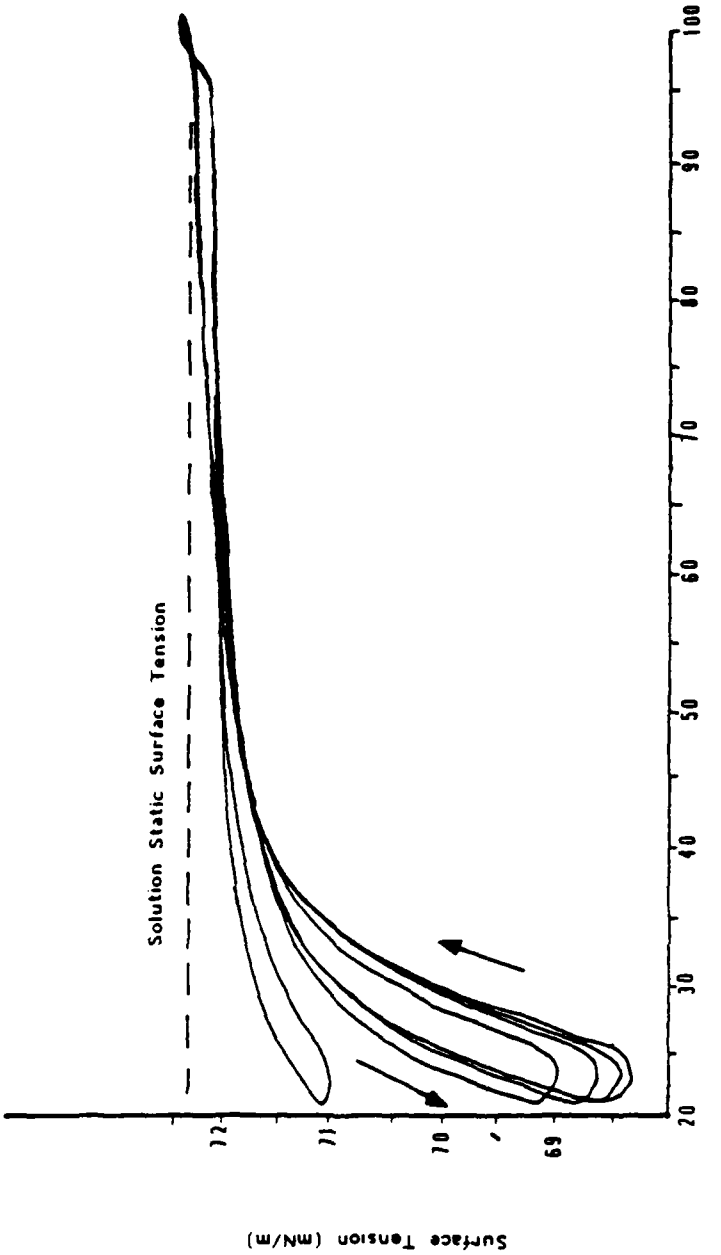

Figure 7. The Variation of Dynamic Surface Tension with Area for a 1.68×10^{-5} M Solution of Recrystallized Sodium Dodecyl Sulfate in Water at 21.0°C and a Cycling Frequency of 0.10 cpm.

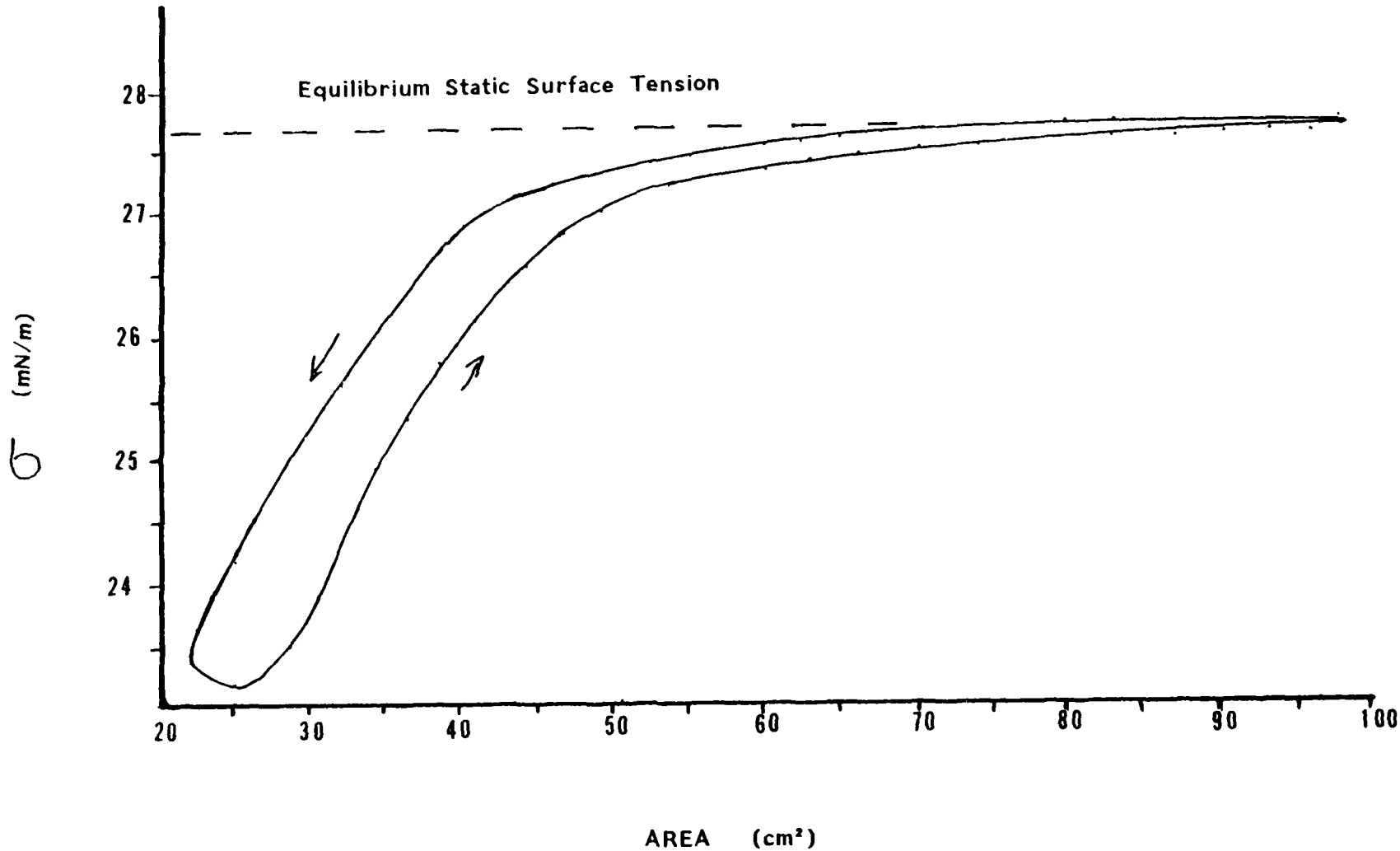

Figure 8. The Variation of Dynamic Surface Tension with Area for a 3.5%(w/w) Solution of N-Phenyl-1-naphthylamine in Tmp-heptanoate at 60.0°C and a Cycling Frequency of 0.20 cpm.

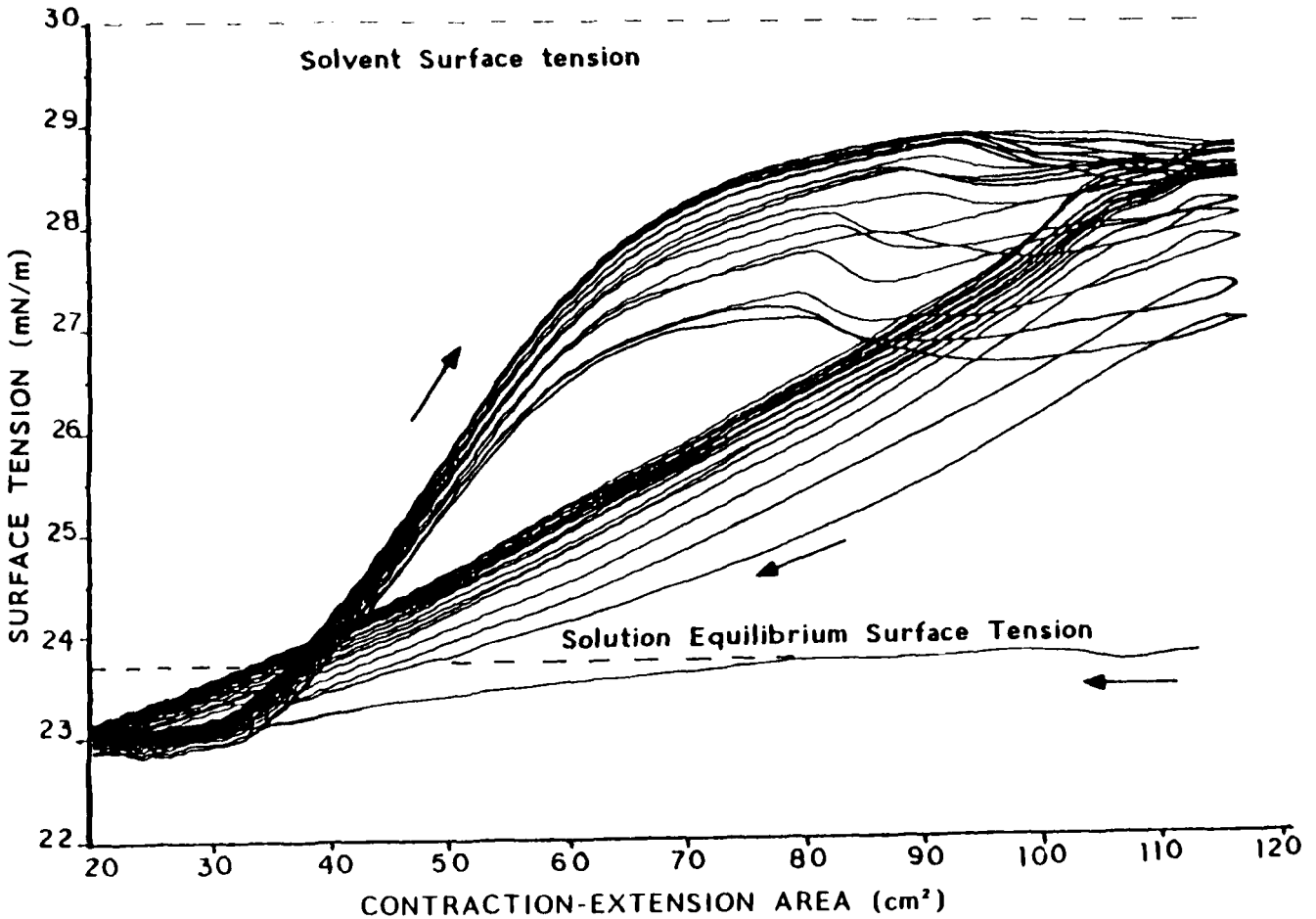

Figure 9. The Variation of Dynamic Surface Tension with Area for a 14 ppm Solution of Polydimethylsiloxane in Tmp-heptanoate at 21.0°C and a Cycling Frequency of 1.02 cpm.

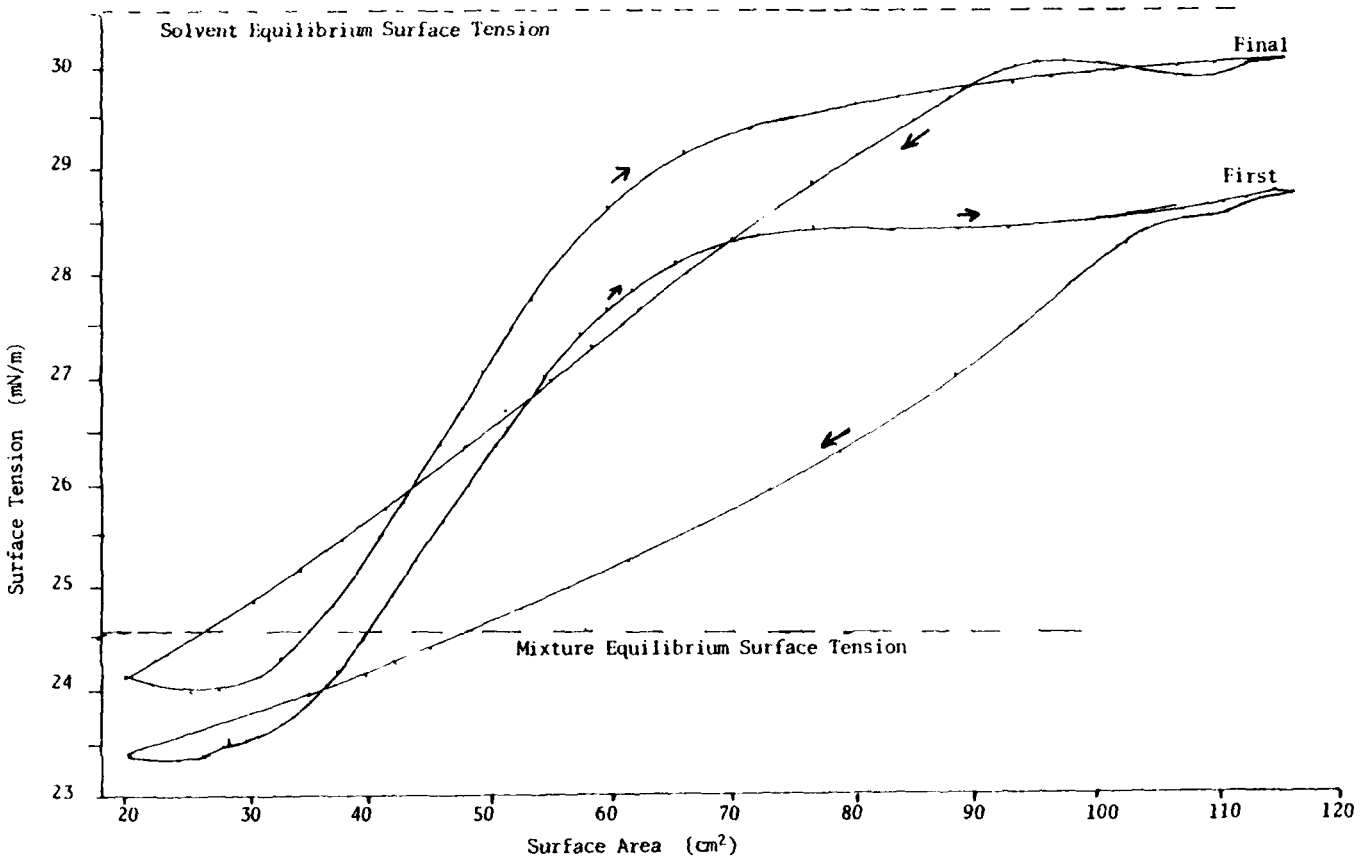

Figure 10. Surface Contraction-Extension Hysteresis of Surface Tension, showing the *First and the Final (Steady State) Hysteresis loops. Temperature* = 295 K. Solution of Polydimethylsiloxane 6.34 ppm in Tmp-Heptanoate.

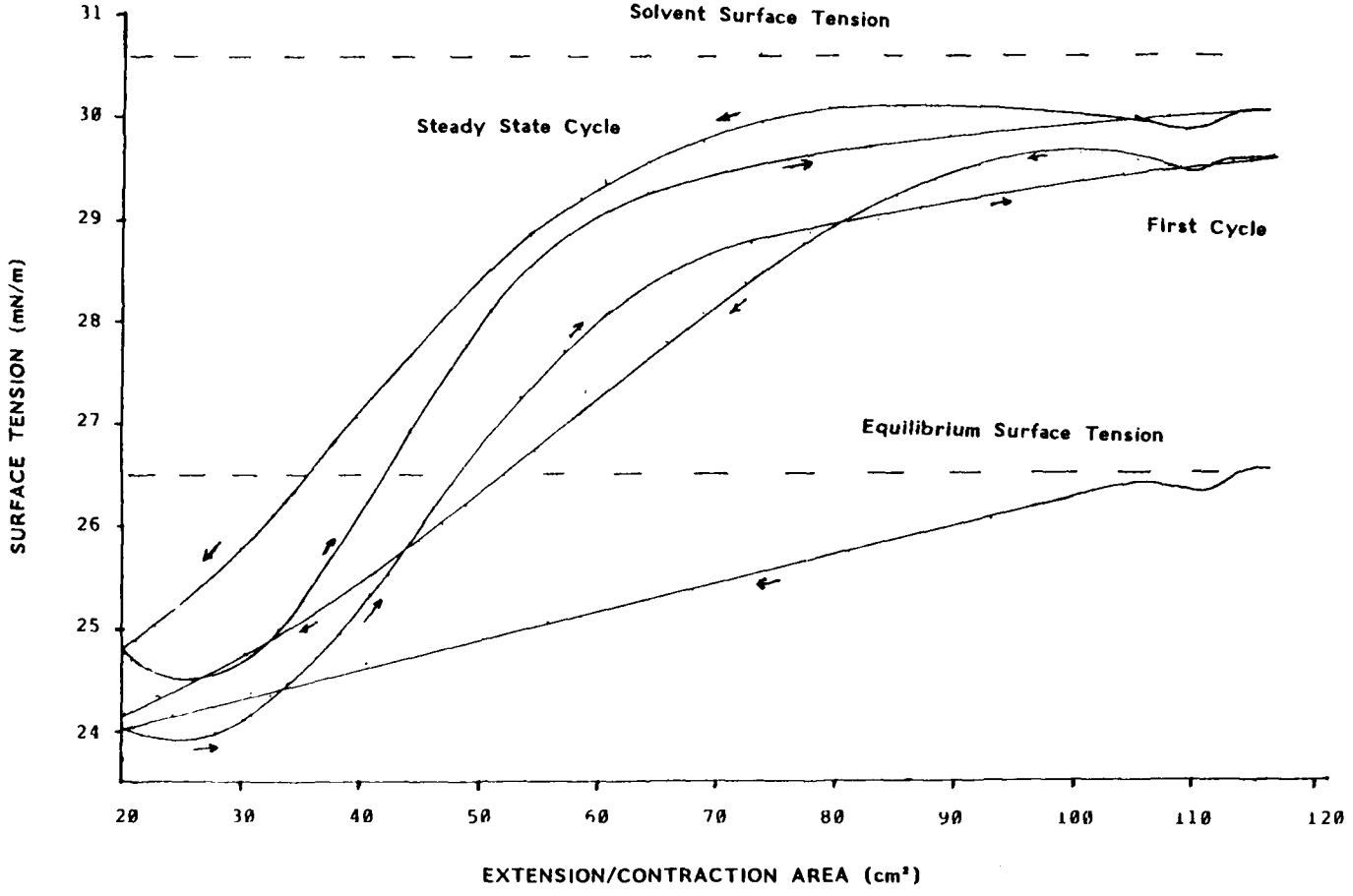

Figure 11. Surface Contraction-Extension Hysteresis of Surface Tension, showing the First and the Steady-State Cycles.
Temperature ≈ 22°C.
Solution of Polydimethylsiloxane (100 cSt), 1.96 ppm, in Tmp-Heptanoate.

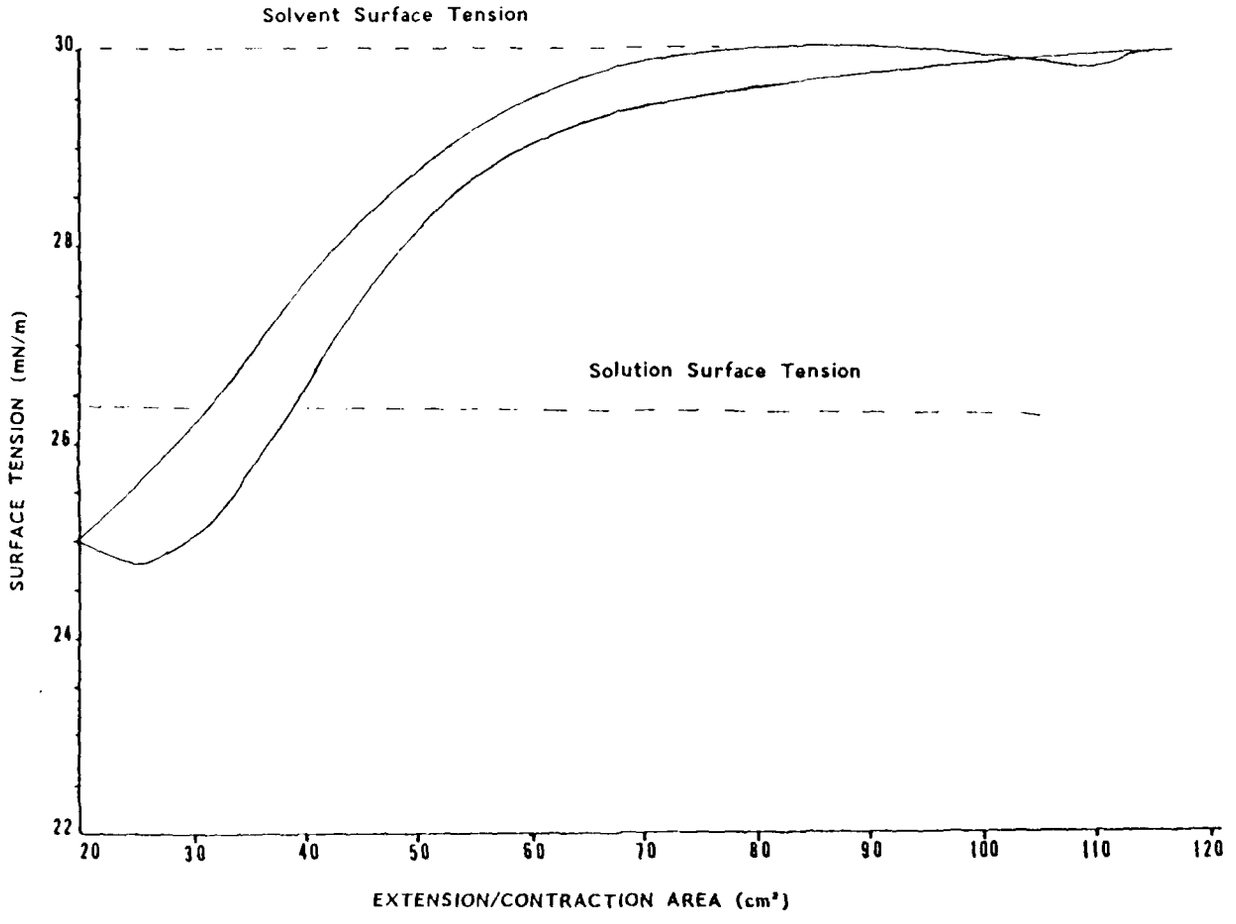

Figure 12. Surface Contraction-Extension Hysteresis of Surface Tension, showing the First Cycle.
Temperature = 22°C.
Solution of Polydimethylsiloxane (100 cSt), 0.49 ppm, in Tmp-Heptanoate.

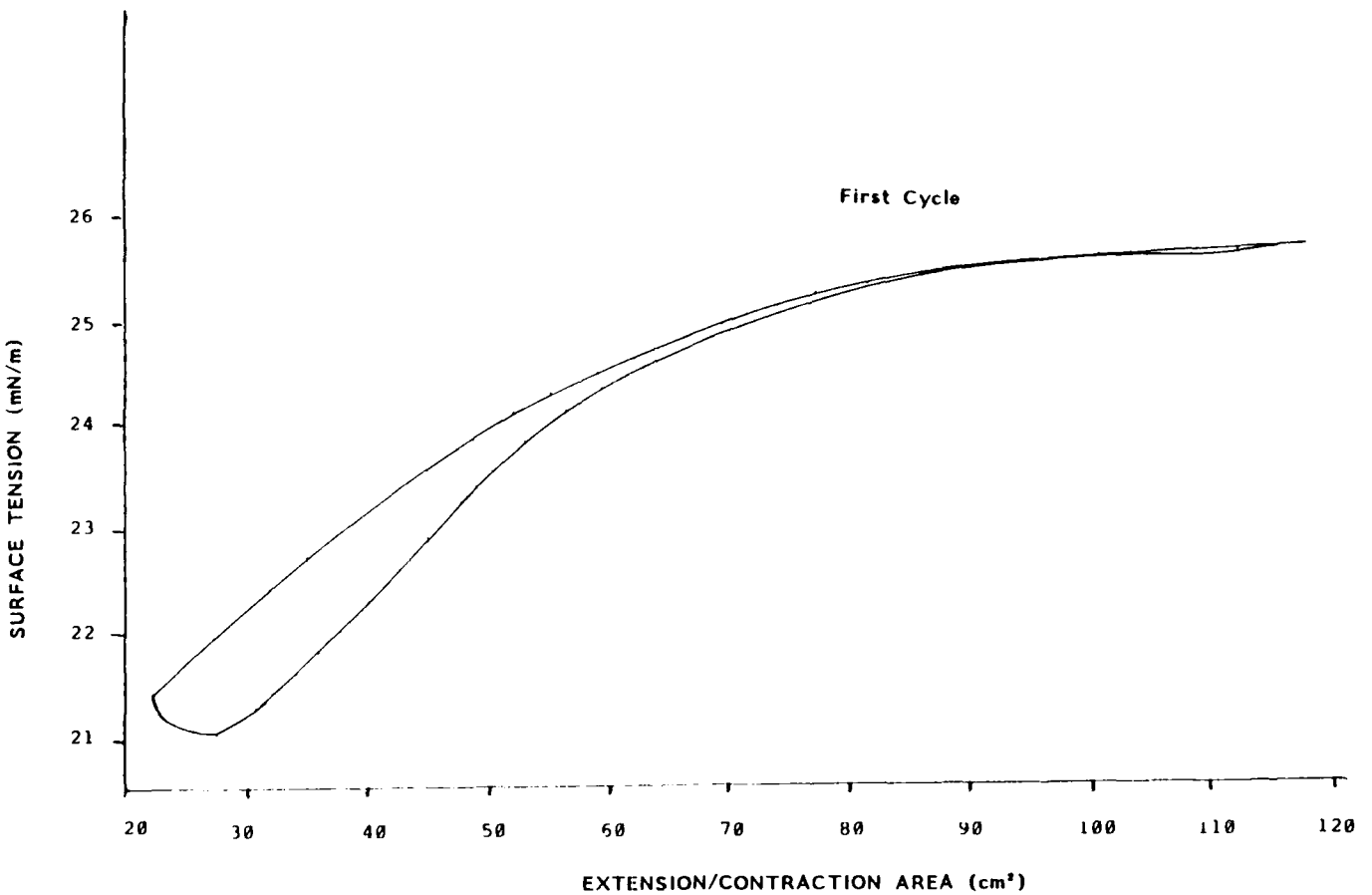

Figure 13. Surface Contraction-Extension Hysteresis of Surface Tension, showing the First Cycle.
Temperature = 72.9°C.
Solution of Polydimethylsiloxane (100 cSt), 0.49 ppm, in Tmp-Heptanoate.

equation. On repeated cycles of contraction and extension of area, the desorption during the contraction portion of the cycle is faster than the adsorption on extension. Therefore, solute is pumped out of the surface into the bulk phase until a steady state is reached at surface tensions larger than the equilibrium value. This description of behavior corresponds to what is observed in this dilute solution.

The concentrated adsorbed film of a 0.819 M solution of 1-butanol in water, has a relatively low equilibrium surface tension and it can be dilatated, but not compressed. Therefore, the rate of adsorption is much faster than the rate of desorption, as predicted by the Langmuir adsorption equation. On repeated cycles of contraction and extension of area, the adsorption during the expansion portion of the cycle is faster than the desorption on contraction; solute is pumped into the surface phase from the bulk phase until a steady state is reached at surface tensions less than the equilibrium value. This description of behavior corresponds to what is observed in this dilute solution.

The intermediate concentration of the adsorbed film of a solution of 0.20 M 1-butanol in water is compressed and dilatated at different parts of the cycle. Therefore, the rates of adsorption and desorption are comparable, as predicted by the Langmuir equation. On repeated cycles of surface contraction and extension of area, adsorption occurs during extension and desorption during contraction. The steady state is reached with the hysteresis loop cycling both above and below the equilibrium value of the surface tension. This description of behavior corresponds to what is observed in this intermediate concentration.

4.2 The Effect of Cycling Frequency

Rapid cycling of the area tends to prevent the transfer of solute between surface and bulk phases, by not providing enough time for sorption processes to occur. The contraction or extension of the surface then affects only whatever adsorbed molecules are on the surface, without adding or subtracting from their number by adsorption or desorption. If the concentration of solute in the surface is initially dilute, neither extension nor contraction of area changes the surface tension significantly: see the region R in Figure 4. The result is that rapid cycling of area of a dilute solution elicits no hysteresis loop. If the cycling frequency is now slowed sufficiently to permit adsorption, which in this dilute range of concentrations is more rapid than desorption, then solute molecules are added to the surface phase each time the area is extended; hysteresis loops appear on cycling; and after a few cycles of continuously diminishing progression a steady state is reached, in which the surface tension is maintained, on continued cycling, at values less than the equilibrium value. If the cycling frequency were slowed still further, the slow desorption process would come into play; the cycling would lag the establishment of equilibrium, and the hysteresis loop would again disappear. The machinery of our equipment is not geared sufficiently low to test this prediction, but it is an obvious result.

Let us now consider the effects of varying the cycling frequency when the concentration of the bulk solution is large enough to bring the surface concentration of solute to near saturation: point P in Figure 4. The rate of desorption at these concentrations is more rapid than the rate of adsorption. The adsorbed layer is too concentrated to be compressed further on contracting the area; therefore, on contraction, solute molecules are pushed out of the surface into the bulk phase (desorption.) On subsequent extension, the compressed adsorbate is dilatated, without adsorption from the bulk phase reducing the effect by adding molecules to the surface, if the cycling rate is sufficiently rapid. Iterated cycling at this frequency continues to remove solute molecules from the surface phase, although by progressively diminishing stages, until a steady state is reached in which the surface tension is maintained at values greater than the equilibrium value. Slower rates of cycling reduce the hysteresis loop by allowing the adsorption process to come into play. And again, rates of cycling sufficiently slow, and they now would have to be very slow indeed, would wait for equilibrium to be established and so finally eliminate any hysteresis.

4.3 Applications to other Systems

The knowledge gained by studying the 1-butanol+water system allows three deductions to be made from surface-tension hysteresis loops of other systems, if their position relative to the equilibrium surface tension is given:[7] the relative concentration of the surface, the direction of the pumping of the solute, and the relative rates of adsorption and desorption, can all be estimated by inspection of the tensiogram. A solution of 14 ppm polydimethylsiloxane in tmp-heptanoate (Figure 9) is similar in dynamic-surface-tension behavior to a concentrated solution of 1-butanol in water. The minimum in the surface tension hysteresis loops is barely below the equilibrium value, which means that the surface layer is concentrated. We infer that solute is pumped out of the surface with great efficiency, since the steady-state hysteresis loop has moved 75% of the way to the upper limit of surface tension; hence the rate of desorption is much greater than the rate of adsorption. The effect of reducing concentration is to increase the portion of the hysteresis that lies below equlibrium and to decrease the dilatational portion; paralleling the behavior of 1-butanol+water (see Figures 10,11 and 12.) The shape of the hysteresis loops and the persistence of these loops at low cycling rates makes the behavior of Polydimethylsiloxane in tmp-heptanoate remarkably similar to that of polypropylene glycol in water (see Appendix B.) Each polymer is comprised of ether linkages and methyl side groups causing them to be adsorbed lengthwise at the air-liquid interface, so the similarity of behavior is not surprising.

The systems N-phenyl-1-naphthylamine (Lot A12A) in tmp-heptanoate (Figure 8) and sodium dodecyl sulfate in water (Figure 7)

---

[7] This important datum is frequently missing in publications on the subject.

both resemble dilute solutions of 1-butanol in water. The hysteresis loops lie entirely below the equilibrium surface tension of each solution, which means that the surface layer is dilute. The steady-state hysteresis loop shows that solute is pumped into the surface from the bulk phase, so we infer that the rate of adsorption is much greater than the rate of desorption.

The similarity of the hysteresis loops of these solutions and of those of dilute solutions of 1-butanol is especially striking, indicating that the surface of a nonaqueous solution like N-phenyl-1-naphthylamine (Lot A12A) in tmp-heptanoate behaves as though it were a dilute aqueous solution of a weakly surface-active solute, or an extremely dilute solution of a detergent, such as sodium dodecyl sulfate in water. Thus, aqueous solutions of precisely known composition may be referred to as models of surface activity for nonaqueous systems, which in an applied context are often of unknown composition.

5. Summary

The rate of adsorption is greater than the rate of desorption for dilute solutions of 1-butanol in water, and therefore, solute is pumped from the bulk phase to the surface on cycles of extensions and contractions of surface area. The rate of desorption is greater than the rate of adsorption for concentrated solutions of 1-butanol in water and solute is pumped in the reverse direction, from the surface to the bulk phase. Intermediate concentrations show both types of behavior. These deductions are generally applicable to any surface-active system that generates a hysteresis loop on varying the area of the surface. The solutions of nonaqueous solutions of weakly surface active solutes are similar in behavior to dilute aqueous solutions of 1-butanol, and also to extremely dilute aqueous solutions of detergent.

6. Polydimethylsiloxane as an insoluble monolayer

The polydimethylsiloxane diagrams above show dilatational effects of surface tension, i.e., extension of the surface reduces the surface concentration of adsorbed solute, and the surface tension moves toward that of the solvent. Such an effect is typical of a solution whose equilibrium surface tension has been notably reduced by the adsorption of a powerful surface-active solute. With tmp-heptanoate as solvent, we have found no solute, other than the polydimethylsiloxanes, that lowers the equilibrium surface tension sufficiently for this dilatational effect to occur. But the observed effect may be interpreted in a different way. Polydimethylsiloxane may form an insoluble monolayer on the surface of the oil (tmp-heptanoate) as it does on water, rather than a soluble layer adsorbed from the solution. The observed lowering of the equilibrium surface tension may be due equally well to the presence of an insoluble layer or to the presence of a layer of solute adsorbed out of a solution. Surface tension data alone, whether equilibrium or dynamic, can be interpreted in either way. Perhaps other physical properties of the solution, such as its foaminess, can be used to choose between these alternatives.

The surface activity of silicone polymers in solution in a synthetic oil such as tmp-heptanoate may be better understood by a few parallel studies of an insoluble monolayer of polydimethylsiloxane on a water substrate. The equilibrium force-area diagram of polydimethylsiloxane (100 cSt) on distilled water is shown in Figure 14. The "steady-state" hysteresis loops, after continuous compression-expansion cycling of the same monolayer at 0.19 cycles/minute and 0.05 cycles/minute, are shown in Figures 15 and 16, respectively. The latter diagrams are similar in appearance to the results of dynamic surface tensions for solutions. An apparent lowering of equilibrium solution surface tension could also be caused by increasing the amount of the insoluble material at the surface, thereby increasing the surface concentration.

As a test of whether the adsorbed solute forms a soluble or an insoluble layer, an aliquot of 0.02 ml of a solution of 100 cSt polydimethylsiloxane (2.5×10^{-4} gm/ml) in pentane was placed on the surface of tmp-heptanoate, which had been demonstrated to be a "clean" substrate by its giving a flat trace on a surface-tension cycle. Figure 17 shows the hysteresis loops of the initial cycle and Figure 18 shows another initial cycle measured after 48 hours of standing. Taking this system as a true solution, its concentration is about 4 parts per billion. The large effect of such a small quantity of solute on the dynamic surface tension is exceptional, unless it can be interpreted as the effect of an insoluble monolayer. One such hypothesis is that the molecule of silicone uncoils its spiral structure when it is adsorbed at a surface, in response to the discontinuity of the force field; and that the rearrangement thus brought about is not reversible. Alternatively, the silicone is so surface active that it could take several days before it is desorbed and diffuses into the bulk, so it is effectively an insoluble layer as far as the dynamic surface tension measurements can show. Therefore, the system combines solution properties and properties of an insoluble monolayer. This combination of properties is shown in the foam behavior: the dissolved portion of the silicone is a pro-foamer, but no foaming occurs at concentrations less than 14 ppm, because the insoluble monolayer has no effect on the foaming propensity of the solvent up to that concentration; at higher concentrations the profoaming fraction predominates and foaming is observed. At still higher concentrations the insoluble polydimethylsiloxane causes bubbles to coalesce, although it is not an effective inhibitor of foam (see This Report, Part 2, Section III.)

7. Foam Stability and Dynamic Surface Tension

Figure 8 shows a typical first cycle of a contraction and expansion of the surface of a solution of N-phenyl-1-naphthylamine (Lot A12A) at a concentration of 3.50% (w/w) in tmp-heptanoate at 60°C. The diagram shows that the adsorbed film of solute is concentrated by compression during the cycle, as is evident from the reduction of the surface tension below its equilibrium value; but that the adsorbed film is not diluted on extending the surface, since no increase of surface tension above its equilibrium value

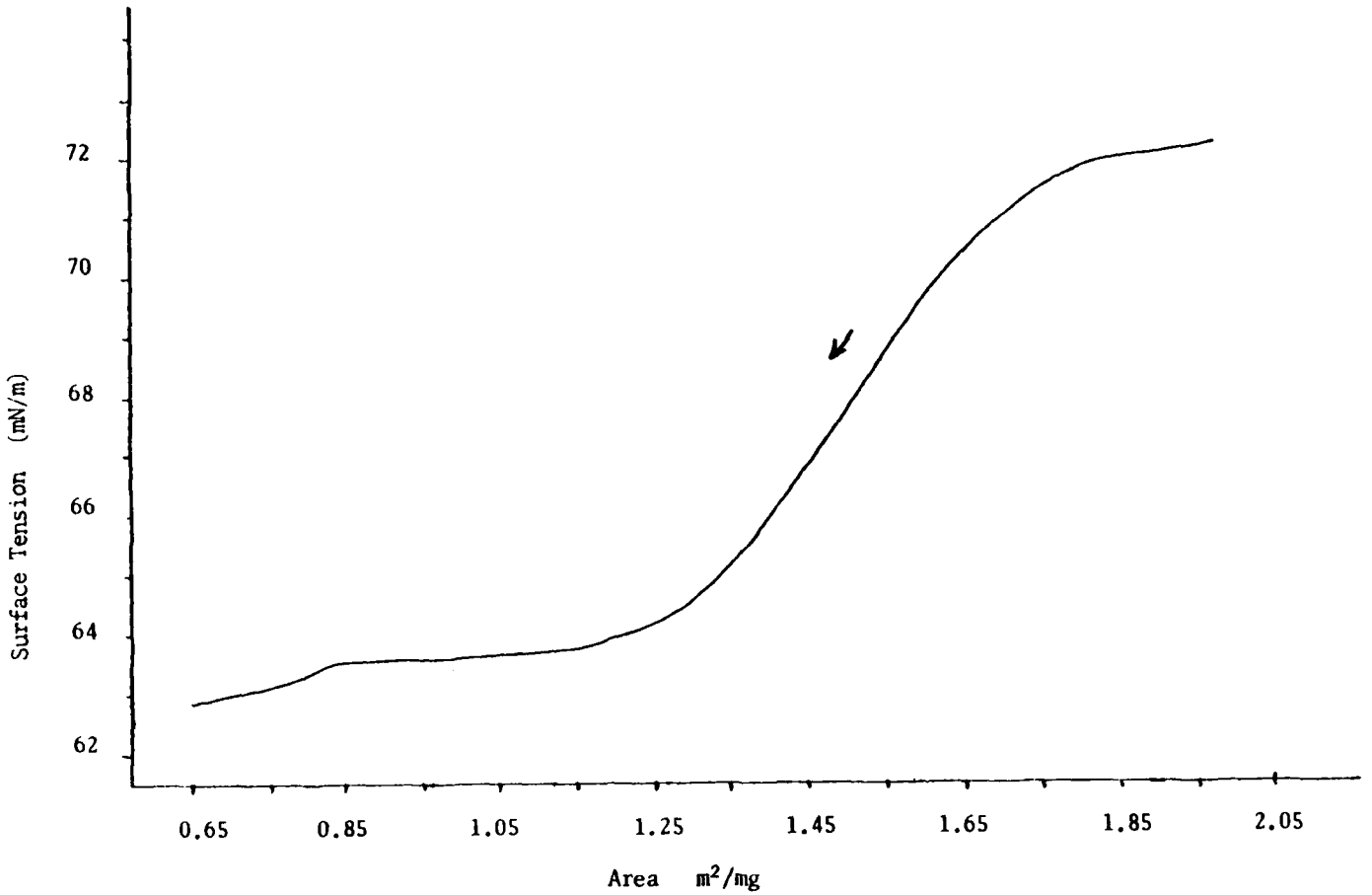

Figure 14. Equilibrium Surface Tension vs Total Area For a Monolayer of Polydimethylsiloxane (100 cSt) on *Distilled Water at 22°C, obtained at* 0.02 cpm.

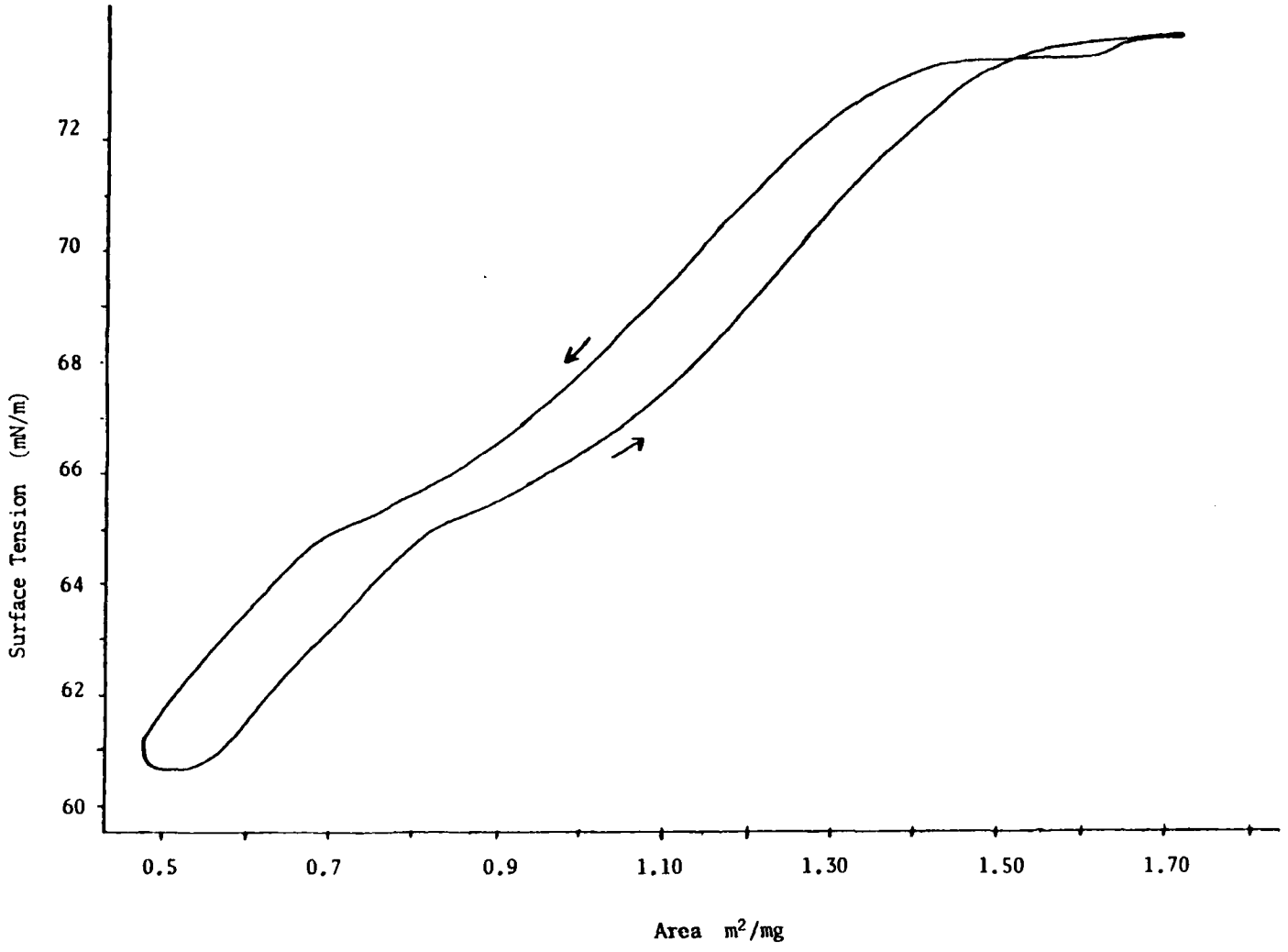

Figure 15. Variation of Compressional-Dilatational Surface Tension with Total Area of Surface for a Monolayer of Polydimethylsiloxane (100 cSt) at 22°C on Distilled Water. Cycling Frequency Of 0.19 cpm.

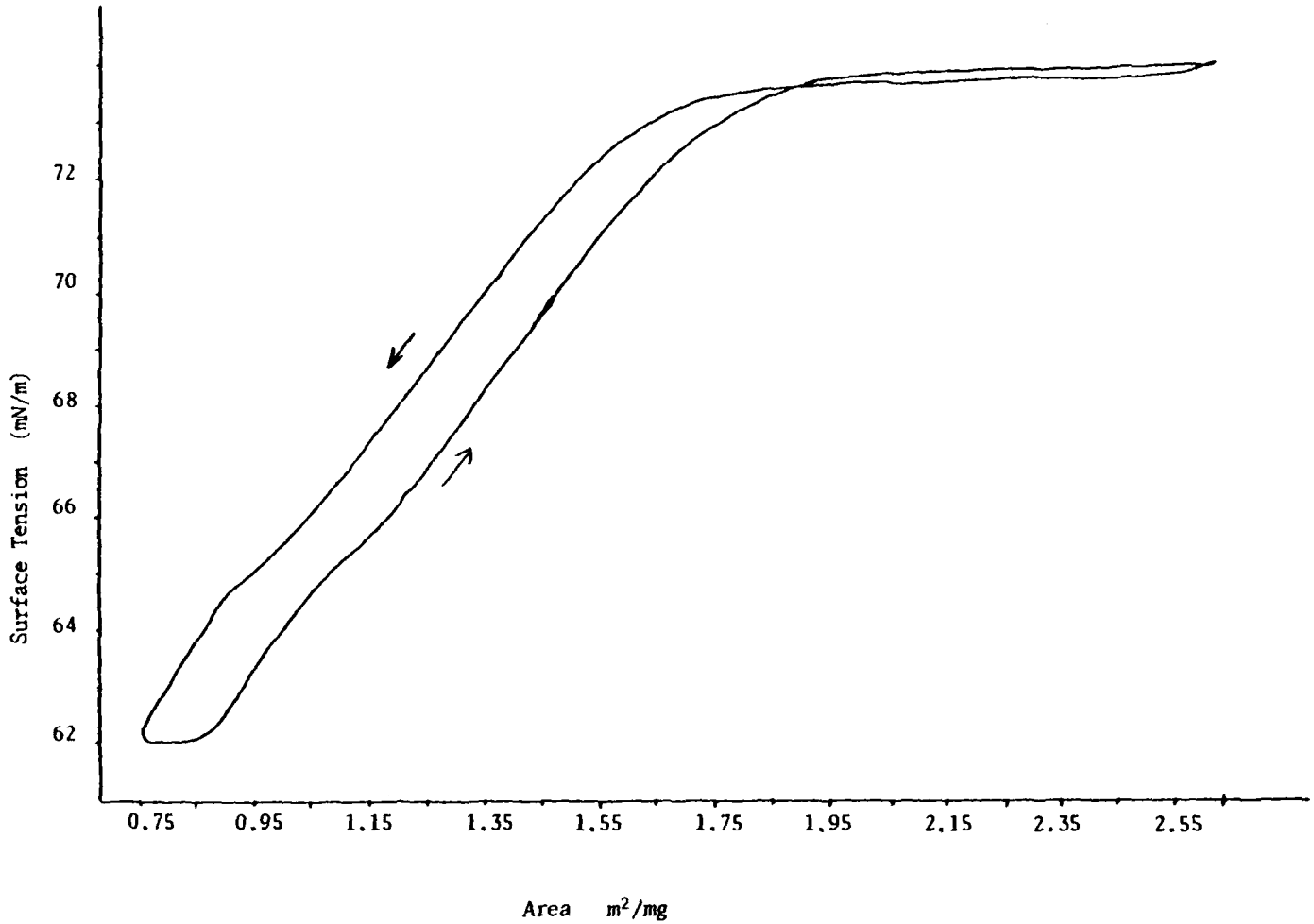

Figure 16. Variation of Compressional-Dilatational Surface Tension with Total Area of Surface for a Monolayer of Polydimethylsiloxane (100 cSt) at 22°C on Distilled Water. Cycling Frequency Of 0.05 cpm.

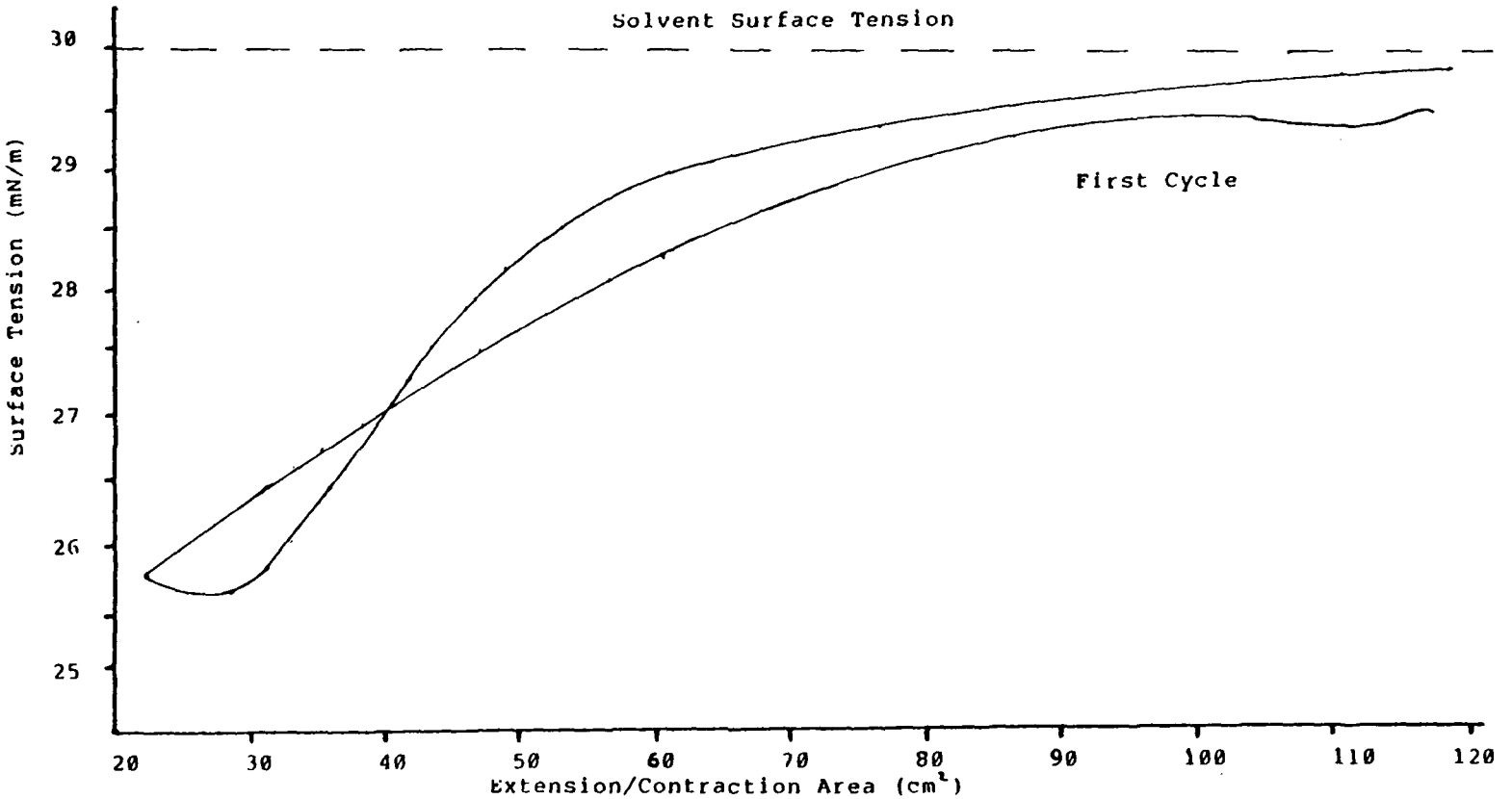

Figure 17. Surface Contraction-Extension Hysteresis of Surface Tension, showing the Initial Cycle (No Aging Time).
Temperature = 22°C.
Solution of Polydimethylsiloxane (100 cSt), 4 ppb, in Tmp-Heptanoate.

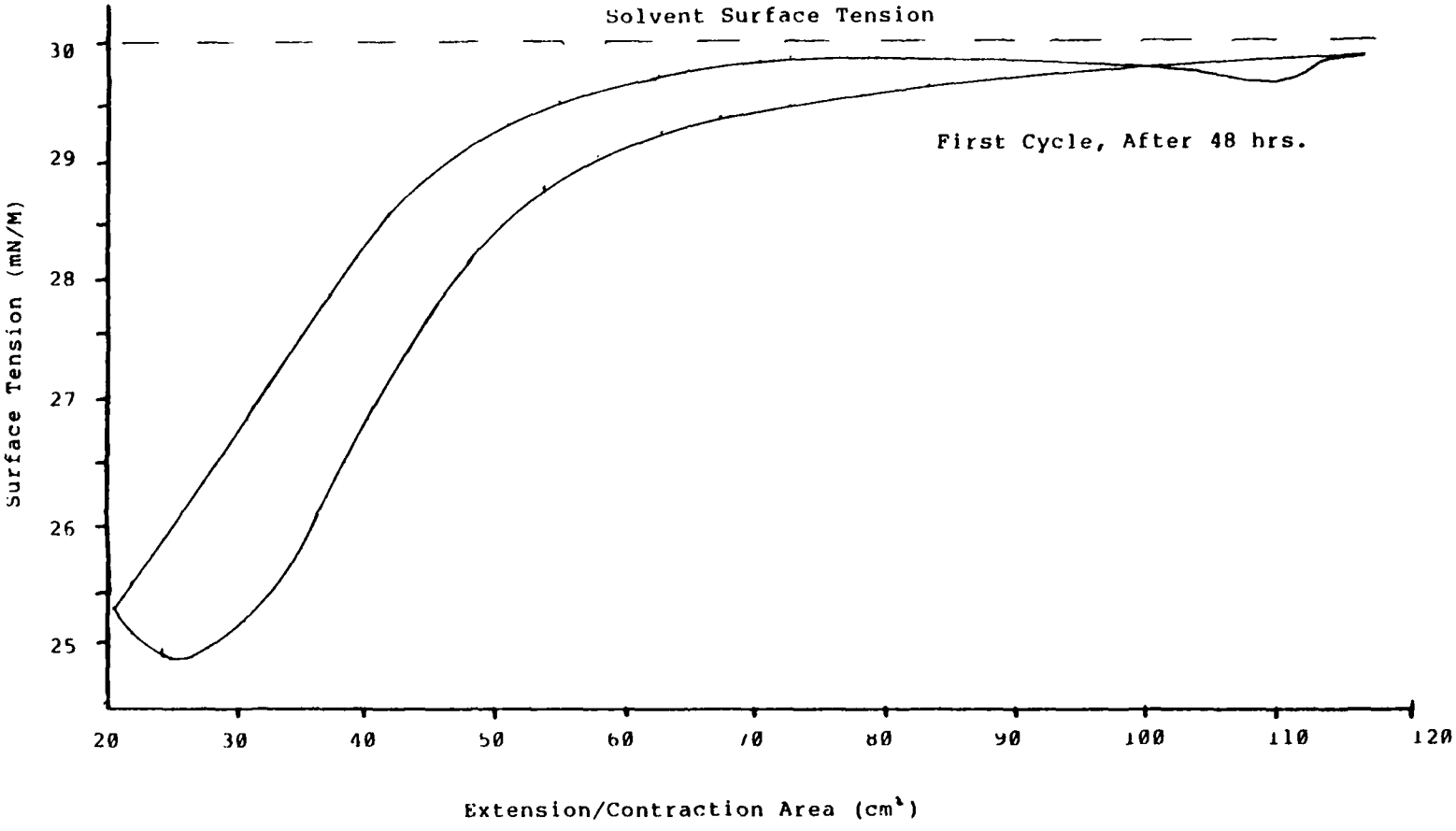

Figure 18. Surface Contraction-Extension Hysteresis of Surface Tension, showing the Initial Cycle after 48 Hours Aging.
Temperature = 22°C.
Solution of Polydimethylsiloxane (100 cSt), 4 ppb, in Tmp-Heptanoate.

occurs at any part of the cycle. The inference drawn from this observation is that the rate of adsorption of the solute is much faster than its rate of desorption.

Direct comparisons between the measurements of foam stability and the range of dynamic surface tensions give qualitative agreements. Figure 19 reports the results of the difference in dynamic surface tension from the top to the bottom of the hysteresis loop ($\Delta\sigma$ in mN/m)) as a function of temperature, for solutions of N-phenyl-1-naphthylamine (Lot A12A) at concentrations of 3.50%, 3.92%, and 4.34% w/w in tmp-heptanoate. Figure 20 reports measurements of foam stability, Σ in seconds, measured by the Bikerman method with a cylinder of diameter 46.2 mm, of solutions in tmp-heptanoate of the same solute, N-phenyl-1-naphthylamine (Lot A12A,) at concentrations of 5.0%, 4.0% w/w, and 3.0% w/w and also a mixture of solutes – namely N-phenyl-1-naphtnylamine (Lot A12A) and tricresyl phosphate – at a concentration of 3.0% w/w of the former and 2.0% w/w of the latter. The increase in $\Delta\sigma$ with temperature up to 40°C is paralleled by an increase in foam stability in each solution; but the subsequent decline in the foam stability at temperatures above 40°C is not reflected exactly in the values of $\Delta\sigma$, which do begin to decline, however, at temperatures above 60°C. A closer agreement is hardly to be expected, as the range of compression of the adsorbed film in the bubbles of a foam is unknown, while the range of compression of the adsorbed film in the cycling device is quite arbitrary. Enough parallelism occurs, however, to suggest that the measured $\Delta\sigma$ is related to the stability of foam, although other variables such as viscosity and bubble size also affect foam stability.

8. Foam Stability and Surface Tensions of Other Systems

Emolein 2917 and a solution of polypropylene glycol (4000 molecular weight) at 5% (w/w) concentration in Emolein 2917 were tested at various temperatures for hysteresis surface-tension loops on expansion and contraction. Both liquids give no sign of a hysteresis loop at any temperature up to 55°C., although the solution has been found to foam at 35°C. and above. Although the dynamic surface tensions of this solution thus gave no sign of activity in our device, the static surface tension was found to be reduced by the presence of the solute, and increasingly so with temperature, as shown in Figure 21.

9. Effect of Varying Lots of N-Phenyl-1-naphthylamine on the Dynamic Surface Tension

Inconsistencies in the results of measuring the dynamic surface tension of the additive N-phenyl-1-naphthylamine from lot to lot indicates the presence of some surface-active impurity that is either working synergistically with the amine or is surface-active alone. Early lots of the additive (1982 production A12A,) at a concentration of 4% (w/w) in tmp-heptanoate (Base Stock 704) showed no hysteresis loops of dynamic surface tension at room temperature, but hysteresis loops form at 35°C, which become more pronounced on

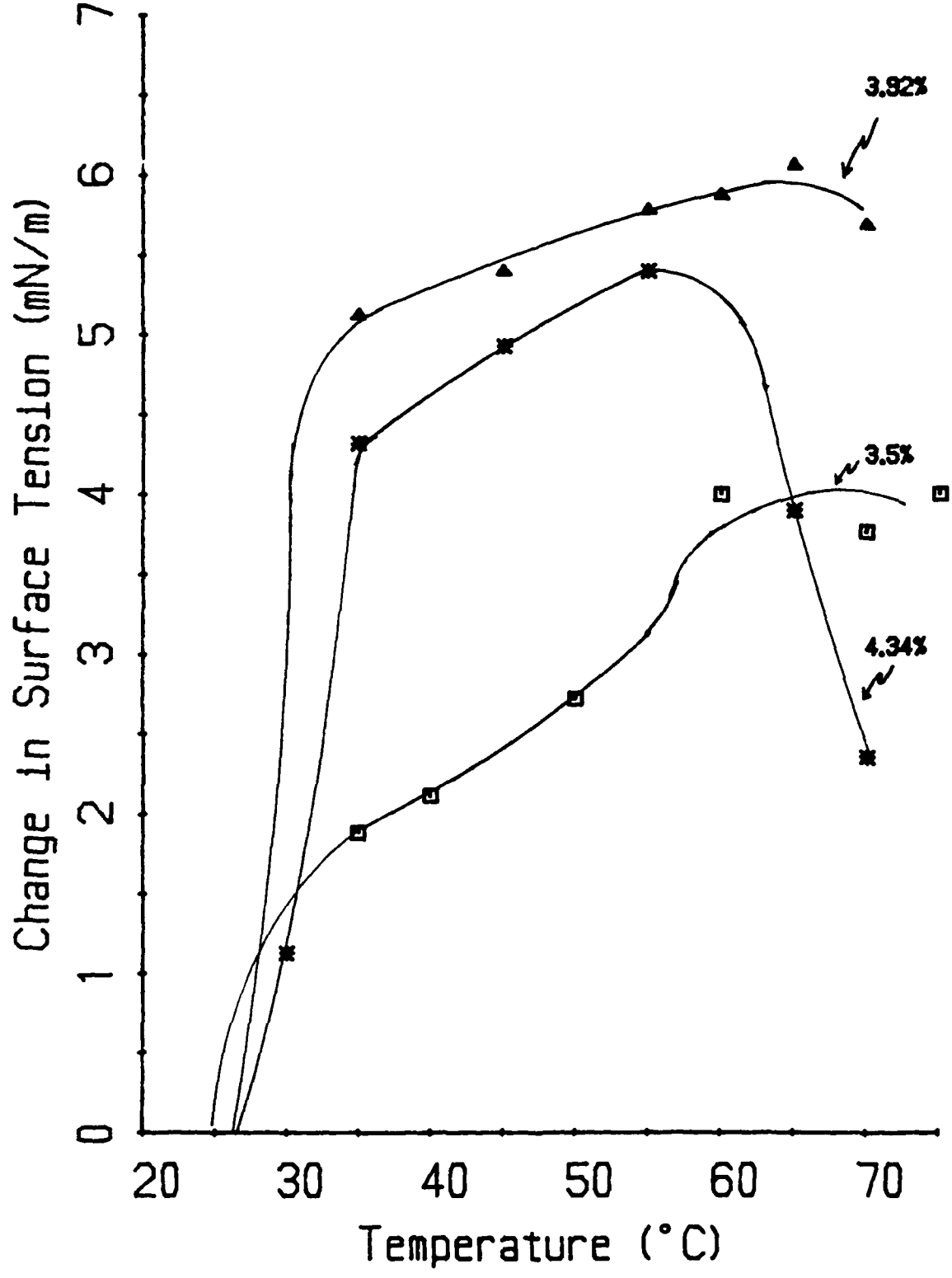

Figure 19. The Difference in Dynamic Surface Tension from the Top to the Bottom of the Hysteresis Loop as a Function of Temperature, for Solutions of N-Phenyl-1-naphthylamine at Concentrations of 3.50%, 3.92%, and 4.34% w/w in Tmp-heptanoate.

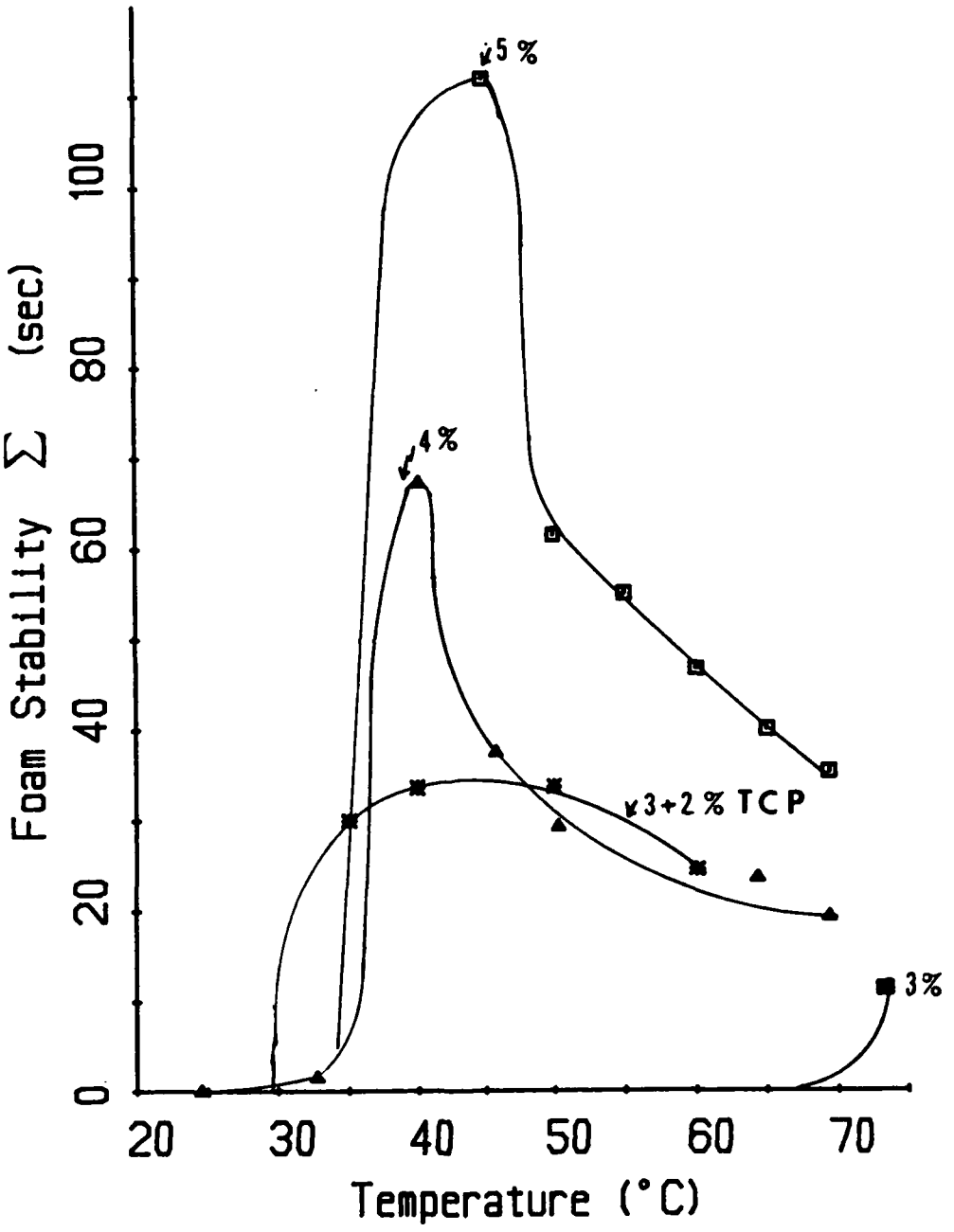

Figure 20. The Variation of Foam Stability with Temperature for Solutions in Tmp-heptanoate of 5.0% w/w, 4.0% w/w, and 3.0% w/w N-Phenyl-1-naphthylamine, as well as a mixture of solutes, 3% w/w N-Phenyl-1-naphthylamine and 2% w/w Tricresyl Phosphate, in the same Solvent.

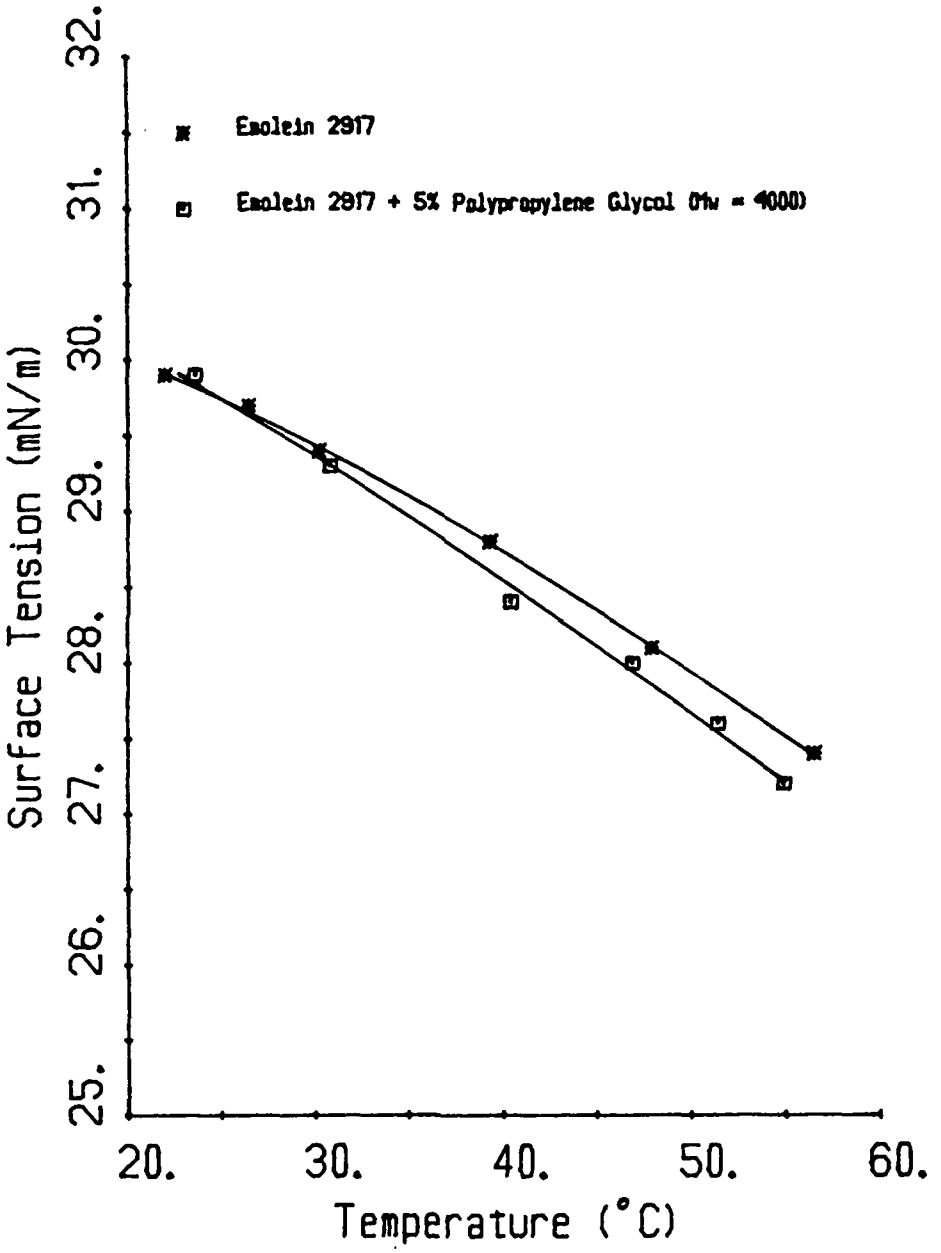

Figure 21. Variation of the Static Surface Tension with Temperature of Emolein 2917 and a Solution of 5% (w/w) Polypropylene glycol (Mw=4000) in Emolein 2917.

raising the temperature still further (see Figure 19.) These results are consistent with the foaminess of the solution, which also increases with temperature (see Figure 20.) The latest batch of the additive (1983 production A13B) gives no indication of surface activity either with dynamic surface tension, foam stability, or bubble rise.

SECTION V

DAMPING OF CAPILLARY RIPPLES

1. Introduction

Marangoni effects are probably responsible for the stability of the foams obtained in our oil systems, but the dilatation-compression cycling of an adsorbed film, as practiced with the dynamic-surface-tension apparatus, is often of too low frequency to detect changes of surface tension that die out rapidly. Another manifestation of a Marangoni effect is the enhanced damping of capillary ripples by an insoluble or a soluble surface film on a liquid. The surface contracts at the crest and expands at the trough of a wave (see Figure 22;) if a surface-active solute is adsorbed, the surface tension then decreases at the crest and increases at the trough; the Marangoni effect that ensues promotes the energy dissipation of the wave by subsurface viscous flow; and consequently leads to a more rapid damping with time or a more pronounced damping over distance than in the surface of the pure solvent lacking the adsorbed film.

Our objective in pursuing this topic is to obtain information about surface properties of oils and oil solutions from the characteristics of capillary ripples. The dynamic properties of a liquid surface determine wave behavior, and to a large extent the production and stability of foam depends on the same dynamic surface properties that govern the propagation of surface ripples. An important factor affecting the properties of surface ripples is the presence of a surface-active solute in the liquid, which creates a layer of adsorbed solute at the surface. This layer of adsorbate has elastic properties, the result of local gradients of surface tension, which resist the periodic surface expansions and contractions accompanying ripple motion. As a result, the damping of surface ripples is more pronounced in such solutions than at the surface of a pure liquid or of a solution in which no surface activity is present, and which consequently lacks surface elasticity. Many experiments have been performed using ripple frequencies larger than 100 Hz,[8,9,10] but few have been performed in the frequency range between 1 Hz and 50 Hz.[11] It is in this range that Lucassen predicts the most pronounced increase in ripple damping, and consequently the most sensitive indication of surface elasticity. The present method is designed, therefore, to investigate this range of frequencies.

---

[8] J.A. Mann and R.S. Hansen, J. Colloid Sci., 18, 757, (1963).

[9] W.D. Garrett and W.A. Zisman, J. Phys. Chem., 74, 1796, (1970).

[10] J. Lucassen and R.S. Hansen, J. Colloid Interface Sci., 22, 32, (1966).

[11] R. Cini and P.P. Lombardini, J. Colloid Interface Sci., 81, 125, (1981).

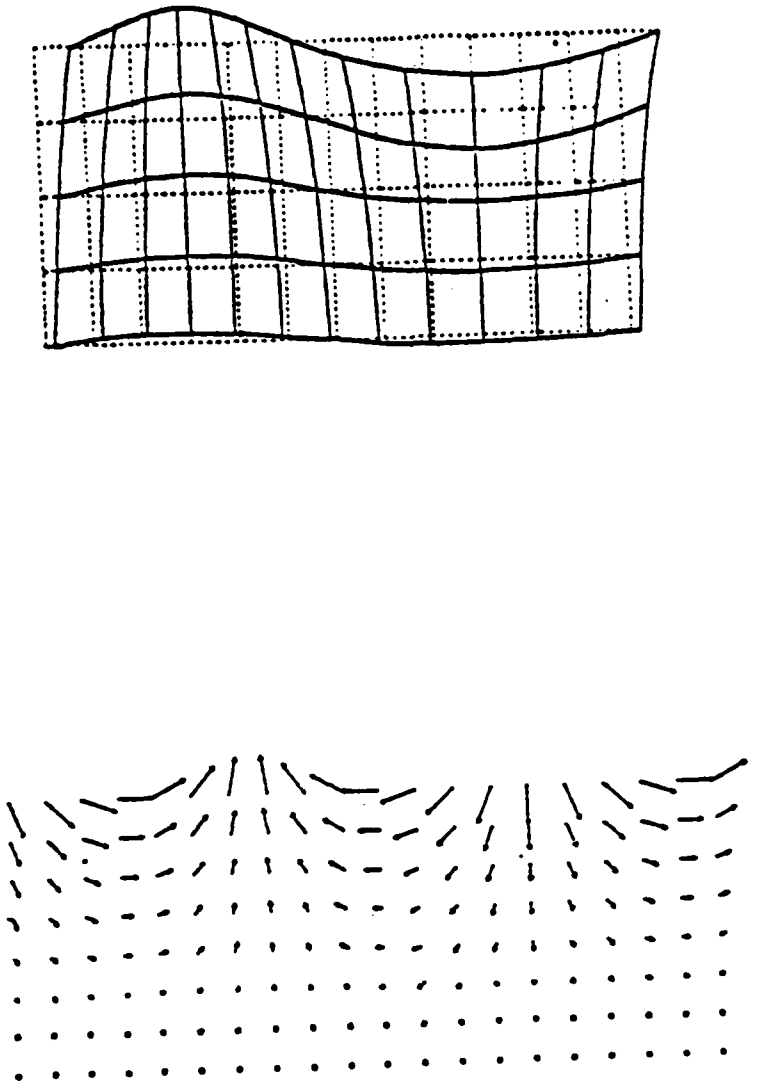

Figure 22. Wave Motion showing Contraction of the Liquid Surface at the Wave Crests and Expansion in the Wave Troughs.

2. Description of Apparatus

Figure 23 is an illustration of the apparatus. This design includes both generation and detection of capillary ripples. The detection system relies on an optical method that does not perturb the fluid surface. The ripples are generated by an electro-mechanical device (a modified Peerless KP 100 WF audio loudspeaker) which is driven by a high-fidelity audio amplifier. The signal source is the SID (Sound Interface Device) integrated circuit within the Commodore 64, and the actual signal is varied to suit the particular experimental conditions (see Types of Experiments below.) The electro-mechanical device drives a plexiglass prism in the surface of the fluid under test, creating a ripple on the surface of the liquid contained in an aluminum channel of rectangular cross section.

The ripple is detected in a manner similar to that described by Thiessen and Sheludko.[12] This method does not perturb the surface; rather, the reflection of a narrow beam of light (a low power He-Ne laser in this case) at the surface of the ripple is deflected by an angular amount equal to twice the slope of the surface. The beam is projected onto a continuous photodiode (Silicon Detector Corporation SD 1166-21-11-391) producing an analog voltage proportional to the slope of the ripple surface. This voltage is pre-conditioned by:

a. A differential amplifier which acts to remove common-mode signals originating from stray electric fields;
b. An eighth-order Chebyshev low-pass filter with a cut-off frequency of 50.0 Hz and 0.5-dB pass-band ripple which precludes signal aliasing and interference from the fluorescent room lighting; and
c. A switchable second-order Butterworth high-pass filter to eliminate low-frequency baseline drifts that originate in the translation of the optical detector.

After pre-conditioning, the signal is converted to an eight-bit digital number by means of a free-running analog-to-digital converter (based on the National Semiconductor Corporation ADC0809,) which performs about 20,000 conversions per second. The combined circuitry is housed as a single unit interfacing directly to the IEEE interface port located on the back panel of the Commodore 64 microcomputer.

The only other electronics necessary to the experiment are housed in a separate unit. This unit synchronizes data sampling and may be operated in one of two modes. In the internal mode, a 100.00-Hz quartz-crystal-based oscillator triggers a one shot (monostable multivibrator) producing 30 μs pulses at the oscillator frequency. In the external mode, an external signal (derived from the ripple-driving signal) triggers the one shot to produce pulses of 30 μs duration at the frequency of the capillary ripple. In this second mode, sampling takes place at equivalent time points allowing 'frozen motion' sampling. The pulses produced are interfaced

---

[12] D. Thiessen and A. Sheludko, Kolloid-Z., 218, 139, (1967).

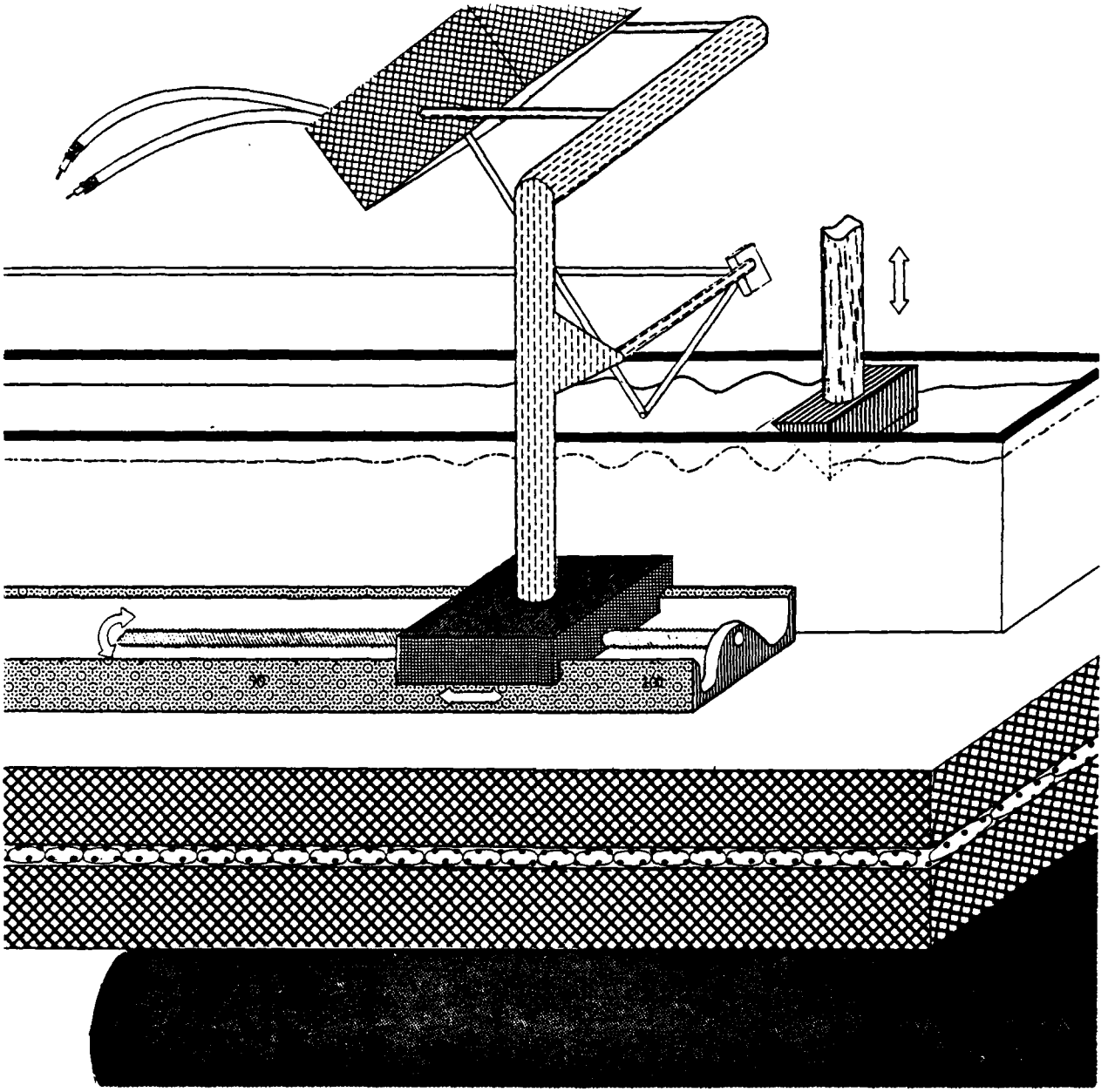

Figure 23. The Experimental Apparatus. A Wheeled Carriage is now used to translate the Optical Detector.

through one of the joystick ports available on the Commodore 64, and software control is accomplished with high-speed machine language (6502 microprocessor) routines. Such software control allows quick and easy changes from one type of experiment to another.

The optical detector is mounted on a wheeled carriage that can move along a flat-ground steel bed by means of a synchronous screw drive. This arrangement permits the detector to be placed anywhere within a 30-cm distance along the channel or, alternatively, to translate along the channel throughout the course of an experiment.

Because of the sensitivity of the optical method, stray vibrations reaching the surface can interfere with the measurement. To reduce noise, the experiment is performed on a shock-resistant table. The resonant frequency of this table is about 3 Hz, thus allowing noise-free measurements down to the frequency at which the residual noise originating in building vibrations degrades the signal. This limits the low frequency measurement of ripple amplitude at about 3 Hz.

The upper frequency limit is set by two factors. One factor is the relative dimensions of laser beam diameter and wavelength. As the wavelength decreases with increasing frequency, the beam begins to be focused by the curvature of the ripple. This destroys the simple geometric relationship that exists when the wavelength is large compared to the beam diameter. With the present system, focusing limits the upper frequency at about 200 Hz.

The second factor that limits the high-frequency response of the equipment is the solution damping. At high frequencies, ripples damp in too short a distance to retain a measurable amplitude at the point of detection. For the oil systems that we studied, the high frequency limit is approximately 40 Hz.

To summarize, the light beam is reflected from a point on the undulating oil surface, and is projected onto a continuous photodiode suitably screened to cut off stray light. The photodetector output is amplified and converted to a digital signal that is read by a Commodore 64 microcomputer. The computer then stores the data in a sequential file on magnetic floppy disks. Data acquisition may proceed in any one of several ways.

3. Types of Experiments

3.1 Moving Optics

Data acquisition is synchronized with the ripple generator. The slope of the ripple surface is digitized at equivalent time points as the optical detector is translated away from the wave source at a speed of 1.323 cm/min. The resulting sequence of digital numbers represents the slopes of the ripple as a function of its distance from the generating source.

The raw data appear in Figure 24, where ripples at three frequencies (3, 9, and 12 Hz) are presented. The data in Figure 24a show the degradation of precision as the ripple frequency approaches the resonant frequency of the shock-resistant table. Figures 24b and 24c show the presence of random noise in the signal. In all cases, a fixed number of data points (4096) is accumulated at a sampling frequency equal to the frequency of the ripple generator. Since the rate at which the optical detector translates is constant, the distance that is scanned by the detector decreases as the ripple frequency increases. The total distance scanned is reported in each part of Figure 24 to display this feature of the instrument, which allows a highly precise wavelength determination to be made over a large range of wavelengths.

Because the information sought, namely, the wavelength and the damping coefficient, are slowly varying with respect to the sampling interval, a digital low-pass filter is ideal to attenuate random noise from the raw data. Such a filter was used to obtain the results shown in Figure 25. These three waveforms correspond to those shown in Figure 24; the resultant sequences can each be analyzed to determine wavelength and damping coefficients with a precision of 0.4%. Each sequence contains several determinations of wavelength, from which the average wavelength may be obtained. Figure 26 allows an estimation of the uncertainty by showing the variation of individually measured wavelengths with the wave number. The scatter in the wavelength determination increases with increasing frequency as seen by comparing Figure 26a with 26c. This trend reinforces the inference that an upper practicable limit exists, and that the highest measurable frequency is of the order of 40 Hz.

The results of wavelength determination with a sample of tmp-heptanoate lubricant are shown in Figure 27. The experimental points were determined by the moving optics method. The solid line is described by the Kelvin approximation, including the depth correction, Equation [14] below, for a Newtonian fluid devoid of surface-tension gradients and with the same bulk characteristics as the ester (see Theory of Capillary-Wave Damping below.) The agreement between observation and theory appears to be excellent; nevertheless, the Kelvin equation contains the wavelength to a high order, thus introducing an amplification of the experimental error at low frequencies in the calculation of surface tension from wavelength. This error is eliminated by using the more exact relation given by Lucassen-Reynders and Lucassen (see Theory of Capillary-Wave Damping below.)

The damping coefficients obtained from these data are reported in Figure 28. Capillary damping is not enough by itself to account for the observed energy loss. A correction for the effects of the walls and floor in a channel of rectangular cross section is given

---

[13] L.D. Landau and E.M. Lifshitz, "Fluid Mechanics," Pergamon Press, London, 1959, p.100

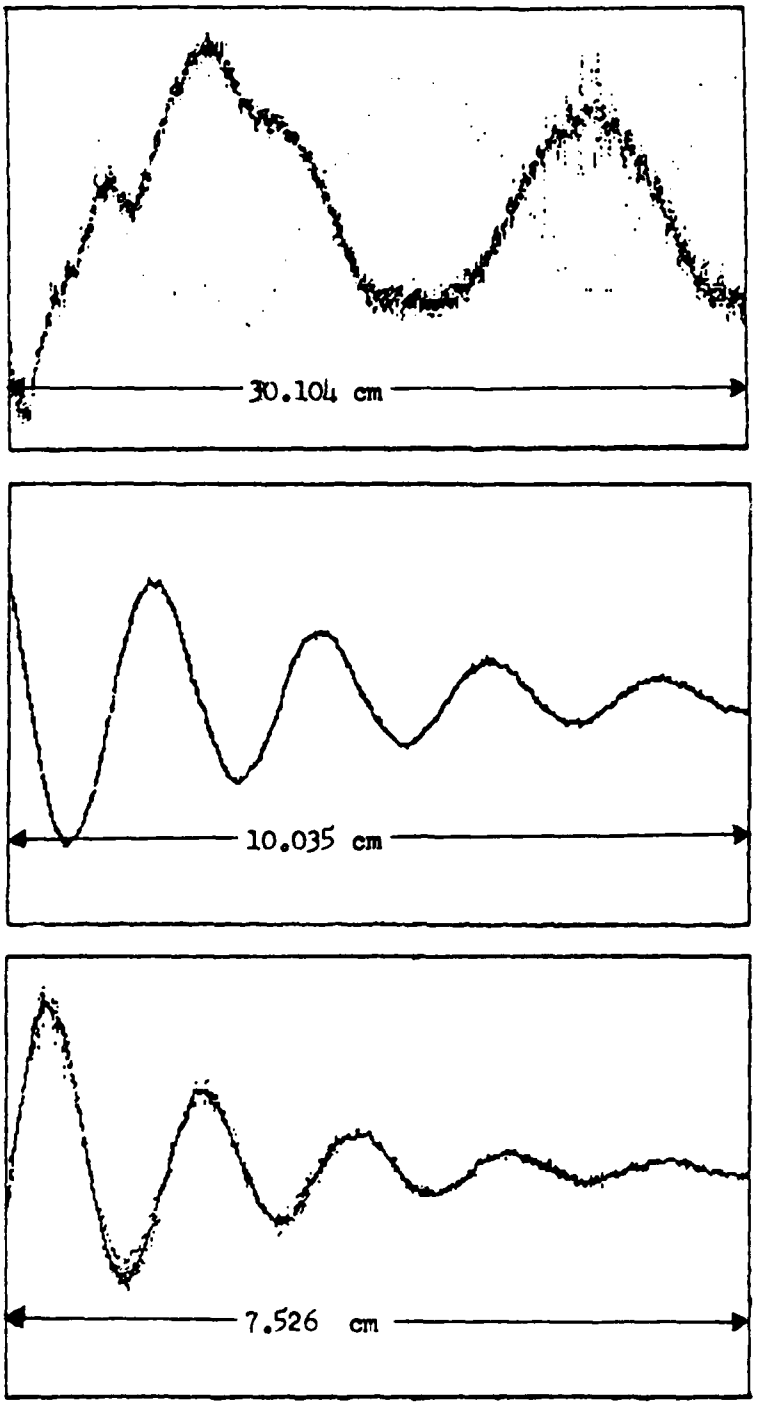

Figure 24. Raw Data as recorded by the Present Automated Equipment. The Parts A, B, and C correspond to Ripples driven at Frequencies of 3.00, 9.00, and 12.00 Hertz.

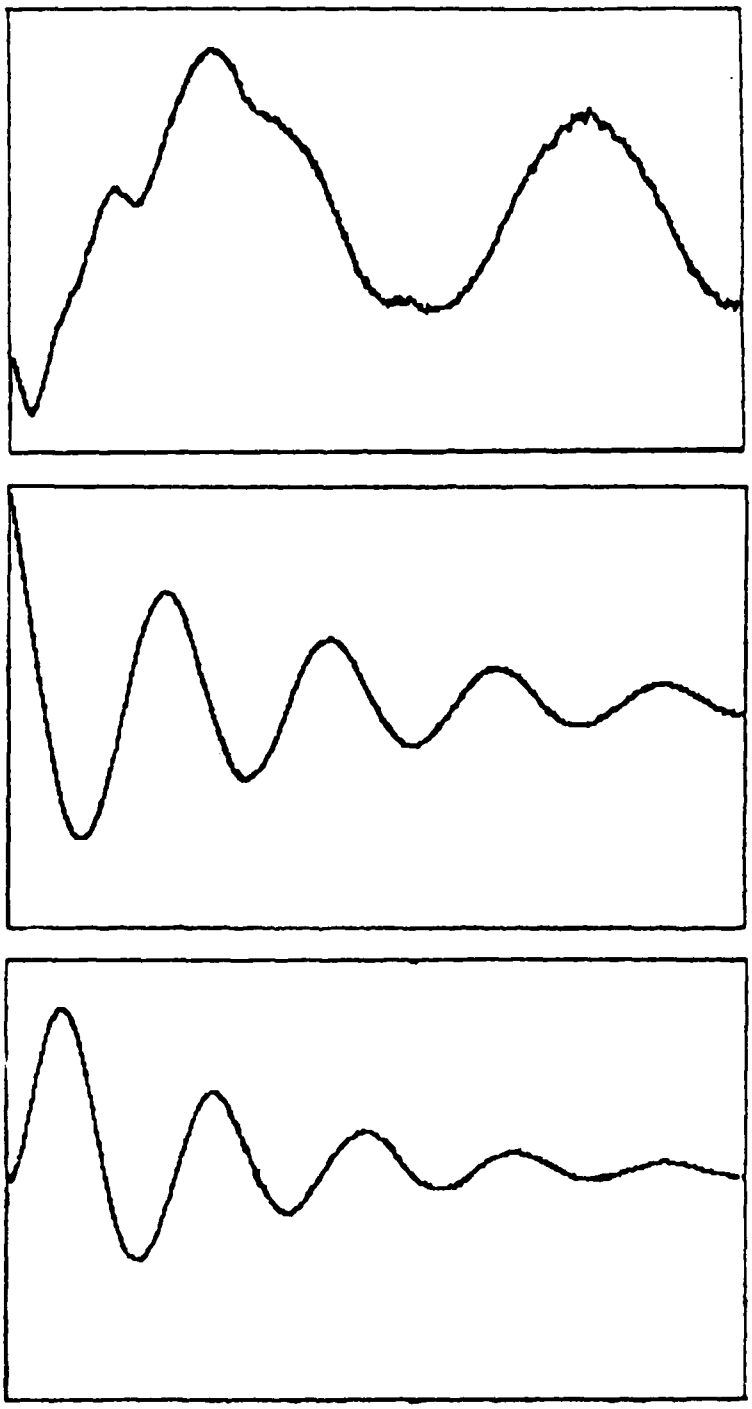

Figure 25. Digitally Filtered Data of Figure 24. Parts A, B, and C correspond to Frequencies of 3.00, 9.00, and 12.00 Hertz.

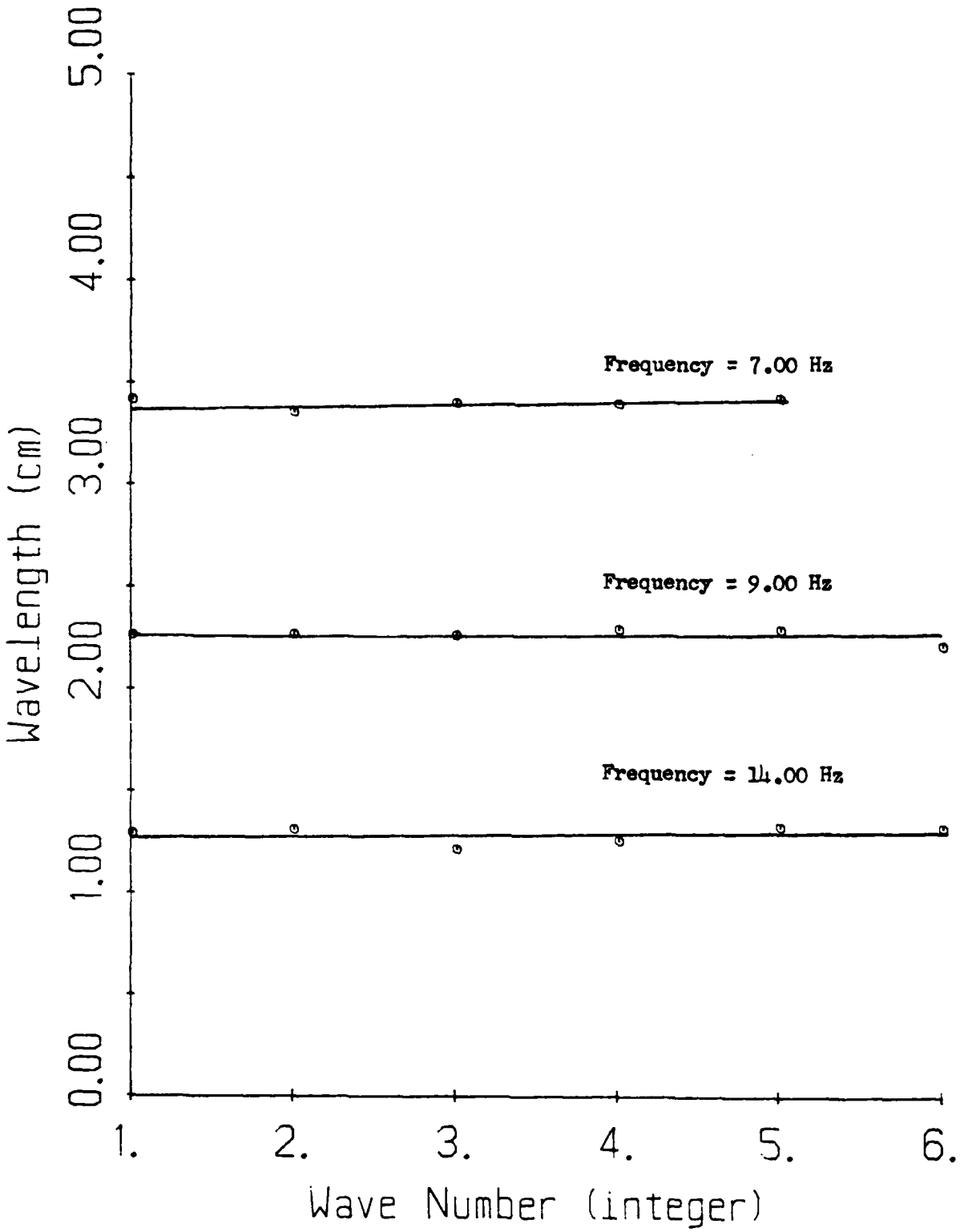

Figure 26. Sampled Wavelengths for Capillary Ripples at Various Frequencies. The Wave Number Represents the Distance from the Ripple Source.

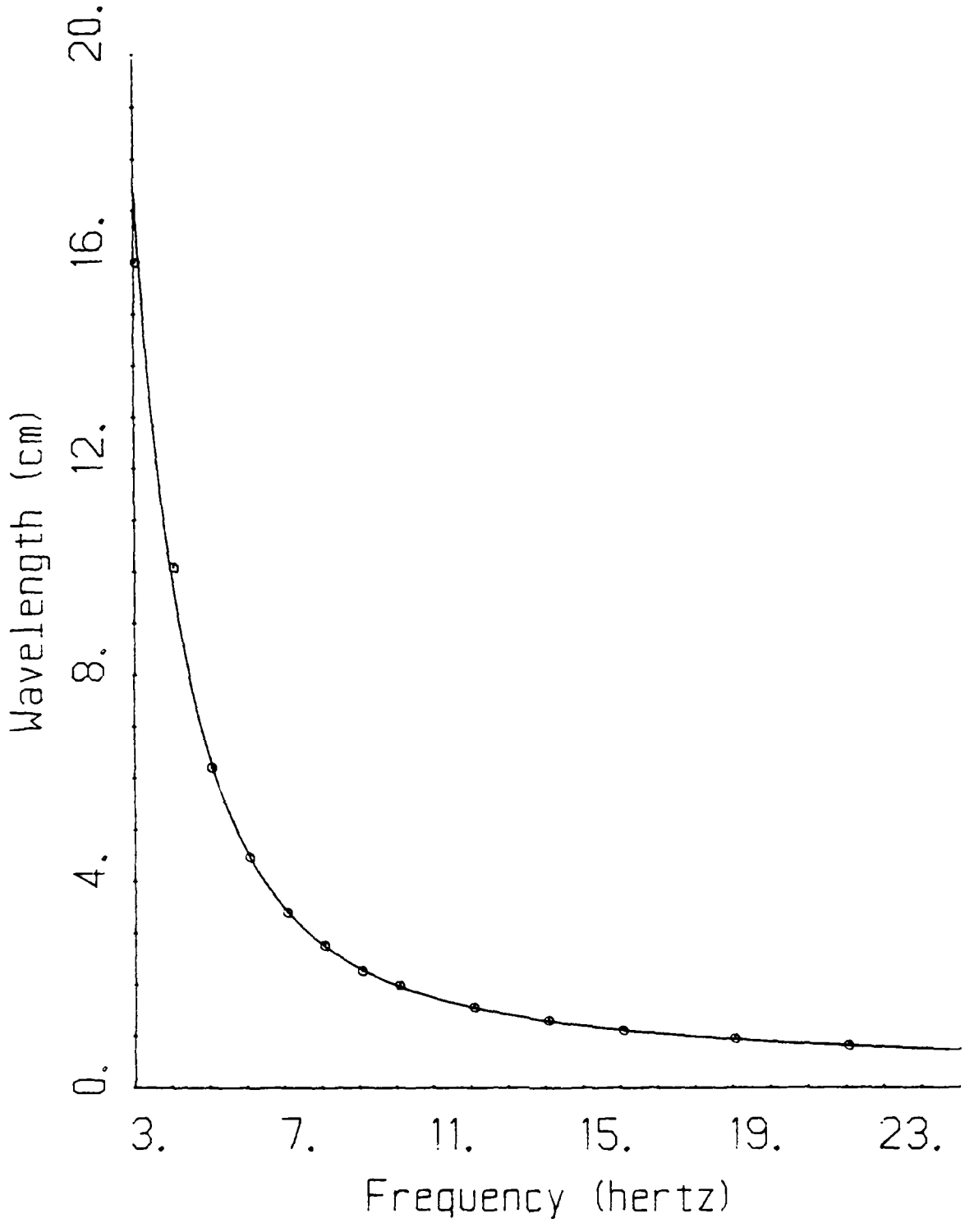

Figure 27. Dispersion Relation of Capillary Wavelength to Frequency for a Pure Theoretical Fluid (Solid Line) and Aged Mobil Ester P-41 (Points).

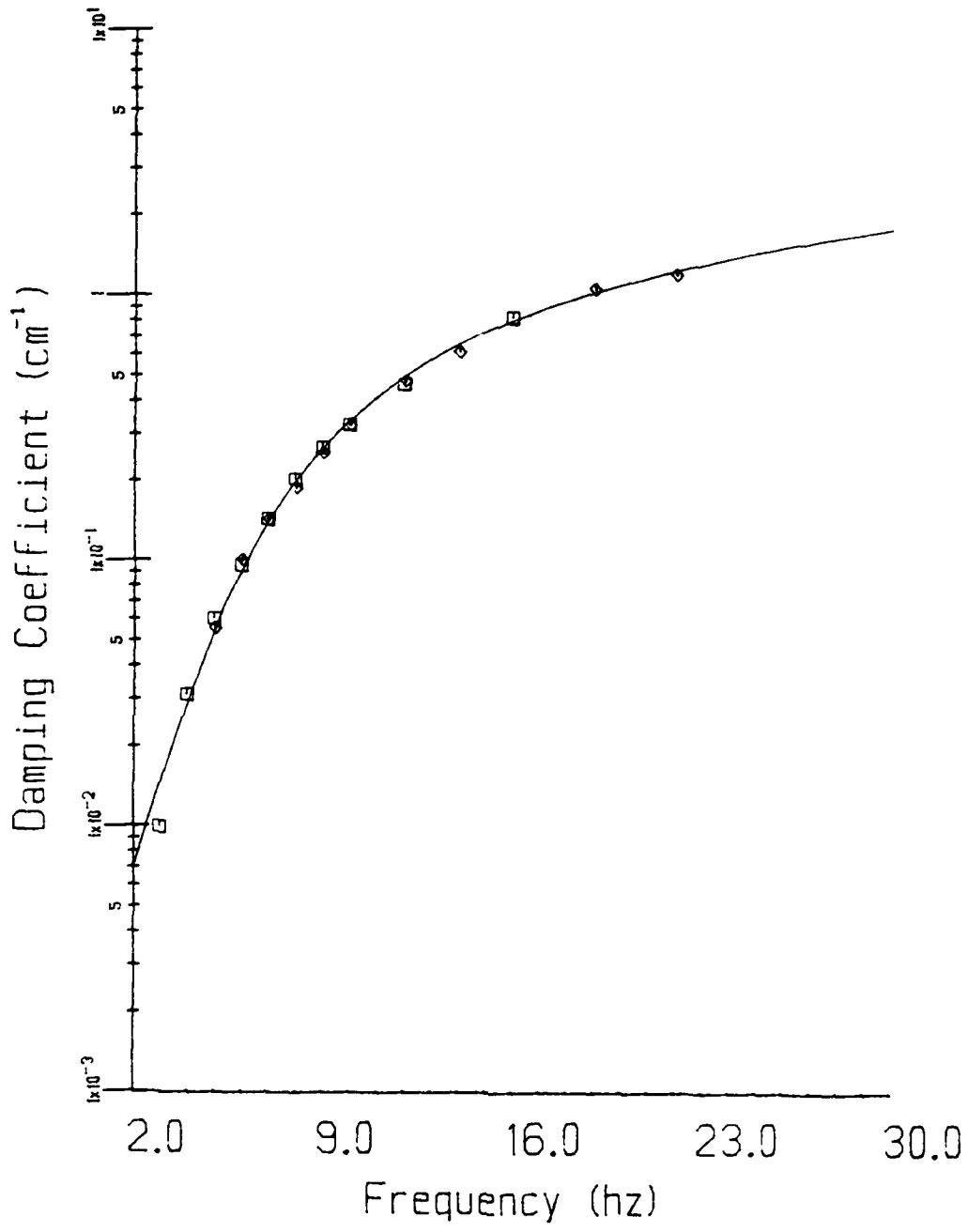

Figure 28. Damping Coefficients vs Frequency. Theoretical *Line from corrected* Lucassen-Reynders Boundary Conditions.

by Landau and Lifshitz;[13] when included, the observations are seen to coincide with the linearized theory, represented by the solid line in Figure 28.

3.2 Stationary Optics

At least two experimental methods do not require the optical detector to be translated during the course of the experiment. The first method allows non-linear and other second-order effects to be observed. The second method is useful for measuring capillary-wave damping of liquids of low viscosity, where back reflection creates standing waves in the channel.

a. Method 1

Data acquisition is synchronized by an internal quartz clock; the slope of the ripple surface is digitized at 0.01 second intervals. The resulting sequence of digital numbers may be converted by a Fast Fourier Transform to a power spectrum, in which peaks corresponding to the fundamental and higher harmonics appear. One example appears in Figure 29, where normalized spectra taken at two distances, 0.5 cm apart, are displayed. The persistence of the higher harmonics, which according to the damping curve of Figure 28 should attenuate more with distance than the fundamental, is an indication of a propagation mode in which non-linear terms are significant. This effect was predicted by van den Tempel and van de Riet;[14] the present observation confirms their prediction. Such experiments provide information about the second-order elastic modulus and other high-order mechanical and rheological properties of liquid surfaces.

b. Method 2

Data acquisition is again synchronized with the 100.00 Hz clock, but in this method, the signal imposed on the electro-mechanical device is not a pure sinusoid of constant frequency. Instead, the imposed signal is a short burst of spectrally filtered white noise created by a gated pseudo-random noise generator within the Commodore 64 SID. The burst is exactly reproducible and has a duration of about 0.6 second. The burst creates a disturbance on the liquid surface that disperses as it travels down the channel, with its frequency content changing as individual frequency components are damped by differing degrees. By recording the ripple profile at several distances from the wave source, the frequency power spectrum of the wave as a function of distance may be obtained by Fast Fourier Transform. The result appears in Figure 30. From this information, the damping coefficients for many frequencies may be determined. Figure 31 shows the damping coefficients determined by this method in a sample of Mobil Ester P-41. Agreement is good at low frequencies, but fails for high frequencies because ripple amplitude falls below the noise level introduced by the numerical method. No real advantage accrues by using the noise-burst method for this lubricant at room temperature because the viscosity is large enough to prevent standing waves. These waves pose a problem, however,

---

[14] M. van den Tempel and R.P. van de Riet, J. Chem. Phys., 42, 2769 (1965).

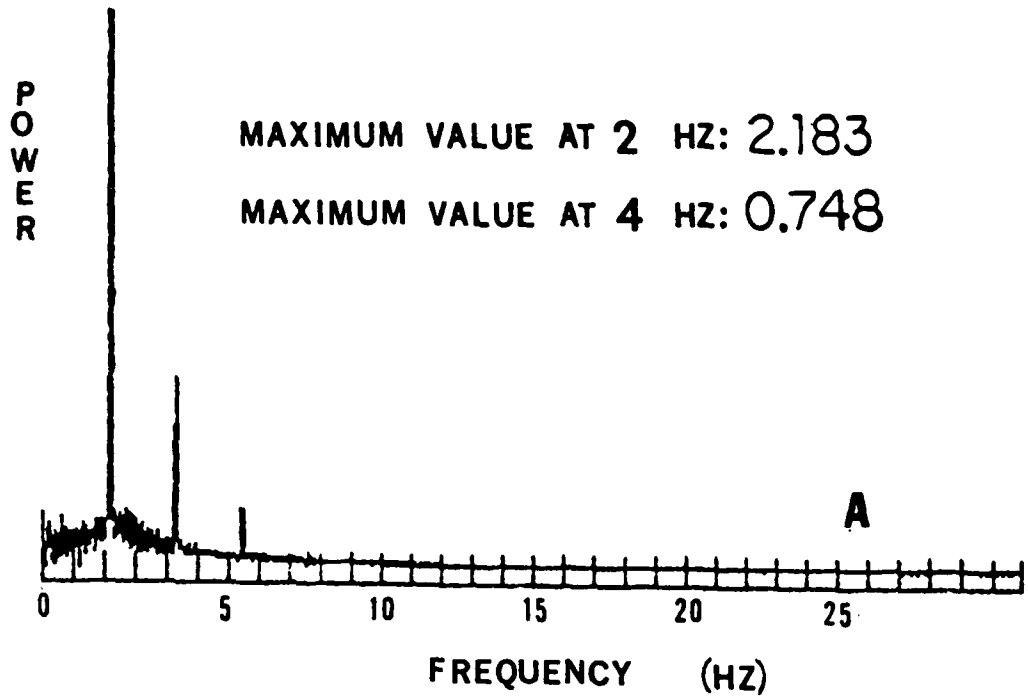

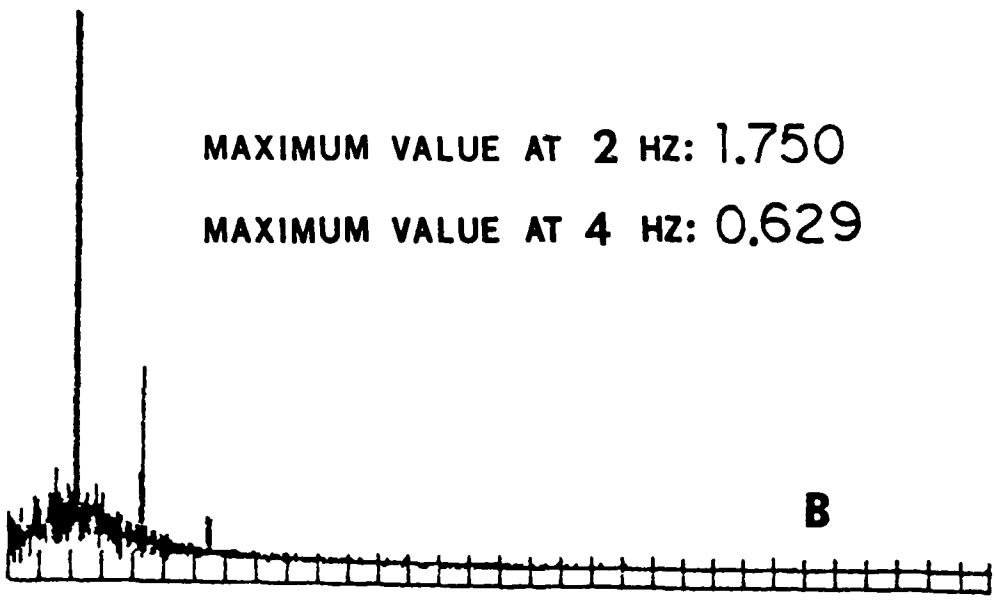

Figure 29. Normalized Power Spectra of a Ripple of Frequency 2.00 Hertz. Numerical Values shown on each Diagram are the Peak Heights of the Fundamental and the Second Harmonic. (A) and (B) represent Data obtained at Places 0.50 cm apart.

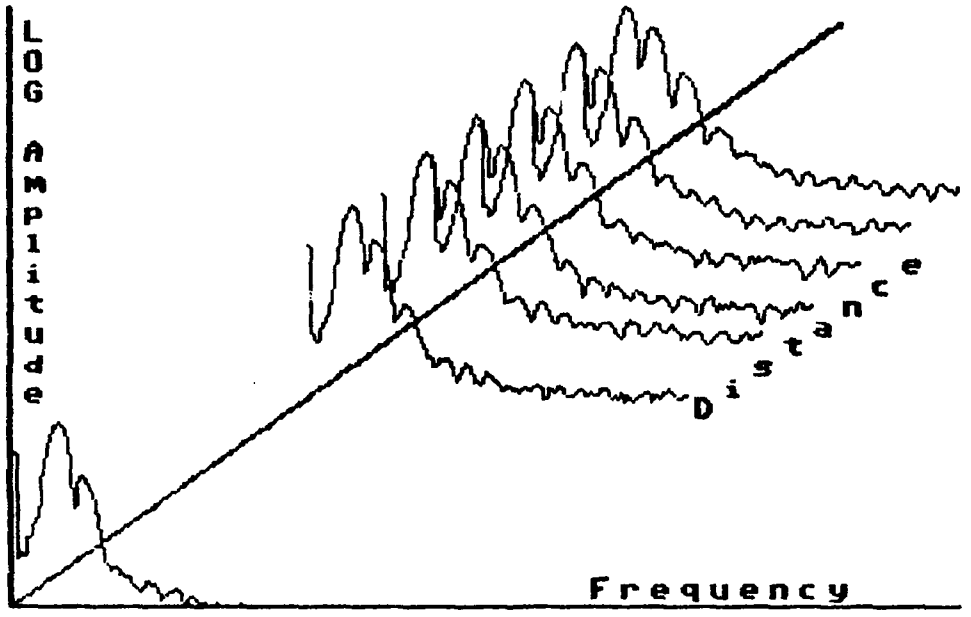

Figure 30. Frequency Spectrum of a Noise Burst as it travels down the Wave Tank. (Method 2)

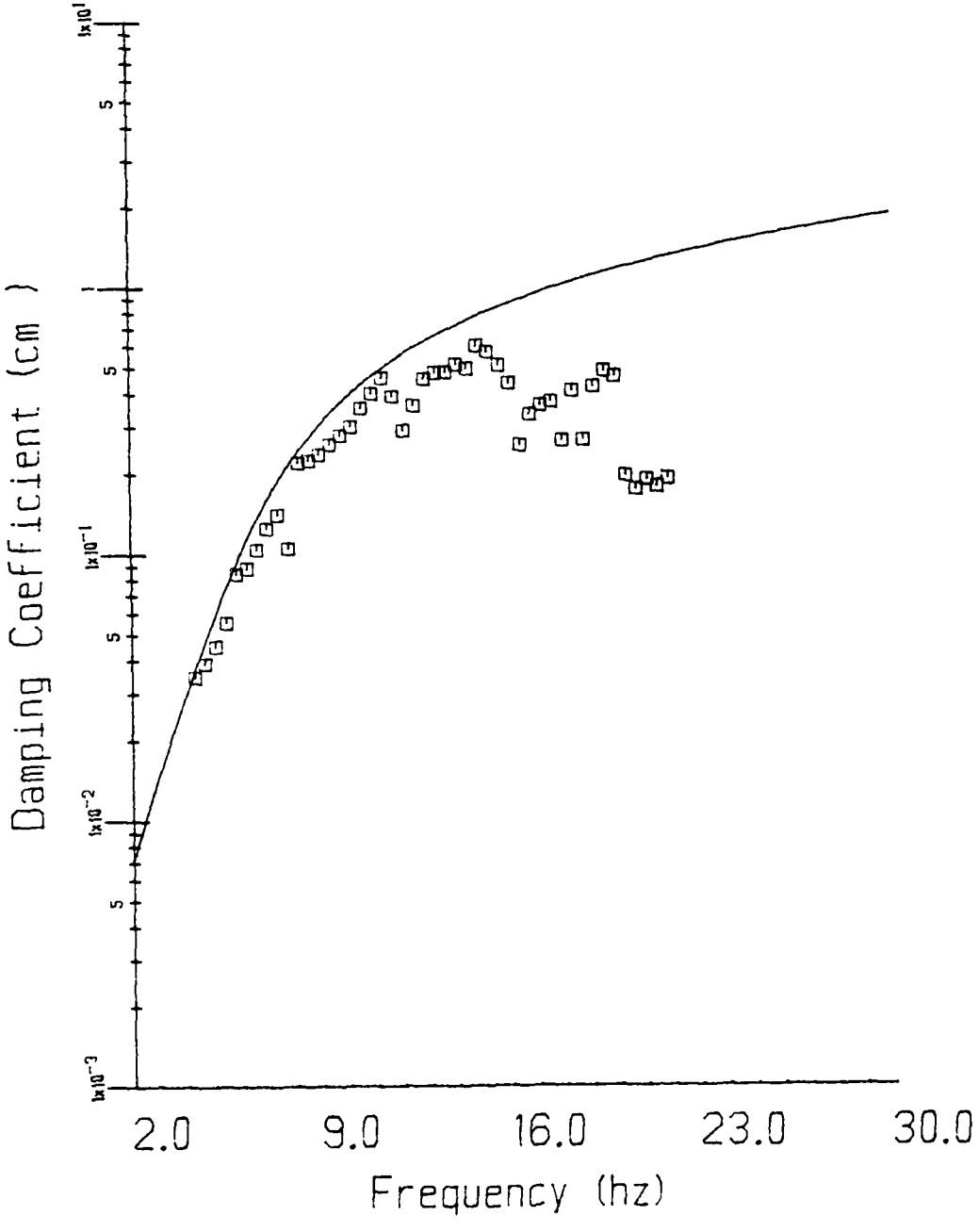

Figure 31. Data from the Noise Burst Experiment with Tmp-Heptanoate.

when the damping coefficients are too small to extinguish the ripples before they are reflected back by the end wall of the channel. The noise-burst technique, therefore, is useful for liquids of small viscosity such as may be encountered with other solvents or at higher temperatures.

3.3 Further Types of Experiment

The record obtained by the moving-optics mode of measurement contains the stress-strain relations of the liquid surface. The rheological properties of the liquid surface, in the form of a rheogram showing the stress variation of apparent viscosity, is therefore implicit in these data. The optical method has the advantage of offering a non-disruptive technique. Another advantage is the ability to vary frequency over a large range, so as to extend the scope of the rheogram. The rheogram can be expressed in fundamental units, by the decomposition and inclusion of the stress tensor as tangential and normal boundary conditions. In all these respects, the capillary-ripple technique is superior to the torsion-pendulum surface viscosimeter, the rotational-torsion surface viscosimeter, and the canal viscosimeter.

4. Theory of Capillary-Wave Damping

The theory of capillary ripples has been worked out in great detail for the limiting case of low-amplitude waves. Lucassen-Reynders and Lucassen[15] have published a review of the analytical solutions to the hydrodynamic problem prior to 1969. At present, the theory of large-amplitude capillary ripples is incomplete and non-general. For this reason, the theoretical treatment presented here is limited to the low-amplitude case.

Two equations of motion necessary to specify the propagation of a capillary ripple are the continuity equation [6] and the Navier-Stokes equation [7].

$$\operatorname{div} \mathbf{v} = \frac{\partial v_x}{\partial x} + \frac{\partial v_y}{\partial y} + \frac{\partial v_z}{\partial z} = 0 \qquad [6]$$

$$\left[\varrho \frac{\partial \mathbf{v}}{\partial t} + (\mathbf{v}\,\operatorname{grad})\,\mathbf{v}\right] = -\operatorname{grad} p + \eta \nabla^2 \mathbf{v} + \mathbf{f} \qquad [7]$$

The right-hand side of equation [7] gives the total force on a fluid element as the sum of three force components. These components are due to:

---

[15] E.H. Lucassen-Reynders and J. Lucassen, "Properties of Capillary Waves" in Advances in Colloid and Interface Science, 2, 347-395 (1969).

a. Differences in hydrostatic pressure between points in the fluid;
b. Momentum transfer through viscous forces between fluid layers with unequal velocities; and
c. External forces, such as gravity.

The inclusion of the term (vgradient)v introduces a non-linearity into the differential equation. If, however, the amplitude of the ripple is small compared to its wave-length, this term is negligible and the wave-length and damping coefficient of the capillary ripple may be determined from the boundary conditions.

With equations [6] and [7] specifying fluid flow within the bulk liquid, only the boundary conditions of the wave remain unspecified. These boundary conditions describe the forces that exist at the interface between the lower liquid phase and the upper air phase. We have found that further conditions specifying the flow in regions near the walls and floor of the wave trough are essential to be included, and can be taken into account after a formal analysis of the interface has been made.

The forces at the wave interface can be resolved into two classes, namely, those normal and those tangential to the wave surface. All treatments based on the hydrodynamic theory use the same boundary condition for the normal force: namely, the normal component of the stress tensor is equal to the capillary pressure across the deformed surface. This pressure is related to the surface tension and the curvature of the surface by the Laplace equation. A tangential surface stress, however, arises when the surface tension does not have the same value everywhere on the liquid surface. This condition exists on the undulating surface of a wave propagating on a solution of a surface-active solute or on a liquid surface covered with an insoluble monolayer, where fluid motion creates contraction of the surface at the wave crests and expansion of the surface at the wave troughs. (See Figure 22.) The contraction of the surface at the crest compresses the adsorbed film there, with a consequent reduction of the surface tension; while the expansion of the surface at the trough dilatates the adsorbed film there, with a consequent increase of the surface tension. These local gradients of surface tension result in a Marangoni flow, in which the crests of the waves are pulled into the troughs; which attenuates the wave energy and gives rise to larger damping coefficients than would occur without these changes of dynamic surface tension.

The formal expression of the wave-boundary conditions requires a tensor to be constructed. This tensor includes elements that are the coefficients of dilatational elasticity and viscosity, as well as the coefficients of shear elasticity and viscosity. If the elements related to the shear properties are neglected, the analysis is simplified. This approximation is justified by the very small shear viscosities found in the ester systems of the present study.

The simplified surface-stress tensor is isotropic and allows the varying surface stress to be described as a surface-tension

gradient, expressed in terms of a surface dilatational modulus, ϵ, where

$$\epsilon = \epsilon_d + \eta_d \frac{\partial}{\partial t} = \frac{d\sigma}{d \ln A_e} \qquad [8]$$

Here, A_e is the area of a surface element.

For small changes of area, ϵ_d and η_d are single valued for any given wave frequency on a given liquid. The value of ϵ, however, is different for different frequencies, except in the particular case where the dilatational viscosity, η_d, equals zero. In this case, the surface of the liquid is purely elastic and the elasticity may be determined from the relation between surface tension and surface concentration. In practice, a few monolayer systems have purely elastic surfaces, but soluble surface-active solutes usually exhibit the more complex viscoelasticity. For such solutions, wave-damping measurements are useful to determine viscoelastic properties.

5. Mathematical Formulation

As a coordinate system we choose that the surface of the liquid at rest lie in the X-Y plane at Z = 0. The force of gravity acts in negative Z direction, and the plane wave moves in the positive X direction. The liquid has a density of ρ, a bulk viscosity coefficient of η, a surface tension of σ, and an elasticity modulus of ϵ. The angular frequency of the wave is ω. Primed symbols refer to the physical constants of the upper phase, which is air. Two parameters are defined to simplify the analysis: these represent the contribution to the liquid flow of the penetration depth of the stream. They are defined by:

$$m^2 = k^2 + \frac{i\omega\rho}{\eta} \qquad [9]$$

$$(m')^2 = k^2 + \frac{i\omega\rho'}{\eta'} \qquad [10]$$

Using this notation, the boundary conditions may be expressed as a set of equations relating the normal and tangential stresses to the liquid flow. Since flow may be either potential flow or vortex flow, four parameters are required to account for the flow in both the upper and lower phases. The symbol A is used for potential flow (A' for the upper phase;) and the symbol B is used for vortex flow (B' for the upper phase.) The normal stress boundary condition requires:

$$\left[-i\omega\rho - 2\eta k^2 + \frac{i\sigma k^3}{\omega} + \frac{i\rho g k}{\omega}\right] A + \left[i\omega\rho' + 2\eta' k^2 + \frac{i\rho' g k}{\omega}\right] A' +$$
$$+ \left[2i\eta k m + \frac{\sigma k^3}{\omega} + \frac{\rho g k}{\omega}\right] B + \left[2i\eta' k m' - \frac{\rho' g k}{\omega}\right] B' = 0 \qquad [11]$$

The tangential stress boundary condition requires:

$$\left[-2i\eta k^2 - \frac{\varepsilon k^3}{\omega}\right] A + [-2i\eta' k^2]\, A' + [-\eta(k^2 + m^2) + \\ + \frac{i\varepsilon k^2 m}{\omega}] B + \eta' (k^2 + m'^2) B' = 0 \qquad [12]$$

and

$$ikA - ikA' + mB + m'B' = 0 \\ A + A' - iB + iB' = 0 \qquad [13]$$

follow from the continuity equations for the horizontal and vertical velocity components through the interface.

These four equations are linear and homogeneous in A, A', B and B'. For a non-trivial solution to exist, a determinant formed from the coefficients of the equation matrix must equal zero. If the viscosity of both phases is neglected, and if the elasticity is taken as zero, the Kelvin equation results from the solution of these equations:

$$\tanh(\kappa d).(\sigma\kappa^3 + \rho g\kappa) = \omega^2\rho \qquad [14]$$

The factor $\tanh(\kappa d)$ is the depth correction, where d is the depth of liquid in the tank, and κ is the wave-number ($\kappa = 2\pi/\lambda$) .

The determinant may be simplified to yield the capillary-ripple dispersion relation as:

$$[\eta(k - m) - \eta'(k - m')]^2 + E \cdot S = 0 \qquad [15]$$

where the functions E and S are shortened notation for:

$$E \equiv \frac{\varepsilon k^2}{\omega} + i[\eta(k + m) + \eta'(k + m')] \qquad [16]$$

and

$$S \equiv \frac{\sigma k^2}{\omega} + i[\eta(k + m) + \eta'(k + m')] + \frac{g(\varrho - \varrho')}{\omega} - \frac{\omega(\varrho + \varrho')}{k} \qquad [17]$$

The solution of this dispersion relation requires the use of a computer, and from its solution all measurable properties of the wave can be obtained. Comparison of experimentally determined wave-damping coefficients with the theoretical results, allows the determination of surface elasticity, which has been reported[16] to correlate with the stability of the foam produced from the liquid. (Our own comparisons between elasticity and foam stability have yet to be made.)

---

[16] K. Malysa, K. Lunkenheimer, R. Miller and C. Hartenstein, Colloids and Surfaces, 3, 329 (1981).

SECTION VI

DYNAMIC SURFACE TENSION BY RATE OF ASCENT OF BUBBLES

Part 1. Behavioral Limits

1. Introduction

The rate of ascent of a single bubble through an oil may be used to reveal whether a surface-active constituent is present therein, which is often a condition not otherwise readily detected in nonaqueous solutions. A hydrodynamic effect of adsorbed solute is to "rigidify" the interface of the rising bubble, which notably reduces its rate of ascent; thus betraying the presence of surface activity. The application of the test is illustrated with a number of synthetic lubricating oils both with and without additives. The results obtained with most of these oils confirm the theoretical calculations of drag coefficients of drops or bubbles with fluid interfaces. One additive widely used as an anti-oxidant was found to convert the behavior of a fluid interface to that of an interface effectively rigid under the dynamic conditions of the experiment, thus disclosing its surface activity in oil solution.

The presence of a surface-active solute in a lubricating oil may cause problems of lubrication due to emulsified water, air entrapment, or foam. Such striking effects, when they occur, at once imply a condition of surface activity as their necessary precursor; but surface activity in a solution does not always make itself manifest by conspicuous phenomena: it may be subtly present. An awareness of the condition is desirable in order to guard against the development of problems, which may arise either by further build-up of the concentration of the surface-active solute or by its synergistic combination with additives. The detection of the condition, in the absence of the clear evidence afforded by foaming or emulsification, is not as straightforward as might appear. Lubricating oils, like most organic liquids, have low surface tensions ($\sigma < 30$ mN/m) and surface activity in such solvents may be a matter of lowering the surface tension by only 1 mN/m or less. The measurement of the lowering of the surface tension of the solvent, which is the direct method to detect the presence of a surface-active solute, is not a feasible procedure with solvents that initially are not chemically pure. Even were the oil a single chemical component, this direct approach is not required, as methods to detect dynamic surface tension are better suited to discover whether a surface-active solute is present. Of these the easiest to perform is the measurement of the rate of ascent of a bubble through the solution. One limitation, however, common to all methods, must be remarked: they can all definitively demonstrate the presence of surface activity in a solution; but the absence of a positive response, by whatever method used, is a necessary but not sufficient reason to conclude that a surface-active solute is not present. The disequilibrium, on which the phenomenon depends, may be over before it is detected.

The rate of rise of single bubbles is determined by the behavior of the gas-liquid interface when it is subjected to dilatation or compression. In a solution that lacks surface activity, a rising bubble moves faster than a solid sphere of the same density, as the mobility of its interface allows lower velocity gradients to be established in the medium than those that develop at an immobile, or rigid, interface. When a surface-active solute is adsorbed at the gas-liquid interface, however, the movement of the interface and of the gas inside the bubble is inhibited; the velocity gradient in the outer fluid is increased, until at the limit the rate of rise of the bubble is the same as that of a solid sphere of the same density.

The simplified descriptions of bubble rise given by Stokes' law for rigid spheres (see Equation [23] below) and the Rybczynski-Hadamard modification of Stokes' law for fluid spheres (see Equation [24] below) are valid only at very small Reynolds' numbers (Re < ca. 1.0,) where Re is given by:

$$Re = 2a.V_c.\rho/\eta \qquad [18]$$

where a is the radius of the sphere;
V_c is the corrected velocity of its motion (see Equation [27];)
ρ is its density; and
η is its viscosity coefficient.

The usefulness of measuring the rate of ascent of a rising bubble to detect the presence or absence of a surface-active solute in a lubricating oil would be greatly curtailed if experimental conditions were to be confined to the narrow range of viscosity and bubble diameter required to ensure such small Reynolds' numbers. No such restriction is introduced in what follows. Higher Reynolds' numbers arise naturally at higher temperatures as the viscosity of the oil decreases; and the effect of temperature on the behavior of lubricating oils is too important practically to be left out of any investigation of their properties. By raising the temperature of our oil samples from 20 to 80°C the Reynolds' numbers are increased to about 20. In the range 0.75 < Re < 20, more recent and more complex theories than those of Stokes for the motion of spherical particles in a fluid medium have to be invoked to interpret the results. In this Section we illustrate how the measurements may be made and the results interpreted.

2. Theories of Rate of Bubble Rise at Moderate Reynolds Numbers

2.1 Spherical bubble.

A perfectly spherical bubble (the Platonic ideal) is the form assumed at the mathematical limit of a Weber number of zero, where the Weber number, W, is defined as:

$$W = 2a.\rho.V_c^{\,2}/\sigma \qquad [19]$$

where σ is the surface tension of the liquid; and
a is the radius of curvature at the top of the rising bubble.

The quantitative relation between the eccentricity of the bubble's shape and the Weber number was investigated experimentally by Wellek et al.,[17] who showed, in particular, that at $W \leq 0.1$ the deviation of the eccentricity from unity does not exceed 0.01. For the materials and conditions of the present experiments, the Weber numbers are sufficiently small ($W = 0.01$ to 0.15) to ensure that the deviation from the sphere is negligible.

2.2 Fluid interface.

Stokes' theory for the terminal velocity of a solid sphere in a viscous medium was extended by Rybczynski[18] and Hadamard[19] to fluid spheres. For a liquid drop or gas bubble of radius a, density ρ_1, and viscosity η_1, moving at constant velocity in an infinite volume of a medium of density ρ_2, and viscosity η_2, the drag coefficient, C_D, is related to the Reynolds number, Re, as follows:

$$C_D.Re = K24 \qquad [20]$$

where $$C_D = 8a.g/3V_c^2 \text{ (g is the gravitational constant)} \qquad [21]$$

and K, the Rybczynski-Hadamard factor, has the value

$$K = (3\eta_1 + 2\eta_2)/(3\eta_1 + 3\eta_2) \qquad [22]$$

The derivation of Equation [20] postulates that the medium exerts a viscous drag on the interface of the bubble or liquid drop, and so promotes a circulation of the fluid contained inside, whether gas or liquid. The theory predicts that a bubble containing a circulating gas, with $\eta_1 << \eta_2$, would move 50% faster ($K = 2/3$) than one in which the gas, for any reason, does not circulate; for in the latter case the Rybczynski-Hadamard factor does not apply, and the velocity of the bubble is given by the unmodified form of Stokes' law:

$$C_D.Re = 24 \qquad [23]$$

Garner et al.[20, 21] demonstrated experimentally the reality of the circulation inside gas bubbles and examined the effects of bubble size and shape. They showed that the validity of the above equations is limited to the range of Reynolds' number less than about one, and to the same conditions as for Stokes' law to hold, including the requirement that the gas bubbles be spheres. Within

---

[17] R.M. Wellek, A.K. Agrawal and A.H.P. Skelland, AIChE J., 12, 854 (1966).

[18] W. Rybczynski, Bull. Int. Acad. Sci. Cracovie, Ser.A, 1911, 40.

[19] J. Hadamard, Compt. Rend., 152, 1735 (1911).

[20] F.H. Garner and A.R. Hale, Chem. Eng. Sci., 2, 157 (1953).

[21] F.H. Garner and D. Hammerton, Chem. Eng. Sci., 3, 1 (1954).

these conditions the Rybczynski-Hadamard expression for an ascending gas bubble whose gas-liquid interface is characterized by a constant surface tension is:

$$C \cdot Re = 16 \qquad [24]$$

Ryskin and Leal[22] recently presented a numerical solution of the problem of an ascending bubble in a liquid, by integrating the forces at the surface, for Reynolds' numbers in the range $0.5 < Re < 200$ and for Weber numbers up to 20.

Ryskin and Leal take the dynamic air-liquid interface to be completely characterized by a constant surface tension, that is, to be spatially uniform; which is to assume, in effect, that it is free of adsorbed surface-active solute and is isothermal.

Theoretically computed rates of rise of bubbles with fluid interfaces at high Reynolds' numbers are tabulated by Ryskin and Leal. Of these computations we require only those that refer to spherical bubbles, that is, to Weber numbers of zero. The numbers from Table 1 of reference (22) for $W = 0$ and for $0.75 \leq Re \leq 20$ are fitted to the following algebraic interpolation:

$$C = -0.0230\ Re + 16.780/Re - 0.244/Re^2 + 1.021 \qquad [25]$$

and for $Re < 0.75$ the Rybczynski-Hadamard equation, Equation [24], applies.

2.3 Effect of surface-active solutes.

Levich[23] was the first to provide a satisfactory explanation of the retardation of the velocity of a rising bubble caused by the presence of surface-active solute in the medium. He postulated that adsorbed solute is not uniformly distributed on the surface of an ascending bubble. The surface concentration on the upstream part of the bubble is less than the equilibrium concentration, while that on the downstream part is greater than equilibrium. This disequilibrium of the concentrations is brought about by the viscous drag of the medium acting on the interface, which in turn creates a gradient of surface tension, with the lower tension where the concentration of adsorbate is greater. The liquid interface then flows (Marangoni flow) from the region of lower tension to that of higher tension, and the direction of this flow offsets the flow induced by the shear stress in the outer fluid acting on the interface. This action restrains the net flow of the interface; its consequent loss of fluidity, or, if you will, its increasing rigidity, reduces the circulation of internal gas to a greater or less degree. When the interface is completely rigidified, by a gradient of surface tension sufficiently large, the circulation of

---

[22] G. Ryskin and L.G. Leal, J. Fluid Mech., 148, 1 (1984).

[23] V. Levich, "Physicochemical Hydrodynamics," Prentice-Hall: New York, 1962; Chapter 8.

internal gas in the bubble is inhibited; both the velocity gradient in the medium and the terminal velocity of rise of the bubble then become indistinguishable from those of a solid sphere of the same density.

The criterion for a rigid interface on a rising bubble is that at Re < ca. 1, its velocity of rise be described by Stokes' law. Kuerten et al.[24] give empirical formulae for rates of motion of solid spherical particles at higher Reynolds' numbers. The following equation is based on numerous experimental measurements of the drag coefficients of solid spheres in fluid media at 0.75 < Re < 20:

$$C_D = 24/Re + 2 \qquad [26]$$

3. Experimental

3.1 Apparatus and procedure to measure rate of bubble rise at different temperatures.

The apparatus previously described[25] was modified slightly (see Figure 32.) Single gas bubbles are generated as before at the tip of a glass capillary tube (d = 0.0323 cm), which passes through a glass stopper specially ground to fit the lower end of the cylinder, of length 70 cm and inner diameter 3.04 cm, that contains the liquid (see Figure 32.) A Haake circulator, F-3K, pumps thermostatically controlled water through the cylinder's jacket; the temperature is monitored, with a precision of ± 0.1°C, by means of a thermistor equipped with a digital indicator. To minimize temperature gradients, the cylinder is enclosed in thermal insulation. The diameter of the spherical bubble is calculated by measuring the length of the air slug in the calibrated capillary tube before its release into the liquid, using a cathetometer with a precision of ± 0.01 mm.

The time for each released bubble to rise through a specified distance of 42.0 cm is measured with a stopwatch (± 0.1 sec.) Measured velocities, Vm, are corrected for wall effects by the Ladenburg-Faxen formula:[26]

$$V_C = V_M(1 + 2.1\ d/D) \qquad [27]$$

where V_C = corrected rate of rise;
V_M = measured rate of rise;
d = bubble diameter;
D = diameter of cylinder.

---

[24] H. Kuerten, J. Raasch and H. Rumpf, Chemie-Ing. Tech, 38, 941 (1966).

[25] Y. Suzin and S. Ross, J. Colloid Interface Sci., 103, 578 (1985).

[26] R.B. Bird, W.E. Stewart, and E.N. Lightfoot, "Transport Phenomena," Wiley, New York, 1960, 206.

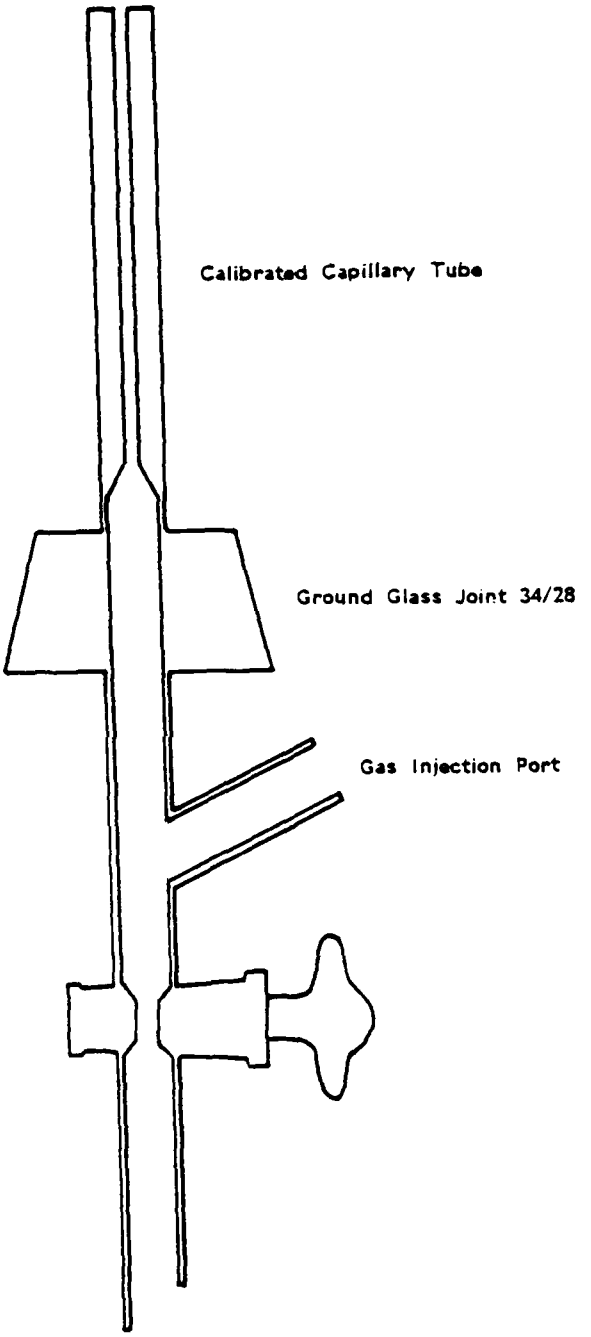

Figure 32. Schematic Diagram of a Part of the Apparatus to measure Bubble Size and rate of Bubble Ascent at a controlled Temperature.

3.2 Measurement of physical properties.

Kinematic viscosities were measured with a Cannon-Fenske viscosimeter in a water thermostat, the temperature of which was controlled by the same thermistor used in the apparatus described above. Densities were measured with a hydrometer, and surface tensions by the Wilhelmy-plate method.

4. Results

To obtain the rate of bubble rise in any solution at any temperature, ten separate measurements were made. Since it is impossible to replicate the same bubble size each time, these data give the variation of bubble velocity with diameter. The Rybczynski-Hadamard theory embodies an implicit supposition that the factor **K** in equation [22] is independent of the bubble size, within certain well understood limits. If bubbles are too small ($2a < 0.03$ cm, according to Garner and Hammerton)[27] the surface-tension gradient has too limited a scope to set up a vigorous toroidal circulation of the internal gas, and the theory is inapplicable; and if bubbles are too large they depart too far from the spherical for either Stokes' law or its Rybczynski-Hadamard modification to apply. Within these limits of size, the velocity of the bubble should vary with the square of the bubble diameter, so that the factor **K**, or the product $C_D Re$, is independent of bubble size. Our first treatment of the data, therefore, is to plot the corrected velocity, V_c, against the square of the bubble diameter, $4a^2$. These plots are shown in Figure 33: they demonstrate that the implicit assumption of the Rybczynski-Hadamard theory is supported by the observations.

The next treatment of our data for each system investigated is to reduce the variety of measured bubble radii to that of a single representative value; which can readily be done by using the linear relation, obtained by least squares, between the square of the bubble diameter and velocity of rise (Figure 33 reports a selection of typical data;) then to interpolate for the value of the velocity corresponding to any desired radius of bubble (we have taken a = 0.042 cm), from which drag coefficients can be calculated by Equation [21]. For the comparison on the theoretical side, we make use of Ryskin and Leal's tabulation of drag coefficients, C_D, at various values of Re and W, taking W = 0 for our near-spherical bubbles. The relation between C_D and Re (W=0) for $0.75 < Re < 20$ is given by Equation [25], and for $Re(W=0) < 0.75$ by Equation [24]. In Figure 34, Equations [24] and [25] are plotted on a log-log scale; for comparison the experimental data for C_D vs Re for several synthetic oils and oil solutions are shown as points on the same diagram. All these systems were measured for different sizes of bubbles and at various temperatures in the range 20 to 80° C., which, on account of different bubble sizes and of changes of kinematic viscosity with temperature, give a series of different Reynolds' numbers for the same solution in each system.

---

[27] F.H. Garner and D. Hammerton, Chem. Eng. Sci., 3, 1 (1954).

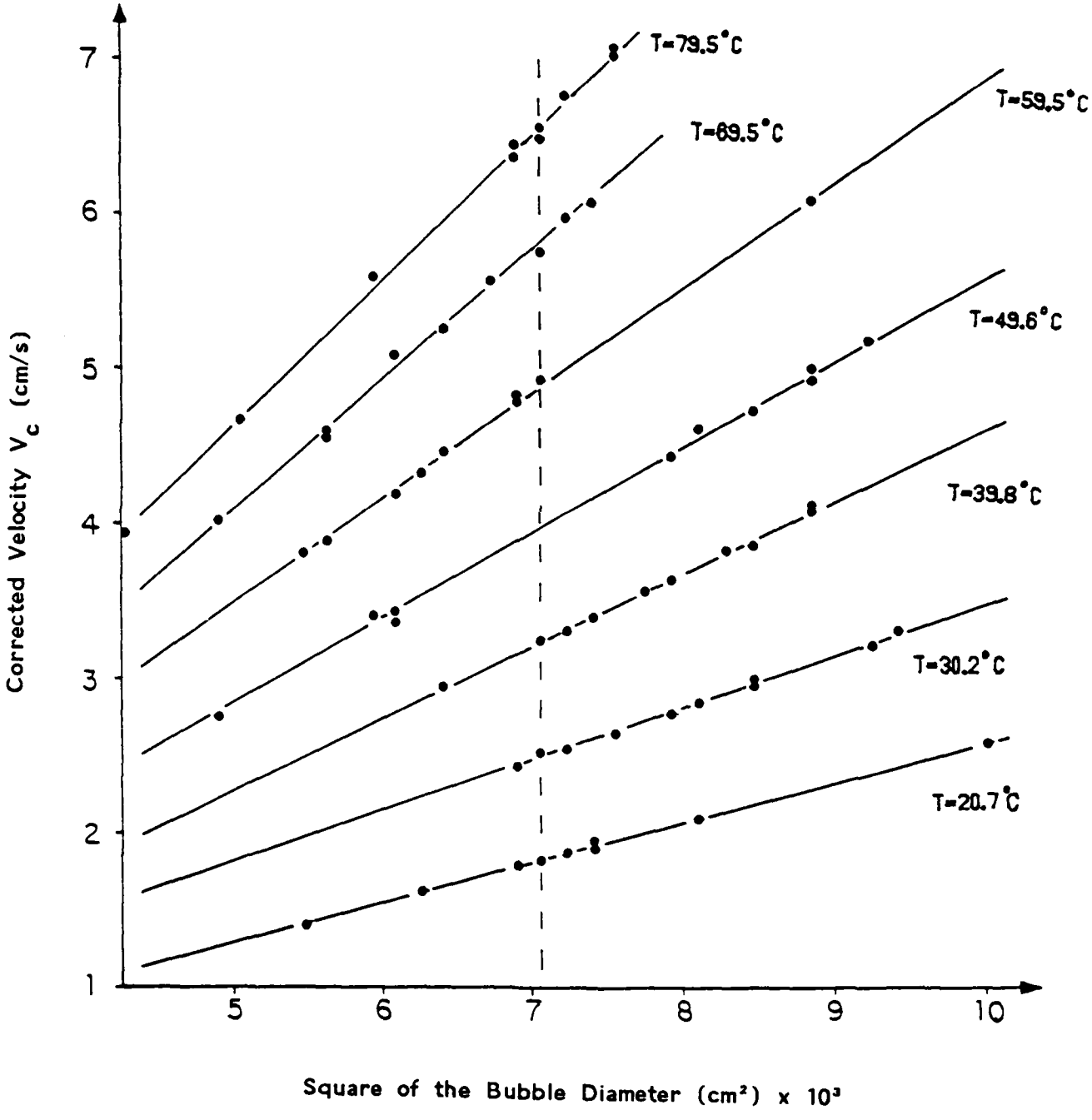

Figure 33. Linear Relations between the Corrected Velocity of Bubble Rise (cm/sec) versus the square of the Diameter (cm) of Bubble, for a Series of Isotherms measured on Mobil Ester P-41. The Vertical Broken Line indicates an Interpolation at 2r = 0.084 cm

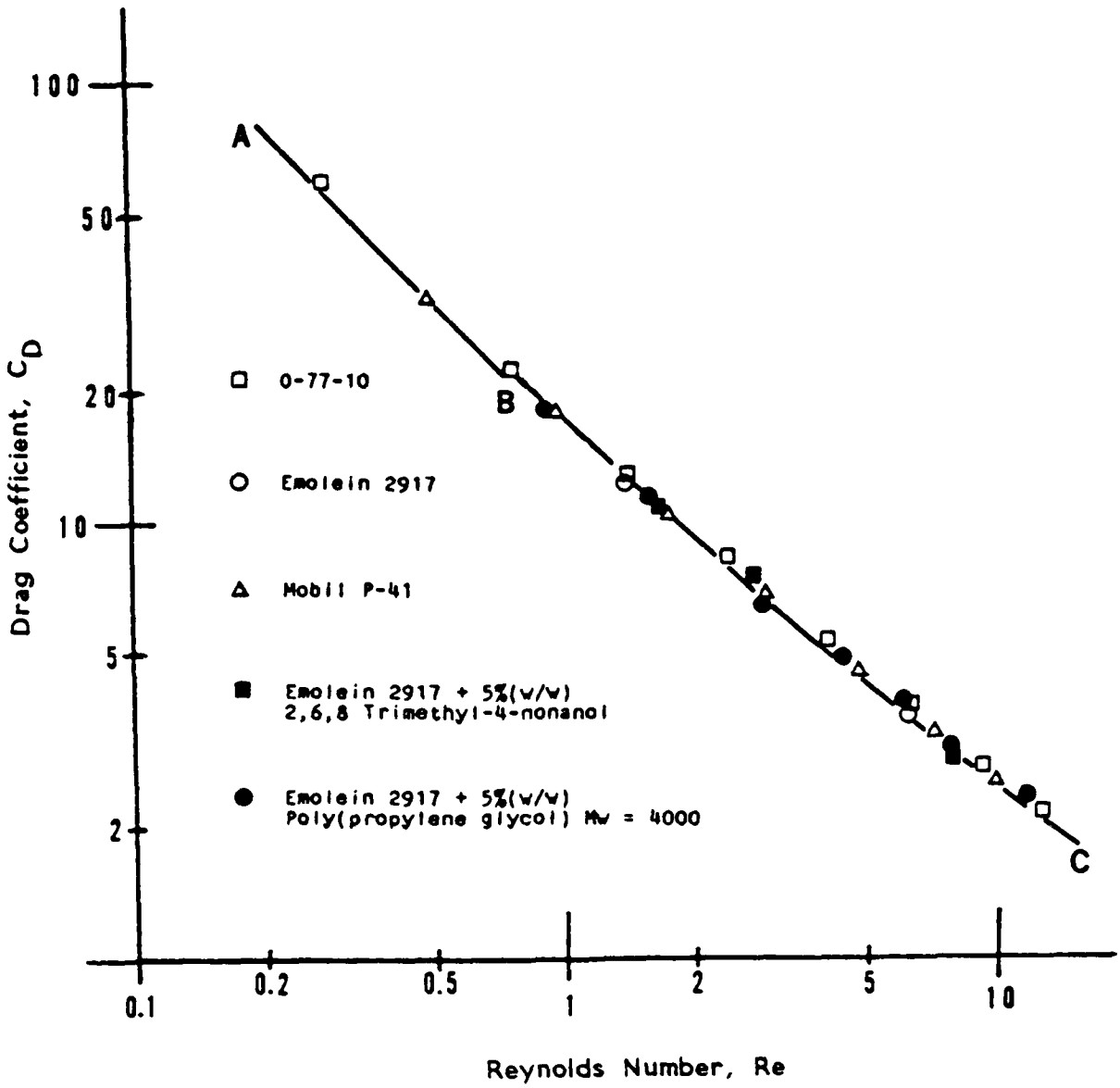

Figure 34. Variation of Drag Coefficient C_D with Reynolds Number Re. Solid Lines are Theoretical Equations; Points are Observational Data. AB is Rybczynski-Hadamard Law, Equation [24]; BC is Ryskin-Leal Theory, Equation [25].

The agreement between theory and observation can be seen to be excellent. The meaning of this finding is that several of the oil systems that have been measured in the course of this work can be correlated by a unitary theory. These systems are alike in that they show no evidence of dynamic surface tension; that is, their surface tension is not affected by any solute that may be present. All the systems contain solutes; even the oils without purposely added solute are not chemically pure; but whatever solutes are present show little or no surface activity at any of the temperatures measured. The systems that conform to this theoretical description are:

(a) Emolein 2917
(b) 0-77-10 Blended Ester
(c) Mobil ester P-41
(d) Emolein 2917 + 5% w/w trimethyl-4-nonanol
(e) Emolein 2917 + 5% w/w polypropylene glycol (Mw = 4000)
(f) Hercolube C;
(g) Hercolube C + 5.16% (w/w) N-phenyl-1-naphthylamine (Lot A13B);
(h) Hercolube C + 4.74% (w/w) N-phenyl-1-naphthylamine (Lot A13B) + 8.29% (w/w) tricresyl phosphate.
(i) Mobil Ester P-41 + 4.99%(w/w) N-phenyl-1-naphthylamine (Lot A13B)
(j) Mobil Ester P-41 + 5%(w/w) N-phenyl-1-naphthylamine (Lot A12A)

The data are tabulated in full in Tables 6-12:

Key to Footnotes in Tables 6-12:

(1) Rybczynski-Hadamard Equation [24]
(2) Stokes Equation [23]
(3) Kuerten-Raasch-Rumpf Equation [26]
(*) Interpolated Diameters

An exception to the general agreement may be found in (b), where the values are consistently larger by about 5% than those computed for a perfectly fluid interface, indicating that a trace of a surface-active solute is already present in this oil.

The observations for the oil designated Mobil Ester P-41, (c) above, agree with the Ryskin-Leal theory for a fluid interface; but the observations for the same oil containing 5% w/w N-phenyl-1-naphthylamine (Lot A12A), (j) above, do not conform to this description. They agree instead with an empirical equation suggested by Kuerten et al. based on numerous experimental observations of the drag coefficients of solid spheres in fluid media at $0.75 \leq Re \leq 10$, namely, Equation [26]; and at $Re < 0.75$ with Stokes' equation, Equation [23].

The comparisons of the results for the solvent, Mobil Ester P-41, and the solution, Mobil Ester P-41 + 5% (w/w) N-phenyl-1-naphthylamine (Lot A12A), are shown in Figures 35 and 36, where the solid lines represent Equations [23], [24], [25], and [26] while the observational data are represented by the positions of points. Figure 35 shows the nature of the variation of C_D with Re for the

Table 6. Experimental Conditions, Dimensionless Groups, and Velocities of Bubbles Rising in Emolein 2917.

Temp [°C]	d [cm]	ν [cm²/s]	V_c [cm/s]	Re	C_D	$C_{D,calc}$
20.0	0.095	0.1760	3.826	2.065	8.486	9.042
20.0	0.077	0.1760	2.561	1.120	15.351	15.783
20.0	0.087	0.1760	3.213	1.588	11.019	11.454
20.0	0.091	0.1760	3.471	1.795	9.876	10.252
20.0	0.081	0.1760	2.781	1.280	13.694	13.952
20.0	0.083	0.1760	2.842	1.340	13.437	13.377
20.0	0.093	0.1760	3.658	1.933	9.088	9.592
20.0	0.092	0.1760	3.495	1.827	9.848	10.090
20.0	0.083	0.1760	2.894	1.365	12.958	13.152
20.0	0.083	0.1760	2.874	1.355	13.139	13.241
20.0	0.084	0.1760	2.988	1.426	12.302	12.635*
50.0	0.098	0.0727	7.016	9.458	2.603	2.575
50.0	0.093	0.0727	6.507	8.324	2.872	2.842
50.0	0.080	0.0727	5.037	5.543	4.123	3.913
50.0	0.101	0.0727	7.565	10.510	2.305	2.374
50.0	0.090	0.0727	6.257	7.746	3.006	3.005
50.0	0.078	0.0727	4.801	5.151	4.425	4.151
50.0	0.081	0.0727	5.219	5.815	3.888	3.766
50.0	0.106	0.0727	8.198	11.953	2.062	2.148
50.0	0.083	0.0727	5.476	6.252	3.619	3.555
50.0	0.084	0.0727	5.472	6.323	3.668	3.523
50.0	0.084	0.0727	5.439	6.284	3.713	3.541
50.0	0.084	0.0727	5.509	6.365	3.619	3.505*

Table 7. Experimental Conditions, Dimensionless Groups, and Velocities of Bubbles Rising in 0-77-10.

Temp [°C]	d [cm]	ν [cm²/s]	V_c [cm/s]	Re	C_D	$C_{D,calc}$	
9.4	0.083	0.3987	1.320	0.275	62.286	58.182	
9.4	0.085	0.3987	1.383	0.295	58.108	54.237	
9.4	0.083	0.3987	1.321	0.275	62.192	58.182	
9.4	0.087	0.3987	1.467	0.320	52.859	50.000	
9.4	0.094	0.3987	1.710	0.403	42.033	39.702	[1]
9.4	0.091	0.3987	1.614	0.368	45.677	43.478	
9.4	0.085	0.3987	1.402	0.299	56.543	53.512	
9.4	0.086	0.3987	1.419	0.306	55.846	52.288	
9.4	0.097	0.3987	1.828	0.445	37.956	35.955	
9.4	0.089	0.3987	1.535	0.343	49.389	46.647	
9.4	0.084	0.3987	1.355	0.285	59.822	56.140*	[1]
21.0	0.087	0.2398	2.411	0.875	19.570	19.859	
21.0	0.092	0.2398	2.679	1.028	16.761	17.089	
21.0	0.090	0.2398	2.591	0.972	17.529	18.004	
21.0	0.091	0.2398	2.586	0.981	17.793	17.850	
21.0	0.079	0.2398	1.931	0.636	27.703	25.157	[1]
21.0	0.095	0.2398	2.822	1.118	15.598	15.809	
21.0	0.095	0.2398	2.804	1.111	15.799	15.901	
21.0	0.089	0.2398	2.459	0.913	19.246	19.086	
21.0	0.089	0.2398	2.515	0.933	18.398	18.704	
21.0	0.099	0.2398	3.103	1.281	13.444	13.942	
21.0	0.084	0.2398	2.215	0.776	22.387	22.222*	
30.0	0.089	0.1722	3.318	1.715	10.571	10.683	
30.0	0.088	0.1722	3.225	1.648	11.063	11.075	
30.0	0.085	0.1722	2.972	1.467	12.583	12.312	
30.0	0.084	0.1722	2.961	1.444	12.527	12.491	
30.0	0.095	0.1722	3.683	2.032	9.158	9.173	
30.0	0.090	0.1722	3.304	1.727	10.780	10.616	
30.0	0.089	0.1722	3.291	1.701	10.745	10.762	
30.0	0.087	0.1722	3.144	1.588	11.508	11.454	
30.0	0.084	0.1722	2.931	1.430	12.785	12.603	
30.0	0.091	0.1722	3.478	1.838	9.837	10.036	
30.0	0.084	0.1722	2.939	1.434	12.716	12.571*	

Table 7. Continued

Temp [°C]	d [cm]	ν [cm²/s]	V_c [cm/s]	Re	C_D	$C_{D,calc}$
40.0	0.081	0.1245	3.321	2.161	9.603	8.684
40.0	0.086	0.1245	3.829	2.645	7.670	7.269
40.0	0.086	0.1245	3.825	2.642	7.686	7.277
40.0	0.083	0.1245	3.549	2.366	8.616	8.015
40.0	0.087	0.1245	3.947	2.758	7.302	7.010
40.0	0.087	0.1245	3.871	2.705	7.592	7.129
40.0	0.088	0.1245	4.036	2.853	7.064	6.807
40.0	0.082	0.1245	3.461	2.280	8.951	8.281
40.0	0.089	0.1245	4.191	2.996	6.625	6.526
40.0	0.086	0.1245	3.815	2.635	7.726	7.293
40.0	0.084	0.1245	3.634	2.452	8.317	7.767*
50.0	0.076	0.0924	3.658	3.009	7.427	6.501
50.0	0.084	0.0924	4.498	4.089	5.429	5.016
50.0	0.076	0.0924	3.638	2.992	7.508	6.533
50.0	0.083	0.0924	4.459	4.005	5.458	5.103
50.0	0.081	0.0924	4.148	3.636	6.156	5.534
50.0	0.077	0.0924	3.685	3.071	7.414	6.389
50.0	0.089	0.0924	5.027	4.842	4.605	4.365
50.0	0.084	0.0924	4.702	4.275	4.968	4.834
50.0	0.079	0.0924	4.172	3.567	5.935	5.624
50.0	0.091	0.0924	5.245	5.166	4.325	4.141
50.0	0.084	0.0924	4.538	4.125	5.333	4.980*
60.0	0.077	0.0712	4.568	4.940	4.825	4.294
60.0	0.081	0.0712	5.081	5.780	4.102	3.784
60.0	0.078	0.0712	4.797	5.255	4.432	4.084
60.0	0.077	0.0712	4.611	4.987	4.735	4.261
60.0	0.089	0.0712	5.950	7.438	3.287	3.101
60.0	0.079	0.0712	4.808	5.335	4.468	4.035
60.0	0.080	0.0712	4.952	5.564	4.266	3.901
60.0	0.077	0.0712	4.587	4.961	4.785	4.279
60.0	0.072	0.0712	4.152	4.199	5.461	4.907
60.0	0.083	0.0712	5.370	6.260	3.763	3.551
60.0	0.084	0.0712	5.405	6.377	3.760	3.500*

Table 7. Continued

Temp [°C]	d [cm]	ν [cm²/s]	V_c [cm/s]	Re	C_D	$C_{D,calc}$
70.0	0.075	0.0572	5.078	6.658	3.803	3.383
70.0	0.071	0.0572	4.581	5.686	4.424	3.834
70.0	0.069	0.0572	4.258	5.136	4.976	4.161
70.0	0.080	0.0572	5.787	8.094	3.124	2.904
70.0	0.077	0.0572	5.309	7.147	3.572	3.200
70.0	0.076	0.0572	5.250	6.976	3.605	3.261
70.0	0.076	0.0572	5.238	6.960	3.622	3.267
70.0	0.070	0.0572	4.508	5.517	4.504	3.928
70.0	0.080	0.0572	5.810	8.126	3.099	2.895
70.0	0.080	0.0572	5.833	8.158	3.074	2.887
70.0	0.084	0.0572	6.330	9.296	2.741	2.609*
80.0	0.083	0.0471	7.005	12.344	2.212	2.095
80.0	0.075	0.0471	5.636	8.975	3.087	2.681
80.0	0.073	0.0471	5.445	8.439	3.219	2.812
80.0	0.066	0.0471	4.209	5.898	4.871	3.723
80.0	0.081	0.0471	6.631	11.404	2.409	2.228
80.0	0.080	0.0471	6.349	10.784	2.595	2.327
80.0	0.077	0.0471	6.016	9.835	2.782	2.498
80.0	0.070	0.0471	4.986	7.410	3.682	3.111
80.0	0.078	0.0471	6.263	10.372	2.600	2.398
80.0	0.077	0.0471	6.263	10.190	2.694	2.431
80.0	0.084	0.0471	7.136	12.727	2.157	2.045*

Table 8. Experimental Conditions, Dimensionless Groups, and Velocities of Bubbles Rising in Mobil Ester P-41.

Temp [°C]	d [cm]	ν [cm²/s]	V_c [cm/s]	Re	C_D	$C_{D,calc}$	
20.7	0.074	0.3120	1.406	0.333	48.946	48.048	
20.7	0.083	0.3120	1.799	0.479	33.533	33.403	
20.7	0.079	0.3120	1.632	0.413	38.783	38.741	
20.7	0.086	0.3120	1.934	0.533	30.064	30.019	1
20.7	0.085	0.3120	1.884	0.513	31.312	31.189	
20.7	0.086	0.3120	1.942	0.535	29.817	29.907	
20.7	0.100	0.3120	2.592	0.831	19.462	20.841	
20.7	0.090	0.3120	2.107	0.608	26.508	26.316	
20.7	0.086	0.3120	1.907	0.526	30.921	30.418	1
20.7	0.084	0.3120	1.837	0.495	32.548	32.323	
20.7	0.084	0.3120	1.845	0.497	32.266	32.193*[1]	
30.2	0.085	0.2136	2.549	1.014	17.106	17.309	
30.2	0.092	0.2136	3.015	1.299	13.233	13.764	
30.2	0.087	0.2136	2.650	1.079	16.199	16.338	
30.2	0.090	0.2136	2.852	1.202	14.468	14.785	
30.2	0.097	0.2136	3.320	1.508	11.507	12.006	
30.2	0.092	0.2136	2.971	1.280	13.628	13.952	
30.2	0.089	0.2136	2.782	1.198	15.543	14.830	
30.2	0.084	0.2136	2.531	0.995	17.146	17.616	
30.2	0.083	0.2136	2.447	0.951	18.125	18.374	
30.2	0.096	0.2136	3.224	1.449	12.076	12.452	
30.2	0.084	0.2136	2.496	0.982	17.630	17.833*	
39.8	0.084	0.1539	3.263	1.781	10.316	10.325	
39.8	0.088	0.1539	3.573	2.043	9.013	9.129	
39.8	0.085	0.1539	3.318	1.833	10.095	10.061	
39.8	0.086	0.1539	3.402	1.901	9.716	9.737	
39.8	0.092	0.1539	3.860	2.307	8.074	8.196	
39.8	0.080	0.1539	2.957	1.537	11.963	11.800	
39.8	0.094	0.1539	4.112	2.512	7.269	7.604	
39.8	0.094	0.1539	4.124	2.519	7.227	7.586	
39.8	0.091	0.1539	3.832	2.266	8.103	8.326	
39.8	0.089	0.1539	3.636	2.103	8.802	8.897	
39.8	0.084	0.1539	3.253	1.776	10.379	10.351*	
49.6	0.078	0.1134	3.435	2.363	8.644	8.024	
49.6	0.089	0.1134	4.439	3.484	5.906	5.737	
49.6	0.070	0.1134	2.752	1.699	12.085	10.774	
49.6	0.077	0.1134	3.411	2.316	8.653	8.167	
49.6	0.094	0.1134	4.942	4.097	5.032	5.008	
49.6	0.092	0.1134	4.731	3.838	5.375	5.288	
49.6	0.090	0.1134	4.629	3.674	5.492	5.486	
49.6	0.094	0.1134	5.013	4.155	4.891	4.950	

Table 8. Continued

Temp [°C]	d [cm]	ν [cm²/s]	V_c [cm/s]	Re	C_D	$C_{D,calc}$
49.6	0.077	0.1134	3.369	2.288	8.871	8.256
49.6	0.096	0.1134	5.183	4.388	4.673	4.731
49.6	0.084	0.1134	4.032	2.987	6.756	6.543*
59.5	0.079	0.0857	4.334	3.995	5.499	5.114
59.5	0.083	0.0857	4.787	4.636	4.736	4.523
59.5	0.075	0.0857	3.900	3.413	6.448	5.838
59.5	0.078	0.0857	4.183	3.807	5.829	5.324
59.5	0.083	0.0857	4.823	4.671	4.666	4.495
59.5	0.074	0.0857	3.813	3.292	6.655	6.020
59.5	0.084	0.0857	4.939	4.841	4.503	4.365
59.5	0.083	0.0857	4.812	4.660	4.687	4.503
59.5	0.080	0.0857	4.473	4.175	5.228	4.930
59.5	0.094	0.0857	6.084	6.673	3.321	3.377
59.5	0.084	0.0857	4.925	4.827	4.528	4.376*
69.5	0.084	0.0670	5.755	7.215	3.316	3.176
69.5	0.085	0.0670	5.977	7.583	3.111	3.055
69.5	0.080	0.0670	5.270	6.293	3.766	3.537
69.5	0.075	0.0670	4.596	5.145	4.643	4.155
69.5	0.070	0.0670	4.029	4.209	5.638	4.897
69.5	0.080	0.0670	5.258	6.278	3.784	3.543
69.5	0.086	0.0670	6.079	7.803	3.043	2.988
69.5	0.078	0.0670	5.101	5.938	3.920	3.703
69.5	0.082	0.0670	5.576	6.824	3.448	3.318
69.5	0.075	0.0670	4.544	5.087	4.749	4.193
69.5	0.084	0.0670	5.807	7.280	3.257	3.154*
79.5	0.065	0.0557	3.962	4.624	5.414	4.532
79.5	0.087	0.0557	7.069	11.041	2.276	2.285
79.5	0.084	0.0557	6.524	9.839	2.581	2.498
79.5	0.085	0.0557	6.758	10.313	2.434	2.409
79.5	0.083	0.0557	6.463	9.631	2.598	2.539
79.5	0.071	0.0557	4.673	5.957	4.251	3.694
79.5	0.077	0.0557	5.636	7.791	3.170	2.992
79.5	0.083	0.0557	6.361	9.479	2.682	2.570
79.5	0.084	0.0557	6.714	10.125	2.437	2.443
79.5	0.087	0.0557	7.033	10.985	2.300	2.294
79.5	0.084	0.0557	6.602	9.956	2.520	2.475*

Table 9. Experimental Conditions, Dimensionless Groups, and Velocities of Bubbles Rising in Emolein 2917 + 5%(w/w) 2,6,8 Trimethyl-4-nonanol.

Temp [°C]	d [cm]	ν [cm²/s]	V_c [cm/s]	Re	C_D	$C_{D,calc}$
21.0	0.072	0.1580	2.347	1.070	17.091	16.466
21.0	0.091	0.1580	3.695	2.128	8.715	8.804
21.0	0.081	0.1580	3.018	1.547	11.628	11.730
21.0	0.087	0.1580	3.449	1.899	9.563	9.746
21.0	0.082	0.1580	3.050	1.583	11.526	11.487
21.0	0.085	0.1580	3.251	1.749	10.516	10.495
21.0	0.082	0.1580	2.986	1.550	12.025	11.710
21.0	0.088	0.1580	3.477	1.937	9.518	9.574
21.0	0.099	0.1580	4.343	2.721	6.863	7.092
21.0	0.081	0.1580	2.961	1.518	12.080	11.934
21.0	0.084	0.1580	3.199	1.701	10.733	10.762*
30.2	0.093	0.1160	4.617	3.702	5.705	5.451
30.2	0.080	0.1160	3.419	2.358	8.949	8.039
30.2	0.091	0.1160	4.509	3.537	5.852	5.664
30.2	0.089	0.1160	4.327	3.320	6.215	5.977
30.2	0.096	0.1160	5.101	4.222	4.824	4.885
30.2	0.090	0.1160	4.620	3.584	5.513	5.601
30.2	0.094	0.1160	4.905	3.975	5.109	5.136
30.2	0.092	0.1160	4.762	3.777	5.305	5.360
30.2	0.097	0.1160	5.187	4.337	4.714	4.777
30.2	0.090	0.1160	4.452	3.454	5.937	5.779
30.2	0.084	0.1160	3.846	2.785	7.425	6.951*
50.0	0.088	0.0657	6.918	9.266	2.404	2.616
50.0	0.078	0.0657	5.527	6.562	3.339	3.422
50.0	0.077	0.0657	5.330	6.247	3.544	3.557
50.0	0.094	0.0657	7.391	10.575	2.250	2.362
50.0	0.093	0.0657	7.328	10.373	2.264	2.398
50.0	0.091	0.0657	7.030	9.737	2.408	2.518
50.0	0.074	0.0657	4.917	5.538	4.002	3.916
50.0	0.088	0.0657	6.603	8.844	2.639	2.712
50.0	0.093	0.0657	7.364	10.424	2.242	2.389
50.0	0.084	0.0657	5.972	7.635	3.080	3.039
50.0	0.084	0.0657	6.188	7.912	2.868	2.956*

Table 10. Experimental Conditions, Dimensionless Groups, and Velocities of Bubbles Rising in Emolein 2917 + 5%(w/w) Poly(propylene glycol), M_w= 4000.

Temp [°C]	d [cm]	ν [cm²/s]	V_c [cm/s]	Re	C_D	$C_{D,calc}$
21.2	0.087	0.2202	2.636	1.041	16.867	16.891
21.2	0.086	0.2202	2.597	1.014	16.673	17.309
21.2	0.096	0.2202	3.250	1.417	11.884	12.709
21.2	0.086	0.2202	2.616	1.022	16.432	17.183
21.2	0.088	0.2202	2.718	1.086	15.576	16.240
21.2	0.103	0.2202	3.727	1.743	9.696	10.528
21.2	0.084	0.2202	2.498	0.953	17.602	18.338
21.2	0.088	0.2202	2.749	1.099	15.226	16.062
21.2	0.095	0.2202	3.153	1.360	12.495	13.196
21.2	0.098	0.2202	3.351	1.491	11.411	12.131
21.2	0.084	0.2202	2.472	0.943	17.974	18.519*
30.0	0.095	0.1628	3.964	2.313	7.905	8.177
30.0	0.078	0.1628	2.681	1.285	14.189	13.902
30.0	0.087	0.1628	3.379	1.806	9.963	10.196
30.0	0.084	0.1628	3.047	1.572	11.830	11.560
30.0	0.100	0.1628	4.378	2.689	6.822	7.166
30.0	0.098	0.1628	4.167	2.508	7.380	7.615
30.0	0.092	0.1628	3.721	2.103	8.688	8.897
30.0	0.099	0.1628	4.306	2.619	6.981	7.332
30.0	0.100	0.1628	4.369	2.684	6.850	7.177
30.0	0.083	0.1628	3.048	1.554	11.682	11.682
30.0	0.084	0.1628	3.115	1.607	11.331	11.331*
40.0	0.080	0.1196	3.902	2.610	6.870	7.354
40.0	0.099	0.1196	5.660	4.685	4.041	4.484
40.0	0.087	0.1196	4.412	3.209	5.844	6.153
40.0	0.091	0.1196	4.836	3.680	5.088	5.478
40.0	0.089	0.1196	4.562	3.395	5.592	5.864
40.0	0.080	0.1196	3.724	2.491	7.543	7.661
40.0	0.085	0.1196	4.230	3.006	6.212	6.507
40.0	0.085	0.1196	4.226	3.003	6.223	6.513
40.0	0.086	0.1196	4.328	3.112	6.003	6.316
40.0	0.085	0.1196	4.176	2.968	6.373	6.579
40.0	0.084	0.1196	4.143	2.910	6.399	6.692*
50.0	0.099	0.0912	6.294	6.832	3.268	3.315
50.0	0.090	0.0912	5.369	5.298	4.082	4.058
50.0	0.089	0.0912	5.557	5.423	3.769	3.982
50.0	0.078	0.0912	4.214	3.604	5.743	5.575
50.0	0.100	0.0912	6.566	7.200	3.033	3.181
50.0	0.078	0.0912	4.136	3.537	5.962	5.664
50.0	0.100	0.0912	6.367	6.981	3.225	3.259

Table 10. Continued

Temp [°C]	d [cm]	ν [cm²/s]	V_c [cm/s]	Re	C_D	$C_{D,calc}$
50.0	0.098	.0.0912	6.221	6.685	3.311	3.372
50.0	0.079	0.0912	4.133	3.580	6.047	5.607
50.0	0.097	0.0912	5.973	6.353	3.555	3.510
50.0	0.084	0.0912	4.780	4.403	4.807	4.718*
60.0	0.084	0.0720	5.240	6.113	4.000	3.619
60.0	0.084	0.0720	5.473	6.385	3.667	3.496
60.0	0.077	0.0720	4.378	4.682	5.253	4.486
60.0	0.088	0.0720	5.818	7.111	3.399	3.212
60.0	0.078	0.0720	4.534	4.912	4.961	4.314
60.0	0.088	0.0720	5.847	7.146	3.366	3.200
60.0	0.086	0.0720	5.640	6.737	3.535	3.351
60.0	0.081	0.0720	4.965	5.586	4.296	3.889
60.0	0.074	0.0720	4.098	4.212	5.762	4.894
60.0	0.081	0.0720	5.093	5.730	4.083	3.810
60.0	0.084	0.0720	5.352	6.244	3.834	3.559*
65.2	0.088	0.0644	6.438	8.797	2.776	2.723
65.2	0.084	0.0644	6.012	7.812	3.039	2.985
65.2	0.080	0.0644	5.491	6.821	3.469	3.319
65.2	0.087	0.0644	6.530	8.822	2.668	2.717
65.2	0.084	0.0644	6.148	8.019	2.906	2.925
65.2	0.083	0.0644	5.919	7.629	3.098	3.041
65.2	0.091	0.0644	7.064	9.982	2.385	2.470
65.2	0.082	0.0644	5.809	7.397	3.177	3.115
65.2	0.085	0.0644	6.309	8.327	2.792	2.841
65.2	0.095	0.0644	7.676	11.323	2.108	2.241
65.2	0.084	0.0644	6.071	7.919	2.980	2.954*
79.5	0.067	0.0492	4.293	5.846	4.753	3.750
79.5	0.070	0.0492	4.840	6.886	3.907	3.294
79.5	0.081	0.0492	6.355	10.463	2.622	2.382
79.5	0.074	0.0492	5.437	8.178	3.273	2.881
79.5	0.079	0.0492	5.936	9.531	2.932	2.560
79.5	0.089	0.0492	7.621	13.786	2.004	1.920
79.5	0.074	0.0492	5.497	8.268	3.202	2.857
79.5	0.066	0.0492	4.213	5.652	4.862	3.852
79.5	0.084	0.0492	6.975	11.909	2.258	2.154
79.5	0.072	0.0492	5.114	7.484	3.600	3.087
79.5	0.084	0.0492	6.869	11.728	2.328	2.180*

Table 11. Experimental Conditions, Dimensionless Groups, and Velocities of Bubbles Rising in Mobil Ester P-41 + 5%(w/w) N Phenyl-1-naphthylamine.

Temp [°C]	d [cm]	ν [cm²/s]	V_c [cm/s]	Re	C_D	$C_{D,calc}$	
20.7	0.084	0.3608	1.000	0.233	109.834	103.004	
20.7	0.087	0.3608	1.176	0.284	82.255	84.507	
20.7	0.081	0.3608	0.953	0.214	116.616	112.150	
20.7	0.091	0.3608	1.280	0.323	72.624	74.303	
20.7	0.087	0.3608	1.221	0.294	76.304	81.633	2
20.7	0.091	0.3608	1.419	0.358	59.093	67.039	
20.7	0.084	0.3608	1.085	0.253	93.299	94.862	
20.7	0.091	0.3608	1.346	0.339	65.677	70.796	
20.7	0.084	0.3608	1.053	0.245	99.056	97.959	
20.7	0.086	0.3608	1.145	0.273	85.772	87.912	
20.7	0.084	0.3608	1.060	0.247	97.752	97.166	*2
30.2	0.081	0.2418	1.345	0.451	58.546	53.215	
30.2	0.085	0.2418	1.565	0.550	45.378	43.636	
30.2	0.088	0.2418	1.809	0.658	35.161	36.474	
30.2	0.080	0.2418	1.264	0.418	65.472	57.416	
30.2	0.092	0.2418	1.974	0.751	30.871	31.957	2
30.2	0.085	0.2418	1.580	0.555	44.521	43.243	
30.2	0.083	0.2418	1.522	0.522	46.850	45.977	
30.2	0.083	0.2418	1.538	0.528	45.880	45.455	
30.2	0.084	0.2418	1.589	0.552	43.500	43.478	
30.2	0.084	0.2418	1.550	0.538	45.717	44.610	
30.2	0.084	0.2418	1.554	0.540	45.482	44.444	*2
39.8	0.083	0.1717	1.994	0.964	27.295	26.896	
39.8	0.080	0.1717	1.828	0.852	31.304	30.169	
39.8	0.086	0.1717	2.295	1.150	21.350	22.870	
39.8	0.091	0.1717	2.580	1.367	17.876	19.557	
39.8	0.079	0.1717	1.796	0.826	32.024	31.056	3
39.8	0.091	0.1717	2.655	1.407	16.880	19.058	
39.8	0.083	0.1717	2.138	1.034	23.742	25.211	
39.8	0.085	0.1717	2.267	1.122	21.626	23.390	
39.8	0.086	0.1717	2.240	1.122	22.411	23.390	
39.8	0.084	0.1717	2.279	1.115	21.147	23.525	
39.8	0.084	0.1717	2.146	1.050	23.849	24.857	*
49.6	0.088	0.1249	3.098	2.183	11.989	12.994	
49.6	0.085	0.1249	2.716	1.848	15.067	14.987	
49.6	0.086	0.1249	3.021	2.080	12.321	13.538	
49.6	0.086	0.1249	2.871	1.977	13.642	14.140	3
49.6	0.082	0.1249	2.692	1.767	14.795	15.582	
49.6	0.087	0.1249	3.107	2.164	11.784	13.091	
49.6	0.084	0.1249	2.750	1.849	14.524	14.980	

Table 11. Continued

Temp [°C]	d [cm]	ν [cm²/s]	V_c [cm/s]	Re	C_D	$C_{D,calc}$	
49.6	0.077	0.1249	2.016	1.243	24.772	21.308	
49.6	0.091	0.1249	3.341	2.434	10.660	11.860	3
49.6	0.085	0.1249	2.853	1.942	13.654	14.358	
49.6	0.084	0.1249	2.735	1.839	14.683	15.051	*3
59.5	0.083	0.0932	3.029	2.698	11.829	10.895	
59.5	0.090	0.0932	3.935	3.800	7.600	8.316	
59.5	0.087	0.0932	3.426	3.198	9.692	9.505	
59.5	0.087	0.0932	3.616	3.375	8.700	9.111	
59.5	0.090	0.0932	3.823	3.692	8.052	8.501	3
59.5	0.084	0.0932	3.105	2.798	11.392	10.578	
59.5	0.083	0.0932	3.133	2.790	11.056	10.602	
59.5	0.087	0.0932	3.536	3.301	9.098	9.271	
59.5	0.087	0.0932	3.653	3.410	8.525	9.038	
59.5	0.084	0.0932	3.198	2.882	10.739	10.328	
59.5	0.084	0.0932	3.200	2.884	10.726	10.322	*3
69.5	0.079	0.0718	3.269	3.597	9.666	8.672	
69.5	0.074	0.0718	2.744	2.828	12.851	10.487	
69.5	0.089	0.0718	4.382	5.432	6.060	6.418	
69.5	0.087	0.0718	4.011	4.860	7.071	6.938	
69.5	0.085	0.0718	4.210	4.984	6.271	6.815	3
69.5	0.083	0.0718	3.686	4.261	7.988	7.632	
69.5	0.086	0.0718	3.784	4.532	7.853	7.296	
69.5	0.083	0.0718	3.750	4.335	7.717	7.536	
69.5	0.090	0.0718	4.245	5.321	6.531	6.510	
69.5	0.085	0.0718	4.001	4.737	6.943	7.066	
69.5	0.084	0.0718	3.808	4.455	7.574	7.387	*3
79.5	0.081	0.0586	4.130	5.709	6.209	6.204	
79.5	0.092	0.0586	5.606	8.801	3.828	4.727	
79.5	0.083	0.0586	4.144	5.869	6.320	6.089	
79.5	0.075	0.0586	3.211	4.110	9.511	7.839	
79.5	0.088	0.0586	5.274	7.920	4.137	5.030	3
79.5	0.078	0.0586	3.620	4.818	7.783	6.981	
79.5	0.078	0.0586	3.584	4.771	7.940	7.030	
79.5	0.080	0.0586	3.781	5.162	7.317	6.649	
79.5	0.085	0.0586	4.736	6.870	4.955	5.493	
79.5	0.087	0.0586	5.123	7.606	4.334	5.155	
79.5	0.084	0.0586	4.500	6.451	5.424	5.720	*3

Table 12. Experimental Conditions, Dimensionless Groups, and Interpolated Velocities of Bubbles (diameter = 0.084 cm) Rising in Various Solutions.

	Temp [°C]	ν [cm²/s]	V_c [cm/s]	Re	C_D	$C_{D,calc}$
a	20.0	0.1760	2.988	1.426	12.302	12.635
	50.0	0.0727	5.509	6.365	3.619	3.505
b	9.4	0.3987	1.355	0.285	59.822	56.140[1]
	21.0	0.2398	2.215	0.776	22.387	22.222
	30.0	0.1722	2.939	1.434	12.716	12.571
	40.0	0.1245	3.634	2.452	8.317	7.767
	50.0	0.0924	4.538	4.125	5.333	4.980
	60.0	0.0712	5.405	6.377	3.760	3.500
	70.0	0.0572	6.330	9.296	2.741	2.609
	80.0	0.0471	7.136	12.727	2.157	2.045
c	20.7	0.3120	1.845	0.497	32.266	32.193[1]
	30.2	0.2136	2.496	0.982	17.630	17.833
	39.8	0.1539	3.253	1.776	10.379	10.351
	49.6	0.1134	4.032	2.987	6.756	6.543
	59.5	0.0857	4.925	4.827	4.528	4.376
	69.5	0.0670	5.807	7.280	3.257	3.154
	79.5	0.0557	6.602	9.956	2.520	2.475
d	21.0	0.1580	3.199	1.701	10.733	10.762
	30.2	0.1160	3.846	2.785	7.425	6.951
	50.0	0.0657	6.188	7.912	2.868	2.956
e	21.2	0.2202	2.472	0.943	17.974	18.519
	30.0	0.1628	3.115	1.607	11.331	11.331
	40.0	0.1196	4.143	2.910	6.399	6.692
	50.0	0.0912	4.780	4.403	4.807	4.718
	60.0	0.0720	5.352	6.244	3.834	3.559
	65.2	0.0644	6.071	7.919	2.980	2.954
	79.5	0.0492	6.869	11.728	2.328	2.180
f	14.1	0.480	1.254	0.219	69.888	73.059[1]
	20.0	0.365	1.637	0.377	41.013	42.440[1]
	29.9	0.244	2.351	0.809	19.875	21.371
	39.6	0.168	3.059	1.529	11.740	11.856
	49.5	0.120	3.846	2.692	7.427	7.159
	59.4	0.093	4.814	4.349	4.739	4.766
	68.6	0.075	5.823	6.529	3.232	3.435

Table 12. Continued.

	Temp [°C]	ν [cm²/s]	V_c [cm/s]	Re	C_D	$C_{D,calc}$
g	14.1	0.532	0.974	0.154	115.831	103.896[1]
	20.0	0.407	1.312	0.271	63.836	59.041[1]
	29.9	0.265	1.945	0.616	29.037	25.974[1]
	39.6	0.183	2.626	1.205	15.932	14.751
	49.5	0.129	3.244	2.112	10.439	8.863
	59.4	0.098	4.349	3.728	5.806	5.419
	68.6	0.077	5.401	5.892	3.766	3.726
h	14.1	0.560	0.978	0.147	114.716	108.843[1]
i	20.0	0.370	1.514	0.344	47.909	46.512[1]
	39.6	0.170	3.021	1.493	12.033	12.116
j	20.7	0.3608	1.060	0.247	97.752	97.166[2]
	30.2	0.2418	1.554	0.540	45.482	44.444[2]
	39.8	0.1717	2.146	1.050	23.849	24.857
	49.6	0.1249	2.735	1.839	14.683	15.051
	59.5	0.0932	3.200	2.884	10.726	10.322 [3]
	69.5	0.0718	3.808	4.455	7.574	7.387
	79.5	0.0586	4.500	6.451	5.424	5.720

a is Emolein 2917
b is 0-77-10 Blended Ester
c is Mobil Ester P-41
d is Emolein 2917 + 5%(w/w) 2,6,8 Trimethyl-4-nonanol
e is Emolein 2917 + 5%(w/w) Poly(propylene glycol) M_w= 4000
f is Hercolube C
g is Hercolube C + 5.16%(w/w) N-Phenyl-1-naphthylamine (Lot A13B)
h is Hercolube C + 4.74%(w/w) N-Phenyl-1-naphthylamine (Lot A13B) + 8.29%(w/w) Tricresyl phosphate
i is Mobil P-41 + 4.99%(w/w) N-Phenyl-1-naphthylamine (Lot A13B)
j is Mobil P-41 + 5%(w/w) N-Phenyl-1-naphthylamine (Lot A12A)

AD-A163 696 LUBRICANT FOAMING AND AERATION STUDY PART 2(U) 2/2
RENSSELAER POLYTECHNIC INST TROY NY S ROSS DEC 85
AFWAL-TR-84-2001-PT-2 F33615-80-C-2017

UNCLASSIFIED F/G 11/8 NL

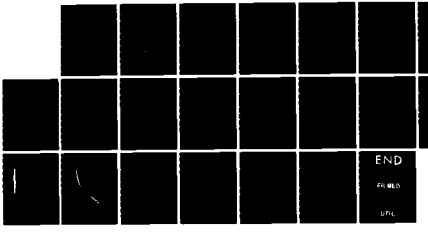

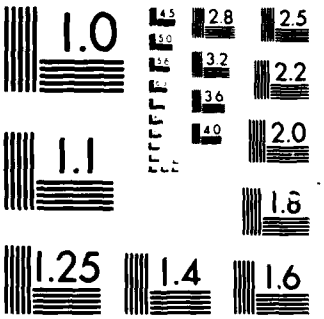

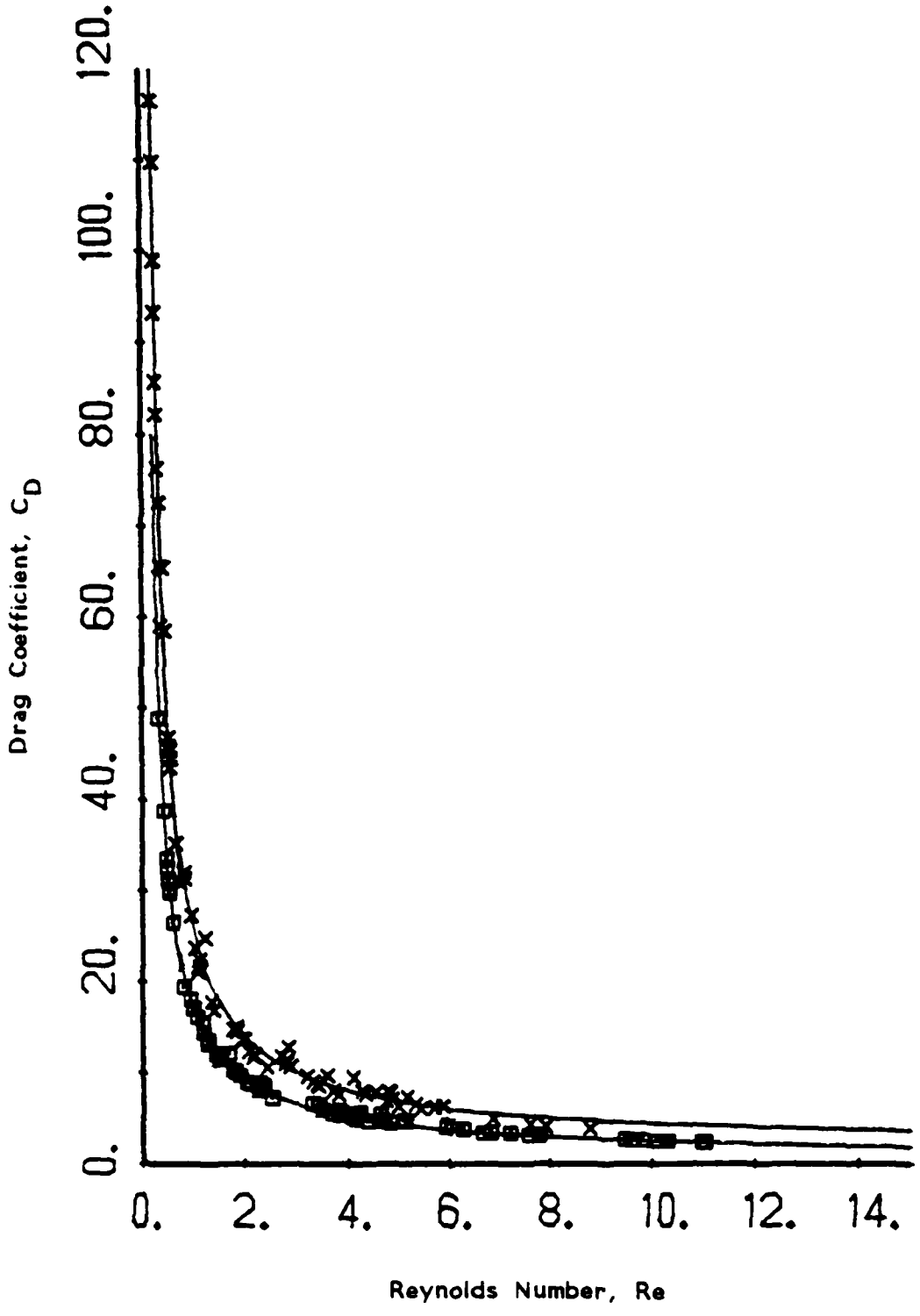

Figure 35. Variation of Drag Coefficient C_D with Reynolds Number Re. Solid Lines are Theoretical Equations; Points are Observational Data. The Lower Curve Refers to Mobil Ester P-41 and the Upper Curve Refers to Mobil Ester P-41 + 5%(w/w) N Phenyl-1-naphthylamine

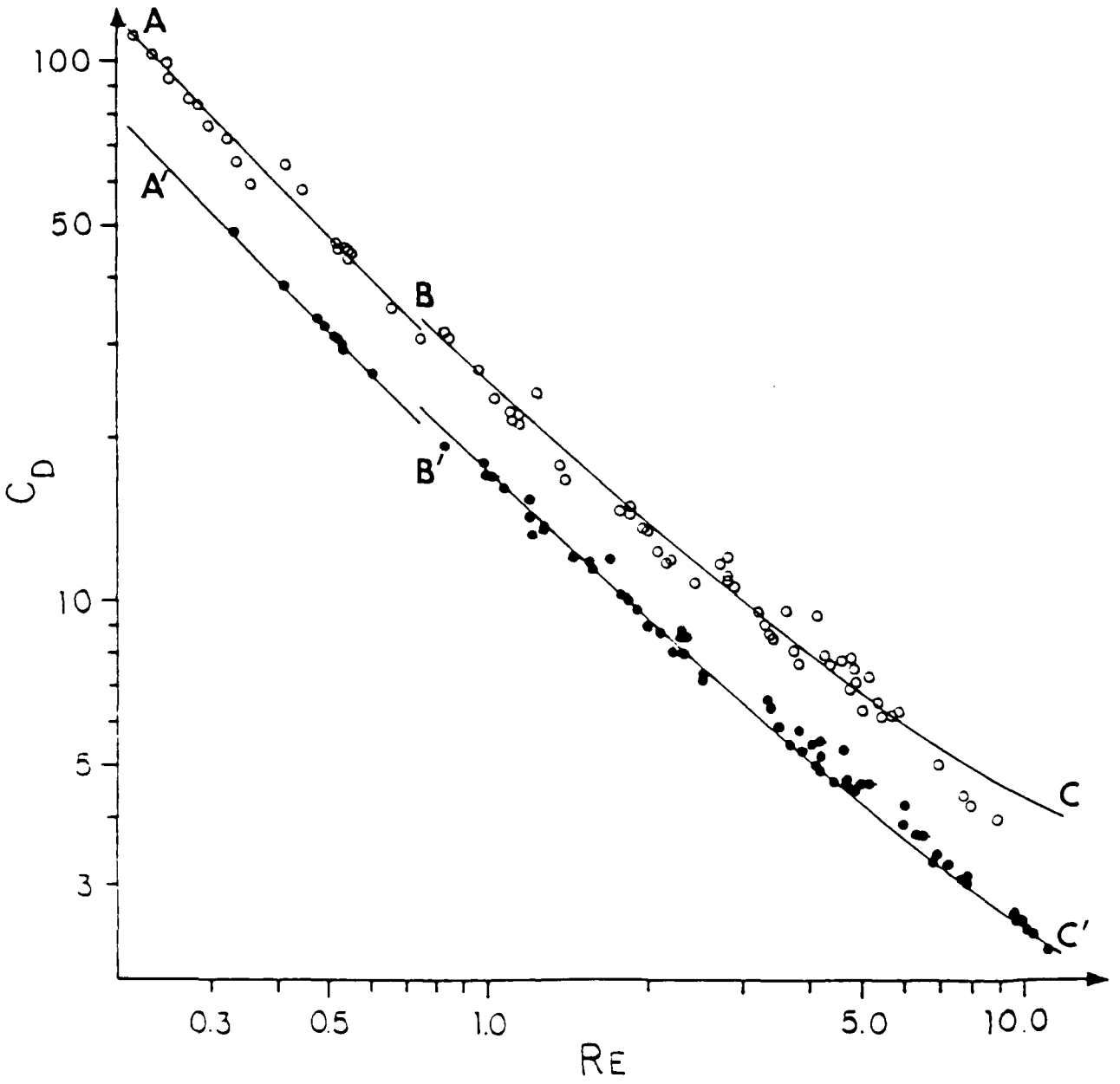

Figure 36. Variation of Drag Coefficient C_D with Reynolds Number Re on Logarithmic Scales. Solid Lines are Theoretical Equations; Points are Observational Data, the same as in Figure 35. AB is Stokes' Law, Equation [23]; BC is Equation [26]; A'B' is Rybczynski-Hadamard Law, Equation [24]; B'C' is Ryskin-Leal Theory, Equation [25].

two cases of bubbles with a rigid and with a fluid interface; Figure 36 shows the same data on a log-log plot, in which the two cases are better distinguished visually. As can be seen in Figure 36, the experimental data conform to the theoretical description of a fluid or a rigid interface, whichever happens to occur in the system observed.

The Mobil Ester P-41 is typical of oil solutions in which the air/liquid interface is fluid; and the data for the solution of N-phenyl-1-naphthylamine (Lot A12A) in Mobil Ester P-41 show that the solute has caused the interface to become effectively rigid under the dynamic conditions of the experiment. Our supplies of the additive N-phenyl-1-naphthylamine were obtained from Eastman Kodak Co. from lots manufactured in 1981, 1982, and 1983. The results of our foam tests reveal that samples from the 1981 lots produced copious foam when dissolved in tmp-heptanoate; that samples from the 1982 lots produced foam synergistically when in an admixture containing tricresyl phosphate, but did not produce foam when used as a sole solute; and that samples from the 1983 lots neither foamed as sole solutes nor in combination with tricresyl phosphate. It seems, therefore, that the manufacturer has gradually improved the purification of this additive. This point is further substantiated by the data reported in Table 13, in which the results of measurements of bubble rise in solutions of different lots of N-phenyl-1-naphthylamine in Mobil Ester P-41 are compared.

Subsequent tests with a different batch of N-phenyl-1-naphthylamine (Lot A13B) from the same supply house (Eastman Kodak Co.) and used at the same concentration of 4.99% w/w, disclosed it to have no effect on the oil Mobil Ester P-41 (see (i) above). The surface activity reported in Figures 35 and 36 for this solute is, therefore, probably due to an impurity in the solute, perhaps a trace of silicone antifoam, which is known to act synergistically as a profoamer with N-phenyl-1-naphthylamine in these synthetic lubricants (see This Report, Part 2, Sections III and IV.)

None of the above oil solutions in which additives had been purposely dissolved showed any measurable reduction of the equilibrium surface tension of the solvent by the additive. This is true even of the system for which a rigid interface was observed. It seems, therefore, that the inability of a solute to reduce the equilibrium surface tension of an oil solution below that of the oil does not necessarily indicate the absence of surface activity. Even the present test, that is, the rate of ascent of a single bubble, is not a definitive indicator of the absence of surface activity in an oil solution. Foam tests showed that some of these solutions for which a fluid interface is demonstrated, are able to stabilize bubbles, albeit briefly; and also that the system for which a rigid interface was observed produced no foam by a standard foam test.[28]

Dynamic surface tension is manifested throughout a wide range

[28] S. Ross and Y. Suzin, Langmuir, 1, 145 (1985).

Table 13. Comparison of Bubble Rise Results with different Lots of N-phenyl-1-naphthylamine

Lot	T (°C)	ν (cm²/s)	d (cm)	V_c (cm/s)	Re	C_D	$C_{D,Theory}$	$C_D/C_{D,Theory}$
A12A	30.2	0.2418	0.084	1.554	0.540	45.482	29.630	1.54 Rigid
B12A	30.1	0.2423	0.084	1.989	0.689	27.775	23.222	1.20
A13B	20.0	0.3736	0.084	1.514	0.340	47.917	47.059	1.02 Fluid

of time scales, depending on various mechanisms of relaxation after the surface has been dilatated or contracted. A test for the effect, such as the present one, may well fail to report its existence if the time required for the operation of the test is much longer than the time required for the system to equilibrate. That appears to have been the case with some of those oil solutions of the present study for which fluid interfaces were demonstrated.

5. Supplemental Results: Rate of Bubble Rise in the Blended Ester 0-77-10, in Solutions of different Additives in 0-77-10 Lubricant, and in Test Lubricant TEL-4041

A sample of 0-77-10 lubricant, supplied by Mr Phillip W. Centers of the Lubrication Branch of the Aero Propulsion Laboratory, is described as a blend of tmp-heptanoate and neopentyl glycol esters of monobasic acids. Our first experiments were to determine if the lubricant exhibited any signs of surface activity in its condition as supplied, and then to test the effects of various additives. This information was obtained by measuring the rate of ascent of air bubbles of measured size in these solutions, and comparing the observed drag coefficient (Equation [21]) to that calculated on the basis of the theory of Rybczynski-Hadamard for Re $\leq$ 0.75 (Eqation [24]) or Ryskin and Leal for Re > 0.75 (Equation [25],) for a fluid surface of the air bubble. The oil as received and different additives in the oil were measured, as well as Test Lubricant TEL-4041, with the results reported in Table 14.

All the liquids have values for the observed drag coefficient that are close to the theoretical value for a fluid surface, demonstrating that:

a. The lubricant as supplied has no adsorbed surface-active impurity;
b. The additives are not surface active in this oil; and
c. The Test Lubricant TEL-4041 shows no contamination by surface-active materials.

6. Correlations with foam

The agreement of the observations with Equation [24] means that the oil systems thus characterized show no dynamic surface tension, and therefore according to the Marangoni-Gibbs-Rayleigh theory should be non-foaming. In fact, all but one are non-foaming: the system
Emolein 2917 + 5% w/w polypropylene glycol (Mw = 4000)
produces a small amount of foam. This system, unlike the others, also shows a small lowering of the equilibrium surface tension of the solvent, despite its lack of dynamic surface tension when measured by the present method.

The systems that show no dynamic surface tension by the method of bubble rise also show no hysteresis loops on contraction-expansion cycling.

Table 14. Comparative Rates of Bubble Rise in the Blended Ester 0-77-10, in Solutions of different Additives in 0-77-10 Lubricant, and in Test Lubricant TEL-4041

System	Temp (°C)	ν (St)	d (cm)	V_C (cm/s)	Re	C_D	$C_{D,Theory}$*
0-77-10	21.0	0.265	0.084	2.215	0.776	22.387	22.222
0-77-10 + 5% (w/w) 3,7-Dioctyl Phenothiazine	21.0	0.319	0.117	3.188	1.169	15.023	15.170
0-77-10 + 1%(w/w) Triphenyl Phosphite	20.6	0.258	0.099	2.929	1.124	15.089	15.731
0-77-10 + 0.05% (w/w) Sebacic acid	20.0	0.261	0.100	2.822	1.081	16.414	16.310
0-77-10 + 2% (w/w) Acryloid HF866	20.0	0.353	0.107	2.588	0.784	20.899	22.009
0-77-10 + 1% (w/w) 3,7-Dioctyl Phenothiazine + 0.5% Triphenyl Phosphite + 0.05% Sebacic Acid + 2% Acryloid HF866	22.5	0.339	0.095	2.256	0.632	24.406	25.316
TEL-4041	21.0	0.313	0.083	1.867	0.495	31.135	32.323

*By Equation [24] or Equation [25]

PART II. TRANSITION BETWEEN BEHAVIORAL LIMITS

1. Introduction

This section reports an investigation of the surface activity of polydimethylsiloxane in a synthetic lubricant, as a function of concentration and temperature. In these experiments, surface activity is measured by the rate of ascent in the solution of a single, near-spherical bubble of known size. Effects of dynamic surface tension influence the rate of ascent. It was shown in This Report, Part 1 Section XIV that between the Rybczynski-Hadamard and the Stokes regimes of concentration, that is, between no effect and the maximum effect of dynamic surface tension as exhibited by the change of the rate of ascent of a single bubble in the solution, an intermediate regime exists in which the surface-active solute influences dynamic surface tensions to various degrees, which are manifested by transitional states of the bubble surface between completely fluid and completely rigid. The previous work explored the intermediate regime as an isothermal function of the concentration of polydimethylsiloxane at room temperature. The present addition to this work extends the scope of that study to a range of isotherms from 14 to 60°C. The data are reported in terms of the variation of drag coefficients with Reynolds' numbers for solutions of various concentrations of a surface-active solute, to show the onset of dynamic surface tension and its gradual growth, as indicated by the transition between the behavioral limits of a completely fluid and a completely rigid interface in the rising bubble. The results show that the surface activity of polydimethylsiloxane in the lubricant increases with concentration at constant temperature and also has a slight increase with temperature at constant concentration.

2. Rate of Bubble Rise in Solutions of Polydimethylsiloxane in Hercolube C

We have found polydimethylsiloxane to be surface-active in every synthetic lubricant that we have tested; Hercolube C had not been tested, and is now added to the others. The rates of bubble rise in a solution of polydimethylsiloxane (1000 cSt) at 43.3 ppm in Hercolube C were found to agree with the theoretical results obtained for bubbles with rigid interfaces, as expressed by Stokes equation, Equation [23] of Part 1 above, for $Re \leq 0.75$ or for $Re > 0.75$ by Equation [26]; that is, polydimethylsiloxane is surface active in Hercolube C.

At values of $Re \leq 0.75$ both Stokes' law and the Rybczynski-Hadamard modification of it are valid descriptions of the terminal velocities of spherical bubbles of rigid and of fluid interfaces respectively. Our results at these lower Reynolds' numbers are most readily understood in terms of the Rybczynski-Hadamard constant **K**, Equation [22], which is how they are reported in Figure 37. Figure 37 shows the variation of **K** with temperature and with concentration of polydimethylsiloxane. At lower concentrations than 14.6 ppm of polydimethylsiloxane (1000 cSt) in Hercolube C, the values of the

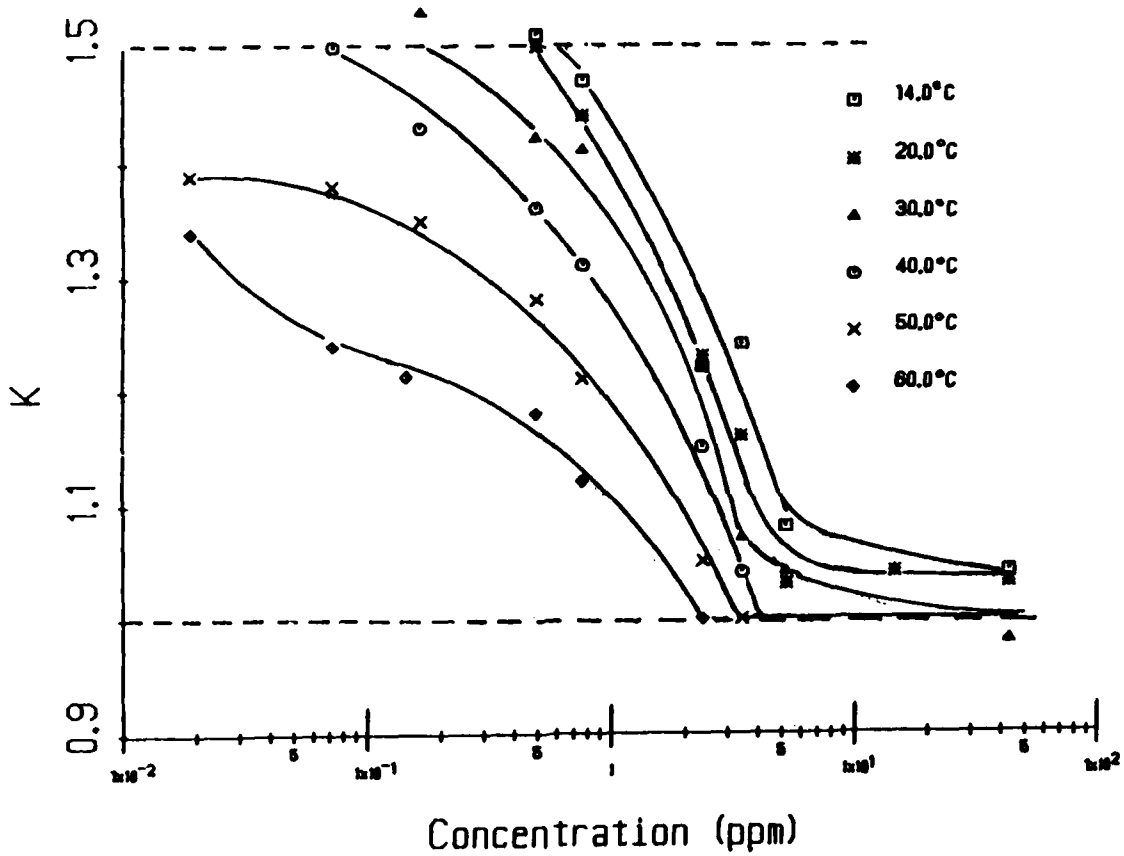

Figure 37. Variation of K with Temperature and Concentration of Polydimethylsiloxane (1000 cSt) in Hercolube C.

comparative rate of rise, **K**, which is the ratio of the observed rate of rise (corrected for wall effects) to the rate calculated by Stokes' law for a rigid sphere, becomes progressively larger, tending to a value of 1.50 (fluid interface) as the concentration is decreased.

The data shown in Figure 37 are reported in another form in Figure 38, in which equal values of **K**, termed cotensiles, are reported as temperature-vs-concentration contours. The cotensiles vary from 1.50 in the Rybczynski-Hadamard regime to 1.00 in the Stokes regime. This diagram makes it clear that the beginning of suface activity of polydimethylsiloxane is manifest at lower and lower concentrations as the temperature of the solution is raised.

The same transition of the interface observed at higher Reynolds' numbers is more conveniently discussed in terms of the variation of drag coefficients with Reynolds' numbers. At lower concentrations than 14.6 ppm of polydimethylsiloxane (1000 cSt) in Hercolube C, the drag coefficient becomes progressively smaller than the value calculated for a rigid interface, tending to an observed drag coefficient that is close to the one calculated from the theories of a fluid interface. Figure 39 shows the variation of the drag coefficient with Reynolds' number on logarithmic scales, for solutions of polydimethylsiloxane of different concentrations in Hercolube C. The data are reported in full in Table 15.

Figure 40 shows the transition in behavior from a fluid to a rigid interface with increasing concentration of polydimethylsiloxane in Hercolube C at Reynolds' numbers of 0.4 and 4.0. The ratio of C_D observed to C_D calculated for a completely fluid interface, using the theory of Hadamard-Rybczynski, as expressed by Equation [24], for $Re \leq 0.75$ and the theory of Ryskin and Leal, as expressed by Equation [25], for $Re > 0.75$, has a value of unity for a completely fluid interface. For a rigid interface the ratio equals 1.50 for $Re \leq 0.75$, and 1.60 for $Re = 4.0$. The points shown are interpolated from the data of Figure 39; the variation of the drag coefficient with Reynolds number for a range of concentrations of polydimethylsiloxane (1000 cSt) in Hercolube C.

Some interesting comparisons can be made by inspection of Figure 37 with Figures 123 and 124 of This Report, Part I.

a. The surface activity of the polydimethylsiloxane is not the same in mineral oil, in tmp-heptanoate, and in Hercolube C: comparing the concentrations of polydimethylsiloxane (1000 cSt) required to obtain an arbitrary value of **K** = 1.10, we find:

   Mineral Oil requires 6 ppm;
   Hercolube C requires 4 ppm;
   Tmp-Heptanoate requires 3 ppm.

   The surface activity in the synthetic lubricants is greater than in mineral oil.

b. The surface activity of polydimethylsiloxane (1000 cSt) in

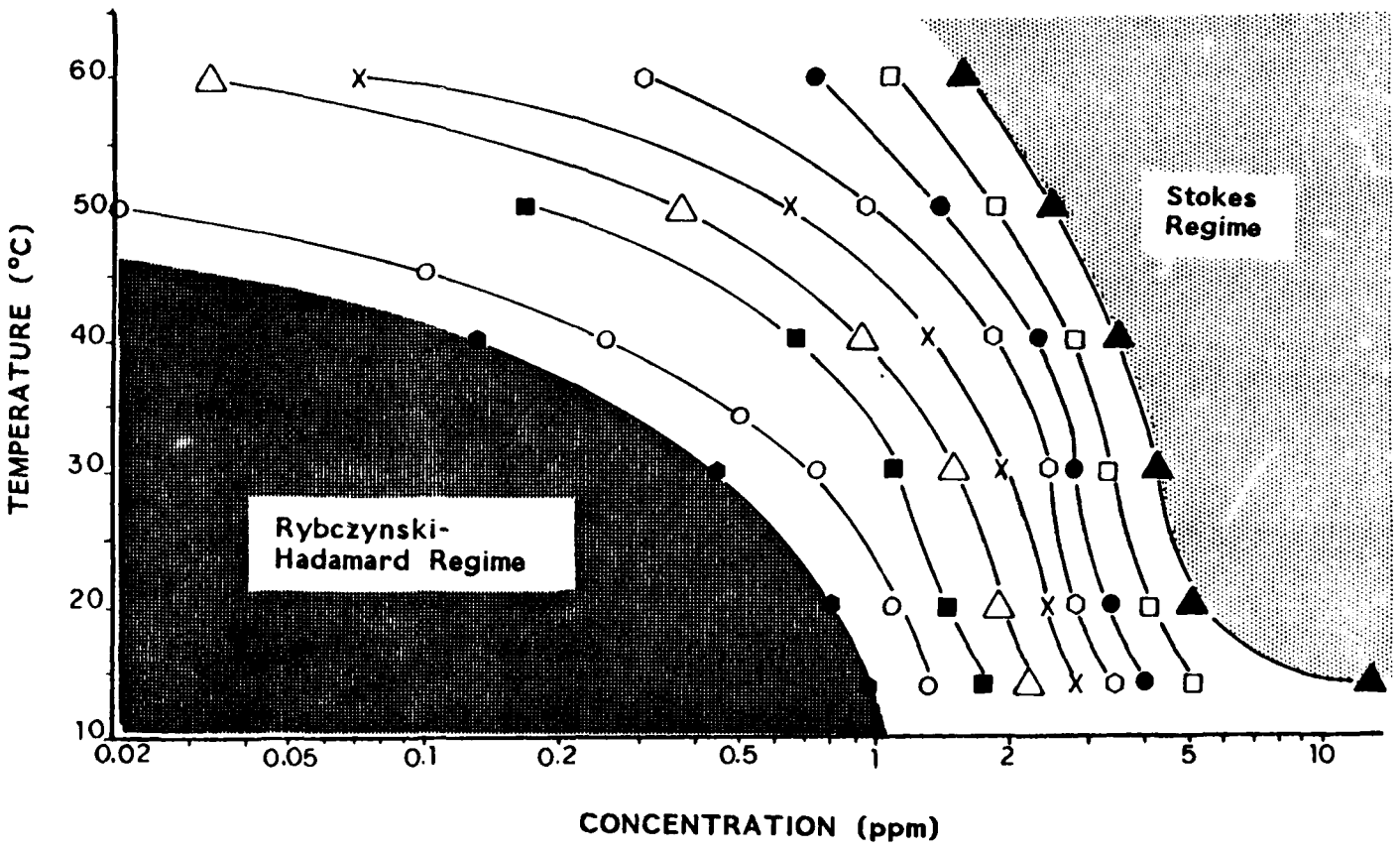

Figure 38. Temperature vs Concentration Contours of Co-Tensiles, or Equal Values of K, Interpolated from the Data in Figure 37.

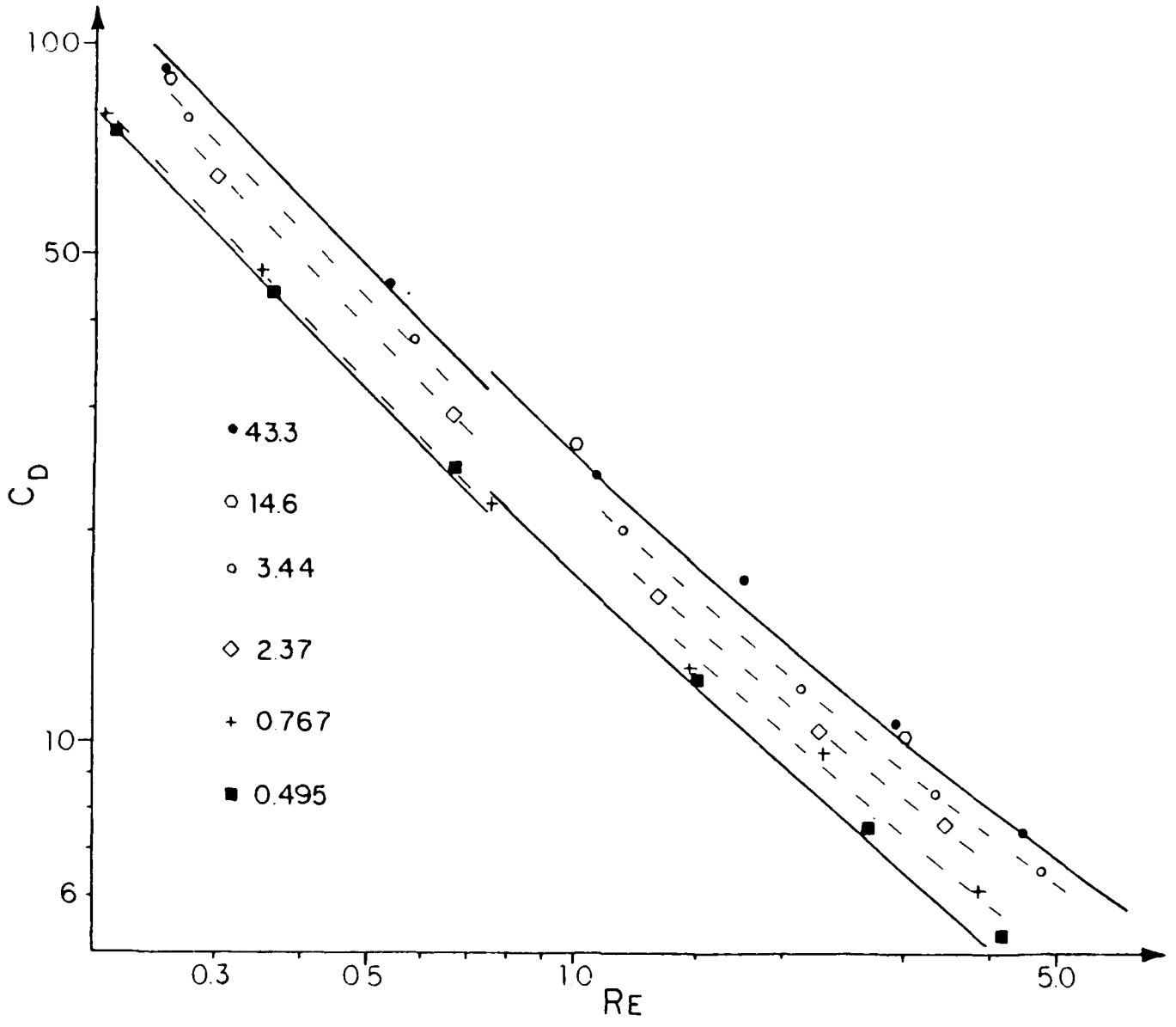

Figure 39. The Limits (Solid Lines) and the transitional States (Dotted Lines) of the Drag Coefficient, C_D, with Reynolds Number, Re, on Logarithmic Scales. Solid Lines are Theoretical Equations; Points are Observational Data. The System is Hercolube C with Various Concentrations of Polydimehtylsiloxane.

Table 15. Experimental Conditions, Dimensionless Groups, and Averaged Velocities of Bubbles Rising in Various Solutions.

	Temp [°C]	d [cm]	ν [cm²/s]	V_c [cm/s]	Re	C_D
a	14.1	0.084	0.480	0.837	0.147	156.691
	20.0	0.084	0.365	1.089	0.251	92.547
	29.9	0.084	0.243	1.554	0.537	45.510
	39.9	0.084	0.167	2.129	1.071	24.227
	49.8	0.084	0.121	2.514	1.746	17.372
	59.7	0.084	0.092	3.182	2.905	10.847
	69.8	0.084	0.073	3.836	4.415	7.462
b	20.0	0.084	0.365	1.103	0.254	90.258
	39.9	0.084	0.167	2.025	1.019	26.773
	59.7	0.084	0.092	3.252	2.969	10.386
c	14.1	0.084	0.480	0.993	0.174	111.431
	20.0	0.084	0.365	1.181	0.272	78.711
	29.9	0.084	0.243	1.698	0.587	38.092
	39.9	0.084	0.167	2.335	1.175	20.138
	49.8	0.084	0.121	3.026	2.118	11.992
	59.7	0.084	0.091	3.591	3.315	8.515
	69.8	0.084	0.073	4.095	4.713	6.549
	39.9	0.060	0.167	1.219	0.438	52.814
	49.9	0.055	0.121	1.365	0.620	38.613
d	14.1	0.084	0.480	0.856	0.150	149.848
	20.0	0.084	0.365	1.089	0.251	92.531
	29.9	0.084	0.243	1.661	0.574	39.795
e	14.1	0.084	0.480	0.978	0.171	114.736
	20.0	0.084	0.365	1.302	0.300	64.812
	29.9	0.084	0.243	1.927	0.666	29.570
	39.9	0.084	0.167	2.610	1.313	16.123
	49.8	0.084	0.121	3.245	2.253	10.431
	59.7	0.084	0.092	3.791	3.462	7.641
f	14.1	0.084	0.480	1.176	0.206	79.464
	20.0	0.084	0.365	1.520	0.350	47.517
	29.9	0.084	0.243	2.231	0.771	22.064
	39.8	0.065	0.167	1.800	0.700	26.241
	49.8	0.060	0.121	1.959	0.971	20.450
	59.7	0.055	0.092	2.009	1.201	17.824

Table 15. Continued.

	Temp [°C]	d [cm]	ν [cm²/s]	V_c [cm/s]	Re	C_D
g	14.1	0.084	0.480	1.210	0.212	75.054
	20.0	0.084	0.365	1.577	0.363	44.190
	29.9	0.084	0.243	2.041	0.672	25.120
	39.9	0.084	0.167	2.965	1.491	12.494
	49.8	0.084	0.121	3.800	2.638	7.606
	59.7	0.084	0.092	4.547	4.152	5.312
h	29.9	0.084	0.243	2.462	0.851	18.118
	39.9	0.065	0.167	1.971	0.767	21.885
	49.8	0.060	0.121	2.193	1.087	16.319
	59.7	0.055	0.092	2.355	1.408	12.971
i	39.9	0.065	0.167	2.073	0.807	19.780
	49.8	0.060	0.121	2.245	1.113	15.571
	59.7	0.055	0.092	2.219	1.327	14.610
j	49.8	0.060	0.121	2.259	1.117	15.500
	59.7	0.055	0.092	2.398	1.434	12.510

a is Hercolube C + 43.3 ppm polydimethylsiloxane
b is Hercolube C + 14.6 ppm polydimethylsiloxane
c is Hercolube C + 3.44 ppm polydimethylsiloxane
d is Hercolube C + 5.23 ppm polydimethylsiloxane
e is Hercolube C + 2.37 ppm polydimethylsiloxane
f is Hercolube C + 0.767 ppm polydimethylsiloxane
g is Hercolube C + 0.495 ppm polydimethylsiloxane
h is Hercolube C + 0.165 ppm polydimethylsiloxane
i is Hercolube C + 0.0724 ppm polydimethylsiloxane
j is Hercolube C + 0.019 ppm polydimethylsiloxane

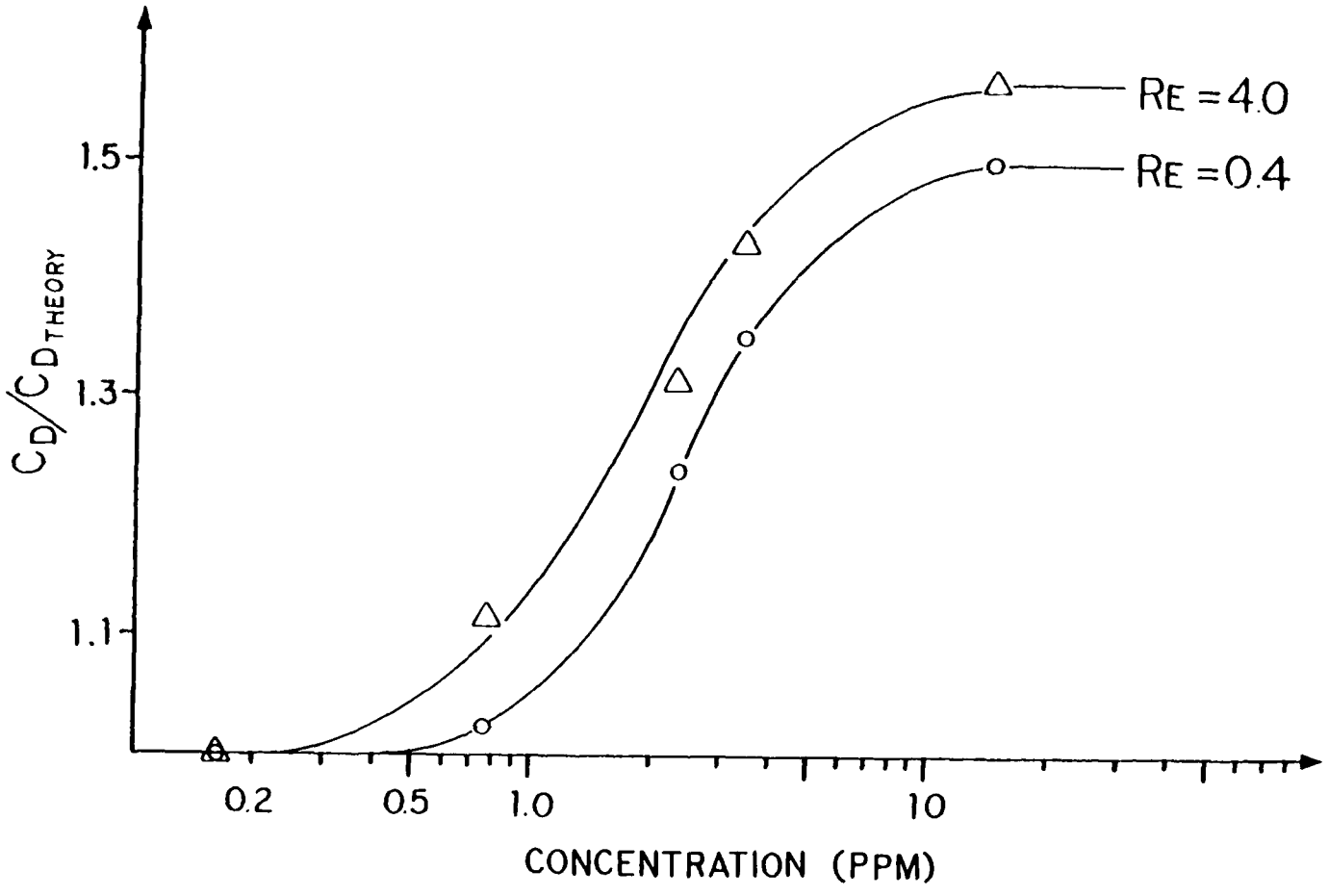

Figure 40. Transition of Behavior from Fluid to Rigid Interface with Concentration of Polydimethylsiloxane in Hercolube C, at Reynolds Numbers of 0.4 and 4.0. The points shown are interpolated from the Data of Figure 39.

Hercolube C is greater the higher the temperature. This result confirms what we have already observed about the foaminess of synthetic lubricants containing polydimethylsiloxane: namely, that the foaminess increases with temperature (see This Report Part I, Figures 11a and 11b.); and at each temperature the foaminess reaches a maximum at a certain concentration. Similar results have been observed with solutions of polydimethylsiloxane (1000 cSt) in Hercolube C. This behavior is consonant with that of a binary system that has a lower consolute point; and indeed the whole pattern of behavior has a strong similarity to the system polypropylene glycol + water, both in the foam behavior and the way in which the surface activity of the solute varies with temperature and concentration. Our results with this aqueous system are shown in Appendix B.

SECTION VII

RECOMMENDATIONS FOR FURTHER INVESTIGATIONS

The recommendations for further investigations given in This Report, Part I, Section XVI, are carried out only partially in the work reported herein. The study of capillary waves, recommended on that occasion, was extended in the sequential work as far as to show that the apparatus as designed and built can be used to validate the theory of Lucassen-Reynders and Lucassen applied to solutions with invariant surface tension. This application was made, as reported herein, for samples of synthetic lubricant without additives, and serves to verify the absence of any surface activity in the lubricant itself. To extend the investigation to take into account situations in which the surface tension changes on contraction or expansion of surface area introduces new elements into the theory, which add to its mathematical complexity and require new software programs for the numerical solution of the elasticity modulus from the observations. I expect that this can be done successfully, only requiring more time.

The study of the rate of ascent of a single bubble in an oil likewise serves to confirm the absence of any surface-active solute in the original oil, and also serves to determine whether any additive or combination of additives creates surface activity in an oil solvent. The technique could be exploited much further for the latter purpose than has yet been done. Both concentration of additive and temperature are variables readily adjusted in the apparatus in its present design. Synergistic interaction between additives to enhance or to diminish surface activity is immediately detectable, even before a foaming problem is evident; and so would provide a warning that the risk of foam has been increased by certain combinations of additives.

Further investigation of this topic should tackle possible Lewis acid-Lewis base interactions between the oil solvent and its additives, and also whether such interactions exist between additives. Surface activity greatly depends on the presence or absence of such interactions. For example, polydimethylsiloxane is insoluble in a hydrocarbon oil because of the absence of an interaction, and acts as a foam inhibitor by virtue of its insolubility. But an acid-base interaction takes place between polydimethylsiloxane and a synthetic-ester lubricant, which increases the solubility of the additive sufficiently so that it acts to promote foam.

The measurement of rates of bubble rise shows these interactions between oil and additive, as it detects the concentration of additive at which surface activity begins to occur. If additives also interact with each other, their concentration for the initiation of surface activity is either increased or decreased.

Another method that we have used to detect interactions is the shift of the proton NMR bands of the additive. By this technique we

have verified the acid-base interaction between polydimethylsiloxane and ethyl acetate (a hard Lewis base,) showing polydimethylsiloxane to be a hard Lewis acid.

An application of this information is to develop a satisfactory foam inhibitor for synthetic-ester lubricants. The underlying theory is to reduce the Lewis acidity of polydimethylsiloxane by means of appropriate substituent groups, e.g., aryl side chains, with the purpose of reducing its interaction, and hence its solubility, in the oil. Reduced solubility is known to convert profoamers to foam inhibitors, as long as the change of structure is not so profound as to destroy the low surface tension of the additive.

The following items of information are significant from this point of view:

Trautman[29] reported the effect of the addition of silicone polymers on the foaming characteristics of lubricating oils and other petroleum products. The particular silicone used was virtually insoluble in the oils tested in concentrations as low as 5ppm or less and was quite effective in suppressing foam. Trautman showed, however, that in the case of a gas oil in which the silicone was soluble to the extent of 0.01%, the addition of silicone below the limit of solubility increased the foam stability. Increasing the amount of silicone beyond 0.1% lowered the foam stability. This indicates that silicones are effective as foam inhibitors only when present in concentrations far exceeding their solubility.

Substituent groups affect the solubility and hence the foam-inhibiting effectiveness of silicones. Haloalkyl siloxanes such as 3,3,3-trifluoropropylmethyl siloxane and its polymers obtained by treatment with sulfuric acid are employed to defoam aromatic solvent solutions.[30]

The measurement of dynamic surface tension by the techniques we have developed, or the use of NMR spectroscopy, would allow the changes of solute-solvent interaction to be monitored as the molecular structure of the additive is altered by adding substituent groups.

The present work brought to light the disturbing fact that samples of the same chemical from the same manufacturer may vary significantly from batch to batch in their propensity to stabilize foam when introduced as an additive to a synthetic lubricant. The tests described in this Report detect and measure dynamic surface tension, and so reveal surface activity of solute samples if it is present. We suggest that the additive in question be synthesized by

---

[29] C.E. Trautman and H.A. Ambrose, "Prevention of Foaming of Hydrocarbon Oils," U.S. Patent 2,416,503 to Gulf Research and Development Co., 25 February 1947.

[30] C.C. Currie, U.S. Patent 3,115,472 to Dow Corning Corp., 24 December 1963.

the usual method of its production, and that it be tested for surface activity at every stage of its purification, so as to isolate and identify the component that causes surface activity.

BIBLIOGRAPHY

J.J. Bikerman, Trans. Faraday Soc., 36, 634 (1938); Idem, "Foams," Springer-Verlag, New York, 1973, pp 78-80.

R.B. Bird, W.E. Stewart, and E.N. Lightfoot, "Transport Phenomena," Wiley, New York, 1960, 206.

R. Cini and P.P. Lombardini, J. Colloid Interface Sci., 81, 125, (1981).

C.C. Currie, U.S. Patent 3,115,472 to Dow Corning Corp., 24 December 1963.

F.H. Garner and A.R. Hale, Chem. Eng. Sci., 2, 157 (1953).

F.H. Garner and D. Hammerton, Chem. Eng. Sci., 3, 1 (1954).

W.D. Garrett and W.A. Zisman, J. Phys. Chem., 74, 1796, (1970).

J. Hadamard, Compt. Rend., 152, 1735 (1911).

H. D. Harkins and R. W. Wampler, J. Amer. Chem. Soc., 53, 850 (1931).

H. Kuerten, J. Raasch and H. Rumpf, Chemie-Ing. Tech, 38, 941 (1966).

J.A. Mann and R.S. Hansen, J. Colloid Sci., 18, 757, (1963).

L.D. Landau and E.M. Lifshitz, "Fluid Mechanics," Pergamon Press, London, 1959, p.100

I. Langmuir, J. Amer. Chem. Soc., 39, 1848 (1917).

V. Levich, "Physicochemical Hydrodynamics," Prentice-Hall: New York, 1962; Chapter 8.

J. Lucassen and R.S. Hansen, J. Colloid Interface Sci., 22, 32, (1966).

E.H. Lucassen-Reynders and J. Lucassen, "Properties of Capillary Waves" in Advances in Colloid and Interface Science, 2, 347-395 (1969).

K. Malysa, R. Cohen, D. Exerowa and P. Krugljakov, J. Colloid Interface Sci., 80, 1 (1981)

K. Malysa, K. Lunkenheimer, R. Miller and C. Hartenstein, Colloids and Surfaces, 3, 329 (1981).

S. Ross and Y. Suzin, Langmuir, 1, 145 (1985).

W. Rybczynski, Bull. Int. Acad. Sci. Cracovie, Ser.A, 1911, 40.

G. Ryskin and L.G. Leal, J. Fluid Mech., 148, 1 (1984).

Y. Suzin and S. Ross, J. Colloid Interface Sci., 103, 578 (1985).

M. van den Tempel and R.P. van de Riet, J. Chem. Phys., 42, 2769 (1965).

D. Thiessen and A. Sheludko, Kolloid-Z., 218, 139, (1967).

C.E. Trautman and H.A. Ambrose, "Prevention of Foaming of Hydrocarbon Oils," U.S. Patent 2,416,503 to Gulf Research and Development Co., 25 February 1947.

R.M. Wellek, A.K. Agrawal and A.H.P. Skelland, AIChE J., 12, 854 (1966).

APPENDIX A

AFAPL TEST METHOD 3213
From Technical Report AFAPL-TR-75-91

The AFAPL Foam Test Method 3213 is basically that outlined in ASTM Method D 892 with the following modifications:

1) A 500 ml graduated cylinder is used in place of a 1,000 ml graduated cylinder.
2) Air flow rate is increased from 25 to 1,000 cc/min.
3) Change in aeration time from 5 to 30 min and procedures for obtaining foam data.

In this test, a measured volume of oil is heated to the required test temperature and then aerated at the required flow rate for thirty minutes using an air-diffuser stone. Foam volumes are recorded every five minutes; these volumes represent the maximum foam volume obtained during the previous five minute aeration period.

1. SCOPE

1.1 This method is used to determine the foaming characteristics of aircraft turbine-engine lubricating oils under specified temperature and air flow conditions.

2. SUMMARY

2.1 The test is basically the ASTM D-892 foam test modified to be substantially more severe. Ratings of synthetic-lubricant foaming tendencies using this method have been consistent with existing operational turbine-engine experience. The modifications primarily involve the use of 500 ml rather than the 1000 ml graduated cylinder and a greatly increased air flow rate.

3. SAMPLE

3.1 The test requires approximately 300 ml of the sample.

4. APPARATUS

4.1 The apparatus is the Foam Test Apparatus; ASTM D-892 (Model 430 or Model 430A, Koehler Inst. Co., 1595 Sycamore Ave., Bohemia, L.I., New York 11716 or equivalent.

The apparatus consists of an air inlet device, 25.4 mm diameter spherical gas-diffusion stone (Norton Co., Worcester, Mass., No. ME-46239, P2180 grade or equivalent,) and a liquid bath equipped with heater, stirrer, and temperature controller. The bath must be capable of maintaining a bath temperature of 80 ± 1°C throughout a test cycle. Maximum stone pore diameter shall not be greater than 80 m. Stone permeability at a water pressure of 250 mm shall be 3000 to 6000 cc of air/min. Refer to ASTM-D892 for maximum pore diameter and permeability test procedures.

4.2 Cylinder, graduated; 500 ml (Standard glass laboratory ware with pouring spout.) Corning Number 3022 or equivalent.

4.3 Stopper, rubber; fitted for air tube.

4.4 Flowmeter; capable of delivering 1000 ± 20 cc air/min as measured at 20°C (68°F) and 760 mm Hg.

4.5 Timer; 1 sec graduations, accurate to 1 sec or better.

4.6 Thermometer; 1°C increments, accuracy of 1°C or better. An ASTM 12C (-20 to +102°C) thermometer is suitable.

4.7 Oven, drying; standard laboratory equipment.

5. MATERIALS

5.1 Solvents, cleaning; Stoddard solvent or petroleum distillate, and toluene conforming to ASTM D-892 specifications. Petroleum ether (Boiling Range 30 to 60°C,) ACS.

"WARNING: Toluene is toxic and flammable. Keep away from open flames. Avoid breathing vapors and contact with skin. Use in a laboratory hood or with adequate ventilation."

6. PREPARATION OF APPARATUS

6.1 The graduated cylinder, air inlet tube and diffuser stone must be thoroughly cleaned after each test. Between tests, these items must be stored in a clean, dust-free area.

6.1.a The cylinder shall be cleaned by rinsing with Stoddard solvent or petroleum distillate, then another rinse with toluene followed by washing with detergent and water. Rinse thoroughly with distilled water and dry in oven.

6.1.b Clean stone and air tube by rinsing with Stoddard solvent or petroleum distillate. Then immerse stone in toluene and, using vacuum and air pressure, flush the solvent back and forth at least 5 times. Finally, rinse stone with petroleum ether and dry using clean air. Wipe the outside of the air tube with a clean cloth moistened with toluene followed by a dry clean cloth.

7. PROCEDURE

7.1 Measure 200 ml of lubricant into clean cylinder. Immerse the cylinder in bath maintained at 80 ± 1°C (bath liquid above 500 ml cylinder mark.) Install air tube and stone so that the stone just touches the bottom of the cylinder and is approximately at the center of circular cross section. Allow 15 minutes for lubricant to reach thermal equilibrium. Make all air-supply connections. Adjust air flow to 1000 ± 20 cc/min.

7.2 Record the maximum foam volume generated during the thirty minute test period. Foam volume is defined as the foam-air interface (ml) minus the foam-liquid interface. If no foam-liquid interface is discernible, the foam-air interface measured in ml shall be defined as the foam volume. At the end of the test period, disconnect the air supply. Record the time required for the foam to collapse to no more than a single ring of bubbles at the periphery of the lubricant surface, or record volume of foam remaining after 5 minutes, whichever occurs first. Disassemble and clean apparatus.

8. REPORT

8.1 Report the following:

Maximum Foam Volume, ml_____
Foam Collapse Time, sec_____
Foam Volume Remaining after 5 min, ml_____

9. PRECISION

9.1 Repeatability. The repeatability of the method depends upon the level of the result. Limited test data indicate the following test repeatability:

Foam Volume	Repeatability
50 ml	10
150 ml	20
250 ml	25

9.2 Reproducibility. This has not been established.

METHOD PREPARED BY
AIR FORCE - AFAPL - 1975

APPENDIX B

SURFACE ACTIVITY OF THE SYSTEM POLYPROPYLENE GLYCOL + WATER

1. Introduction

The present study of isaphroic contours investigates, for the first time, a two-component system with a lower consolute point, namely, the system polypropylene glycol + water. An epicenter of maximum foam stability, which in these dilute solutions of low viscosity probably corresponds closely to the epicenter of maximum surface activity, is located on the coexistence, or solubility, curve.

Further evidence of the surface activity of this region of the phase diagram is shown by comparing measurements of dynamic surface tension with foam stabilities. Neither of these techniques measures a characteristic property of the solution, that is, one that depends only on the state of the solution, so a mismatch in the time scales of the two measurements may well occur; nevertheless, by disturbing the surface of the solution at a rate that is commensurate with the time stability of the foam, the processes are brought into the same temporal framework.

2. Materials

Distilled water, which was obtained from a general supply, was redistilled from alkaline permanganate into phosphoric acid and distilled once again into a quartz container. Polypropylene glycol (Mw = 1000 g/mole, ACS name poly(oxymethyl 1,2 ethanediyl) α-hydro ω-hydroxy, registry number 25322-69-4) was obtained from Aldrich Chemical Co. and was used as is.

3. Experimental

The phase diagram of the system polypropylene glycol + water was determined by visual observation of cloud-points. Solutions were made volumetrically and placed in a test tube with a magnetic stirring bar and a thermistor. A hot-water bath and an ice bath were used to adjust temperatures. A mixture was either allowed to cool until the liquid cleared or it was warmed up (sometimes by a warm hand) until it became turbid. The mixture was observed at a right angle to a beam of light passing through it, with occasional stirring until the cloud point was reached. By approaching the cloud point in both directions, an endpoint was found to within one Kelvin degree.

The solutions of polypropylene glycol in water that were used to determine the phase diagram were prepared by weighing the polymer into a 100 ml volumetric flask. The other solutions were prepared by weighing the polymer into a 2 liter flask to form a 0.10 M stock solution, which was then diluted volumetrically.

Dynamic foam stabilities were measured by the technique described by Ross and Suzin.[31] The foam vessel was made by fusing a 60° funnel to a 4.6 cm diameter graduated cylinder. A water bath regulated the temperature. Foam heights were measured with a cathetometer. Humidified nitrogen was the gas used to make the foam.

Dynamic surface tensions of aqueous solutions of polypropylene glycol were measured using the same procedures as previously described: see This Report, Part 1, Section VIII. The temperature was monitored by placing a thermistor at the surface outside the contained area, but as near to the Wilhelmy blade as possible.

4. Results

A portion of the phase diagram of the system polypropylene glycol + water is shown in Figure B-1 in terms of the logarithm of concentration. This system has a lower consolute point, so the homogeneous region is below the coexistence curve. The isaphroic contours, that is, lines of equal foam stability, derived from measured foaminess, are interpolated on the phase diagram in Figure B-1. These contours circulate around an epicenter, (30°C, 0.016 M), and decrease in value the farther they are from it.

Examples of the variation of surface tension on extension-contraction cycling of surface area at 1.02, 0.20, and 0.05 cycles per minute for a 0.0021 M solution at 10°C are shown in Figures B-2, B-3 and B-4, respectively. Figure B-2 shows an initial compression, which is followed by successively larger dilatations in the course of which solute is gradually pumped out of the surface, more and more slowly, until a nearly flat steady-state hysteresis loop is reached. Figure B-3 also shows an initial compression, but the variation of surface tension reaches a steady-state hysteresis loop that is both above and below the equilibrium surface tension. On still slower cycling, the steady state becomes a hysteresis loop lying almost entirely below equilibrium surface tension (see Figure B-4), that is, the solute is now pumped into the surface. The steady-state loop is reached within three cycles.

These differences in the direction of movement of the solute on continued cycling are entirely due to varying the cycling frequency, and are not due to differences of concentration; the results can be interpreted as a consequence of slow rates of adsorption and desorption of the polymer (see below for the explanation.)

A comparable result for polydimethylsiloxane dissolved in tmp-heptanoate was reported in This Report, Part II, Section IV, Figures 9-12. These diagrams most resemble Figure B-3 of the system polypropylene glycol + water.

---

[31] S. Ross and Y. A. Suzin, Langmuir, 1, 145 (1985).

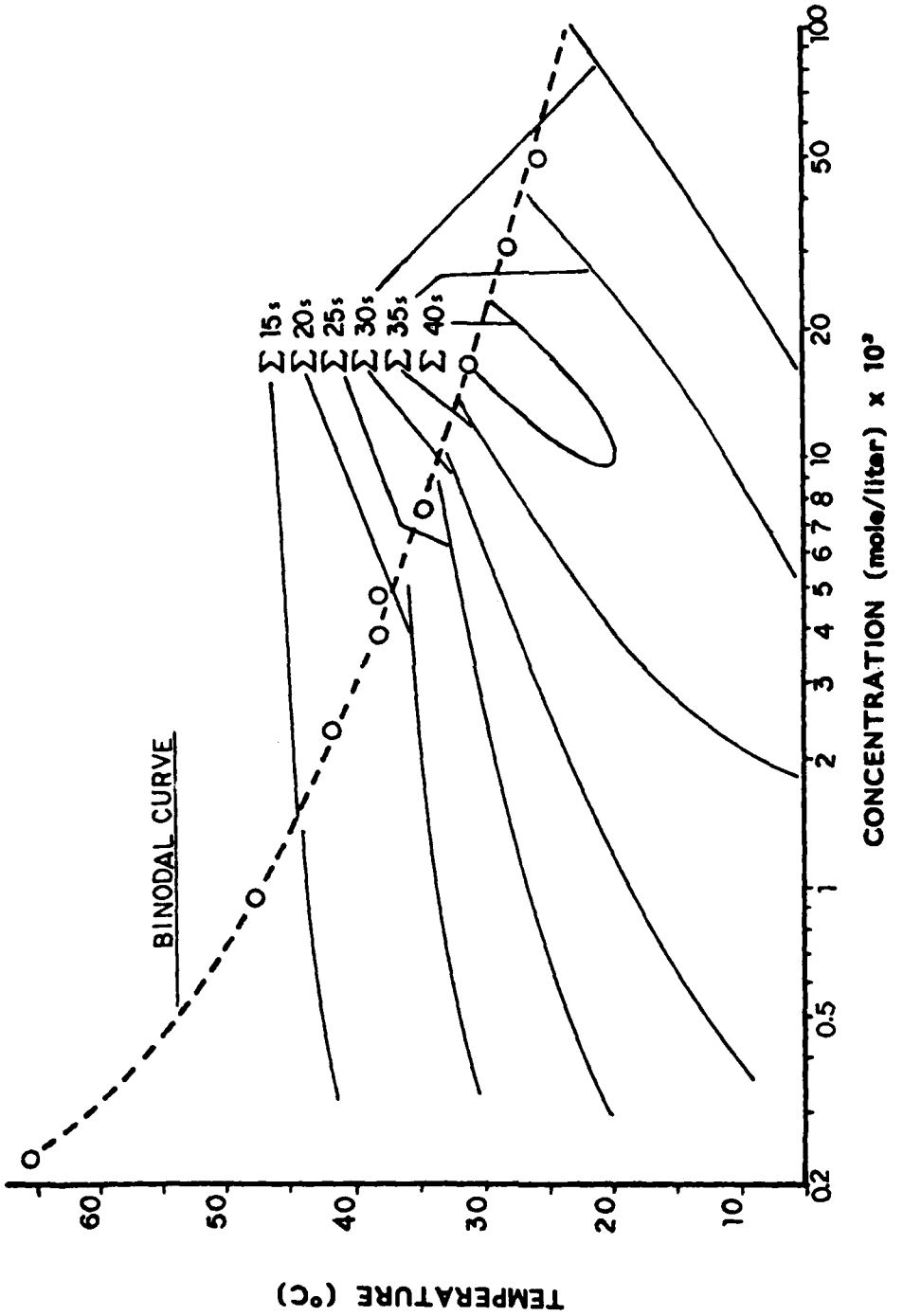

Figure B-1 Phase Diagram and Interpolated Isaphroic Contours of the Two-Component System Polypropylene Glycol and Water.

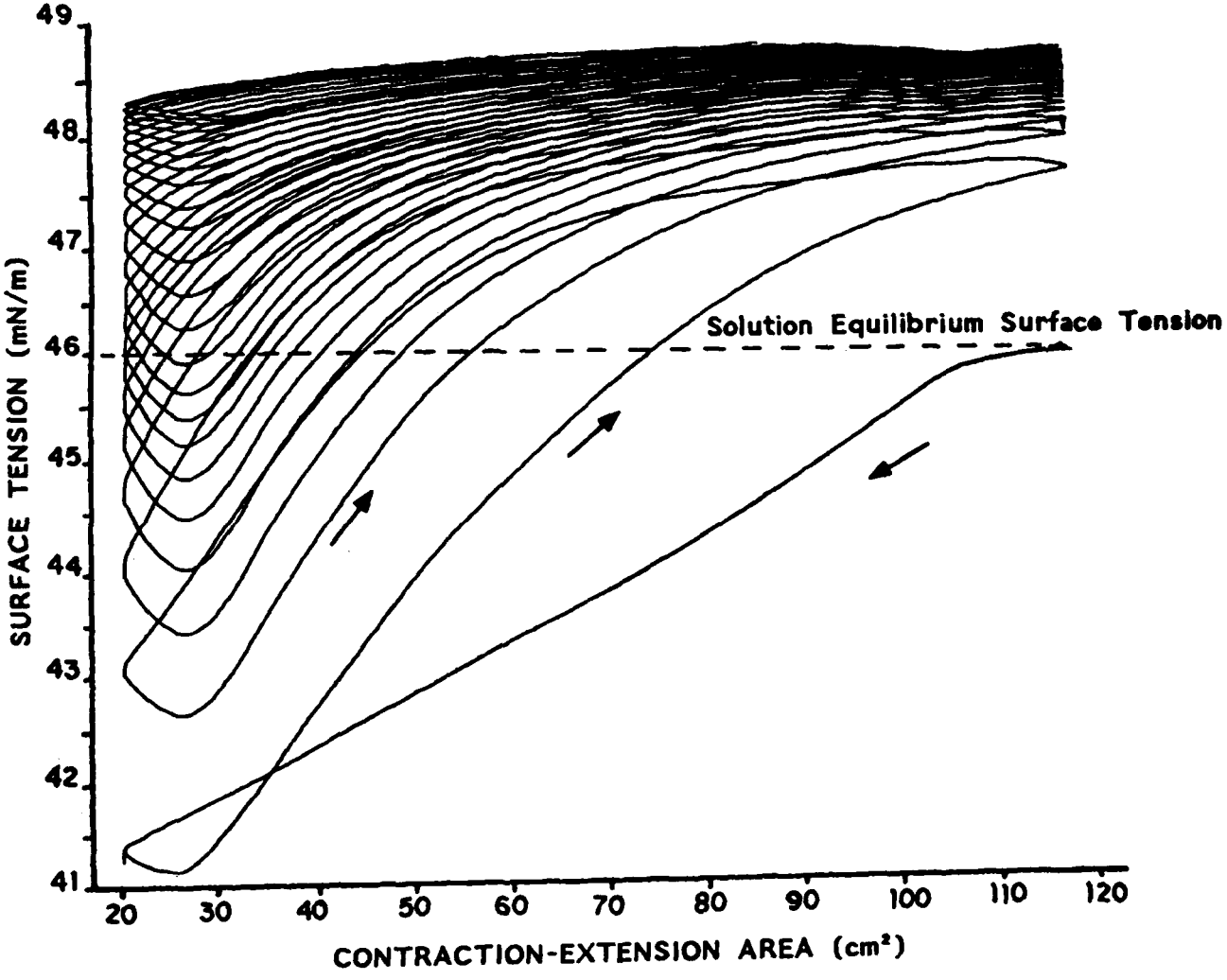

Figure B-2 The Variation of Dynamic Surface Tension with Area for a 0.00205 M Solution of Polypropylene Glycol in Water at 10.0°C and a Cycling Frequency of 1.02 cpm.

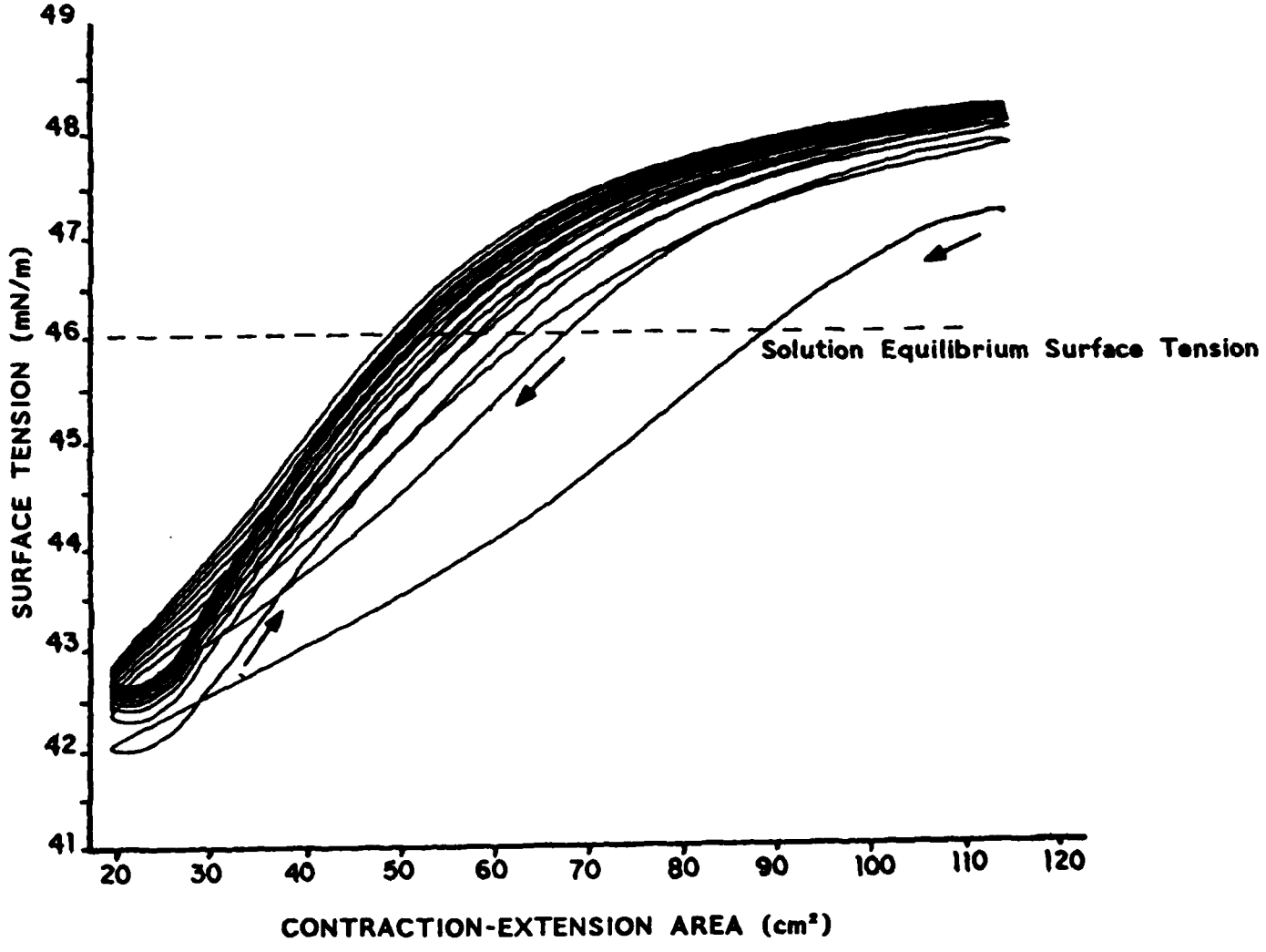

Figure B-3 The Variation of Dynamic Surface Tension with Area for a 0.00205 M Solution of Polypropylene Glycol in Water at 10.0°C and a Cycling Frequency of 0.20 cpm.

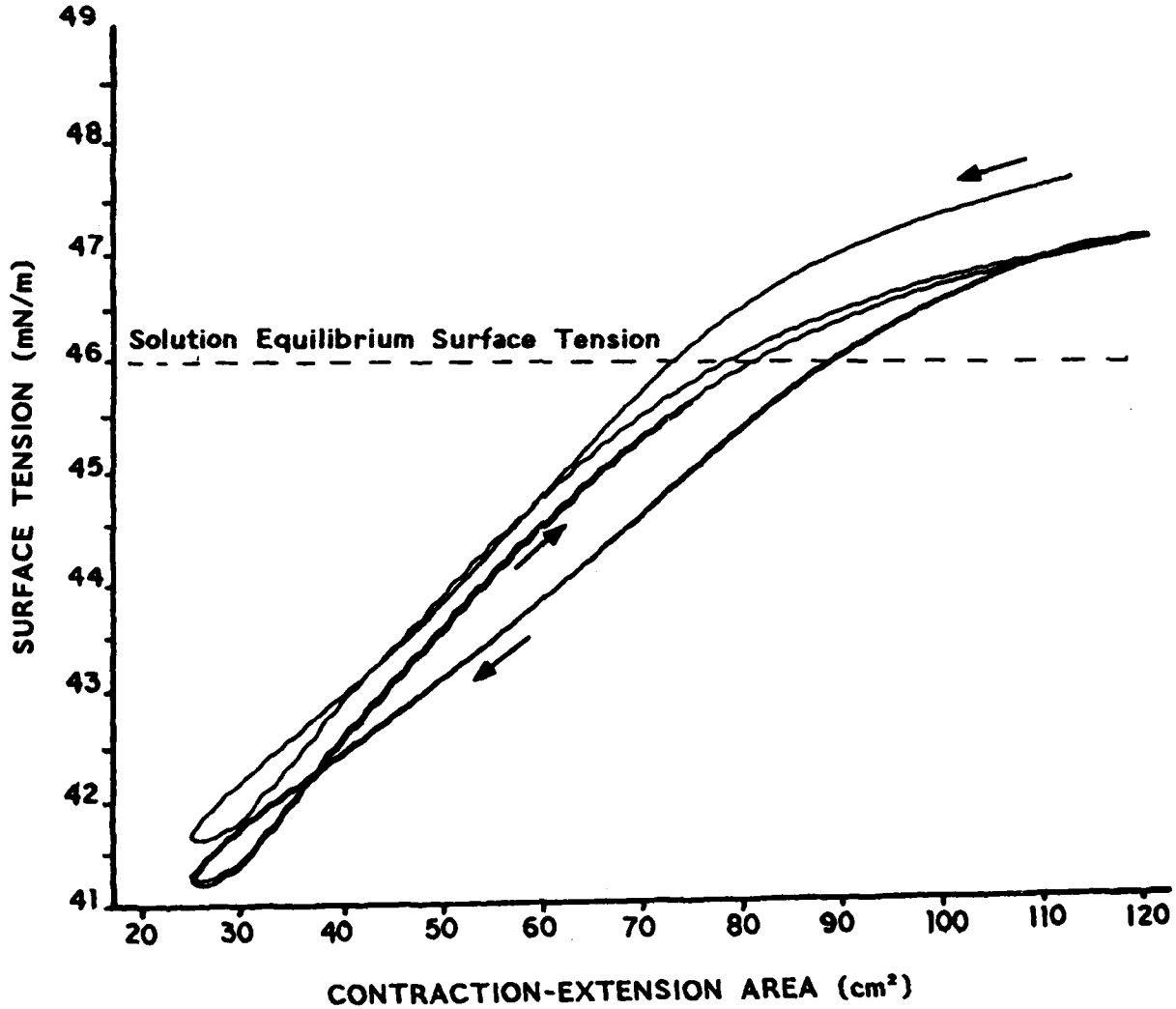

Figure B-4 The Variation of Dynamic Surface Tension with Area for a 0.00205 M Solution of Polypropylene Glycol in Water at 10.0°C and a Cycling Frequency of 0.05 cpm.

The values of $\Delta\sigma$ corresponding to the changes of surface area at 0.20 cycles per minute, are plotted in Figure B-5 as dynamic isotherms, separated into compressional and dilatational components; that is, the difference between the equilibrium surface tension and the minimum in the steady-state hysteresis loop is taken as a compressional component to $\Delta\sigma$, and the difference between the maximum in the steady-state hysteresis loop and the equilibrium surface tension is taken as a dilatational component; these are then plotted against concentration for 10, 15, 20, and 25°C isotherms. For each dynamic-surface-tension isotherm, the compressional component decreases over the same range of concentrations at which occur decreases in surface tension in the equilibrium isotherms, while the dilatational component increases over the same range. Increasing the temperature has little effect on the compressional components in Figure B-5, but the dilatational component is seen to decrease.

The values of $\Delta\sigma$ corresponding to a cycling frequency of 1.02 cycles per minute, are compared directly with the dynamic foam stabilities in Figure B-5. These dynamic surface tensions are determined by the formula for dilatational components, as is suitable for steady-state hysteresis loops that lie mostly above the equilibrium surface tension. The trends of the 10 and 15°C isotherms show a good correlation with foam stability, but the magnitude of the dynamic surface tension decreases with increasing temperature, which reduces the precision of the measurement; hence, the above-mentioned correlation does not hold for temperatures at 20°C and above.

5. Discussion

Three aspects of surface activity have been shown to occur in binary solutions in which an epicenter of surface activity occurs; namely, the existence of a point of perfect wetting, and the existence of epicenters of the isaphroic and cosorption contours. The isaphroic contours of the system polypropylene glycol + water show that a binary system with a lower consolute point exhibits the same behavior, mutatis mutandis, as systems with upper consolute points.

The dynamic surface tensions of this system have the unusual feature that the cycling frequency determines whether the adsorbed film is compressed or dilatated. Rapid cycling produces dilatations on extending the surface; but as the rate of cycling is slowed more and more, compression is observed at the contraction end of the cycle. With solutes of low molecular weight, such as 1-butanol in water, compression of the surface film on contraction of area is a feature of a relatively low concentration of solute in the surface; dilatation on extension of area is a feature of a relatively high concentration of solute in the surface; and the rate of cycling, within the range amenable to our control, hardly affects this aspect of behavior. That a concentrated surface layer should dilatate on extension of area is readily understood as the result of a rate of adsorption too slow to keep up with the rate at which the area is being extended; that it should fail to compress on contraction of

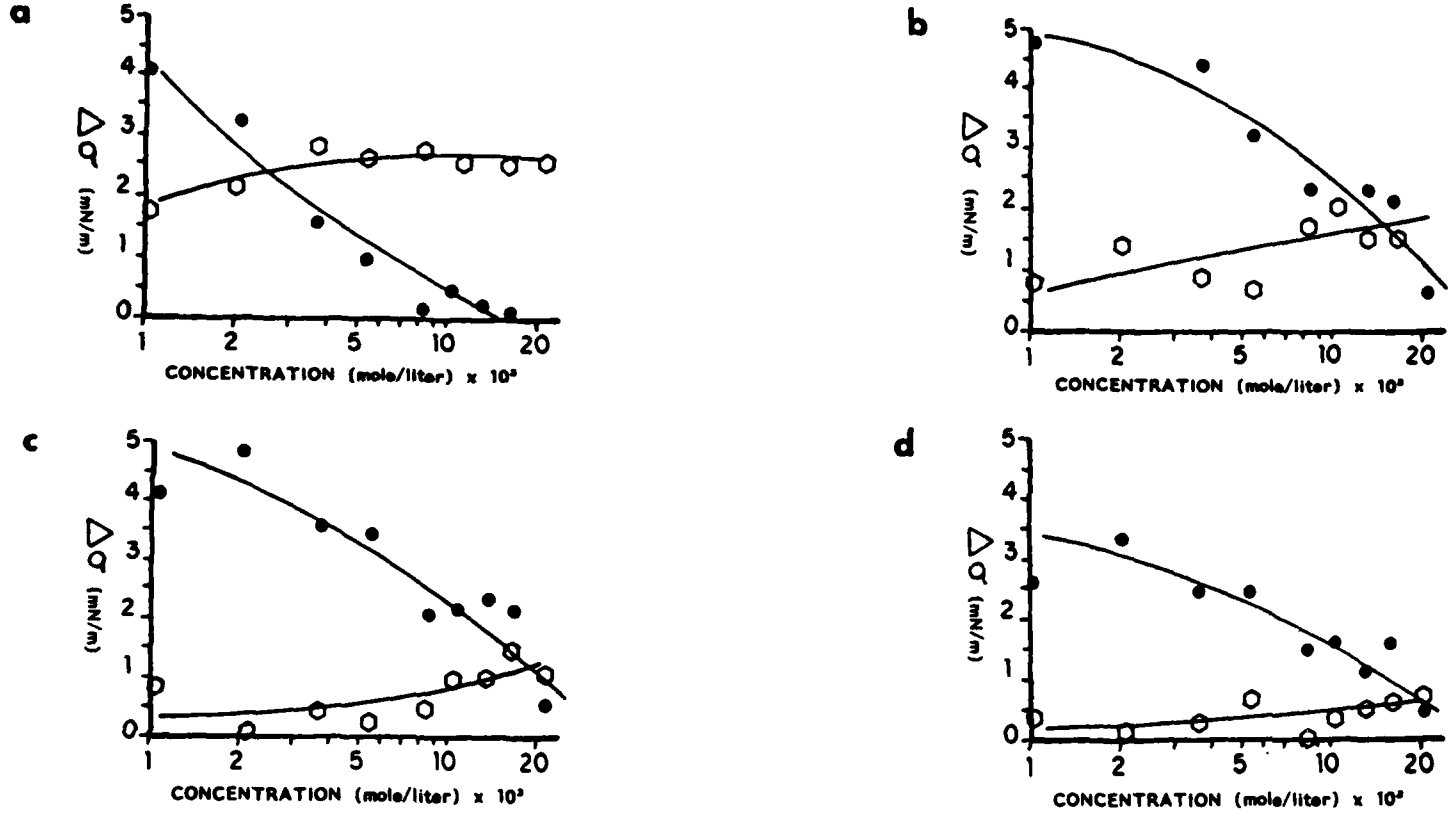

Figure B-5 The Variation of the Compressional Component of the Dynamic Surface Tension, ● ; and the Dilatational Component of the Dynamic Surface Tension, ○ ; with the Concentration of Polypropylene Glycol in Water at (a) 10.0°C, (b) 15.0°C, (c) 20.0°C and (d) 25.0°C.

area indicates that the rate of desorption is rapid enough to allow surface molecules to evade being crowded together on contraction of area: they can escape by desorption. That is, in a concentrated aqueous solution of 1-butanol, the rate of desorption is more rapid than the rate of adsorption. The behavior of a concentrated solution of polypropylene glycol differs in that, even at the slowest rate of cycling available to us, both dilatation and compression persist. Now dilatation depends on a slow rate of adsorption of solute, and compression depends on a slow rate of desorption of adsorbate, both relative to the mechanical rates of extension or contraction of surface area. The behavior of the aqueous solution of polypropylene glycol indicates rates of adsorption and desorption that are slower than the imposed rates of surface extension and contraction. An insoluble monolayer has practically zero rates of adsorption and desorption, and this polymer solution forms an adsorbed layer that behaves much like an insoluble monolayer. The same behavior has been observed in the present work with solutions of polydimethylsiloxane in tmp-heptanoate.

Choosing the correct cycling frequency that would correspond to the time scale of the processes stablizing foam is difficult with this system, since both compressions and dilatations occur depending upon the value of the cycling frequency. Comparing the dynamic surface tensions measured at a specific cycling frequency with the values of foam stabilities, indicates which frequency is most appropriate for the comparison.

The overall trends of the dynamic surface tensions measured at 0.20 cycles per minute show a reduction of total $\Delta\sigma$ with increasing concentration, while the foam is passing through maximum stability. Separating the values of the dynamic surface tensions into the compressional and dilatational components shows that the compression of the surface film predominates over dilatation at this frequency. The compression portions of the steady-state hysteresis loops still do not correspond to the foam stability and the dilatational components, while showing some indications of following the foam stability, are too small, and therefore not precise enough, to establish a definite trend. Poor compressibility of an adsorbed film is attributable to a concentrated surface layer; and that seems a reasonable supposition in the system polypropylene glycol + water, which is borne out by the low equilibrium surface tension. This trend in the surface concentration promotes dilatations on extensions of the surface area of the solution, as seen in the dilatational components in Figure B-5. The magnitude of these dilatations decreases with increasing temperature showing that either the rates of adsorption are increasing or the rates of desorption are decreasing or both. The compressional components, however, are relatively unaffected by the change in temperature, so we conclude that the rates of adsorption are increasing with temperature. Normally the rate of adsorption of a surface-active solute decreases with increasing temperature; but in this system the increase of temperature brings the solution closer to the phase boundary, and so, to a condition of greater surface activity. Thus the apparent anomaly is not anomalous.

U.S.Government Printing Office 1986 646-067,40654

END

FILMED

3-86

DTIC